AN INVESTIGATION OF COSMIC RAYS USING A HIGH PRESSURE WILSON CLOUD CHAMBER.

Thesis

submitted by

Robert A. Donald

B.Sc. (Edinburgh)

for the Degree of

Doctor of Philosophy.

University of Edinburgh.

September 1957.

CONTENTS.

PREFACE.

The research described in this thesis has been carried out in the Department of Natural Philosophy of the University of Edinburgh, under the joint direction of Professor N. Feather, F.R.S. and Dr. G.R. Evans.

Chapter I.

INTRODUCTION.

Section A - The Cosmic Radiation.

Towards the end of last century, experiments by C.T.R. Wilson, Elster and Geitel, on the rate of discharge of electroscopes, led to the suggestion that the surface of the earth was being bombarded by a previously unknown type of radiation, and that this radiation had an extra-terrestrial origin. Later work, using balloons to carry instruments into the upper atmosphere, was carried out by Hess, Gockel and Kohlhorster. This showed that the variation with altitude of the intensity of the radiation was not consistent with terrestrial origin. Since about 1926, the extra-terrestrial origin has been accepted and the rays are now known as cosmic rays.

The radiation detected by the above experiments is in fact of secondary origin. It is now known that the truly extra-terrestrial component interacts with the atoms of the earth's atmosphere, to give a complex radiation in which electrons, γ-rays, protons and other particles are present. In this work, the term "cosmic rays" will be taken to mean this complex secondary radiation.

Experiments on the absorption of cosmic rays by lead, and other materials, showed that the radiation

was made up of two parts. One part was readily absorbed, and is now known to consist of electrons and photons. The other was very penetrating. It was shown by Rossi that particles of this component could penetrate at least one metre of lead. Since particles of positive and negative charge were equally plentiful, it was not possible to identify them as protons. It would have been possible to have explained the absorption experiments by the existence of a particle of mass intermediate to that of the proton and electron. This particle was called a meson and its existence was confirmed by a cloud chamber photograph of Anderson and
1 Neddermeyer[1]. Such a particle had been predicted, on theoretical grounds, by Yukawa in 1935, in an attempt to explain the short-range nuclear forces, and also β-decay. He postulated a particle of mass approximately 150 m_e, which underwent radioactive decay, with a half-life of 0.25×10^{-6} seconds. This particle should have had a strong interaction with nuclei. The particle found by Anderson and Neddermeyer, now called the μ-meson, was of mass 200 m_e and was shown to decay
2 into an electron and one or more neutral particles[2]
3 with a half-life of approximately 2×10^{-6} seconds[3]. However, experiments showed that the μ-meson had very
4 little interaction with nuclei of light elements.[4]
5 A second type of meson, now known as the π-meson[5],

was discovered by workers using nuclear emulsions. This meson has a mass of 273 m_e and decays into a μ-meson and a neutrino with a half-life of 2.53×10^{-8} seconds. The π-meson does interact strongly with the nuclei of all elements and is now regarded as the Yukawa particle.

It has been known for many years[6], that "showers" of penetrating particles can be created in the atmosphere by cosmic rays. Cloud chamber experiments, by Fretter and others, show that these penetrating showers are caused by the interaction of a penetrating particle with the nucleus of an atom. In 1947, Rochester and Butler[7], in an experiment to search for new particles that might have been contained in these showers, discovered two new types of meson. One was a neutral meson, decaying into two charged particles and, possibly, a neutral particle, and the second was a charged meson. Both these types had masses greater than that of the π-meson. The neutral particle was more plentiful than the charged meson, and many examples were found. Investigation of the decay products of the neutral meson yielded strong evidence that, in many cases, the visible products were a proton and a negative π-meson[8], while in a few cases the decay products were two light mesons. However, up to 1953, these decay schemes had not been completely established, neither

had the presence nor absence of neutral decay products been finally settled[9].

Until 1953 much less was known about the charged heavy mesons. It had been established that one type[10], the τ-meson, was of mass approximately 970 m_e and decayed into three charged π-mesons. It was fairly well established that there was a second type, known as the χ-meson, which decayed into a μ-meson and two or more neutral particles. A third type, the χ-meson, decayed into a π-meson, which, within the very limited statistics available, was of unique energy.

In 1953, a joint group from University College of Wales, Aberystwyth (later this group transferred to Edinburgh University) and University College, London, decided to collaborate in an experiment to study the neutral mesons found in penetrating showers. For the study of neutral, decaying particles, a counter — controlled Wilson cloud chamber has very great advantages over the nuclear emulsion technique. It is possible in relatively few photographs to scan a very large volume. The scanning of a comparable volume of emulsion would be a very difficult task. In addition the property of the expansion chamber of associating the visible particles in time is valuable, while the origin of any interaction is relatively easy to determine.

In previous work on the neutral mesons, two types of cloud chamber had been used. In one case the chamber was operated near atmospheric pressure, in a strong magnetic field. This allowed momentum determinations to be made. In the second case, the chamber, again at atmospheric pressure, contained one or more metal plates. Residual range measurements were in this way sometimes available, and it was possible to distinguish between fast electrons and penetrating particles, by means of the cascade showers initiated in the plates. Both these types of chamber had disadvantages. In the magnet chamber, the probability of an interaction occurring in the gas is very small. In the multiplate chamber, interactions will take place in the plates, but full details of these are not visible. It was decided to use a third type - the high pressure chamber. In such a chamber, the probability of an interaction in the gas is increased by the greater density, and full details of any such interaction would be visible. It was intended to study interactions in the gas and it was hoped that examples of neutral mesons originating in an interaction in the gas would be found. In addition it was suspected that the two types of neutral meson mentioned above were always produced in association[11] and examples of this associated production were looked for. A third possibility

was that, in favourable cases of the decay $V^o \rightarrow p^+ + \pi^-$, the proton could be stopped in the chamber. If in addition, its origin, in a star in the gas, or an interaction above the chamber, could be determined, the dynamics of the decay could be very accurately explored, with the possibility of establishing the presence or absence of neutral secondaries in the decay scheme.

Examples of all these types of events have been
12 obtained[12]. Due to the low frequency of penetrating showers at sea level, it was necessary to carry out the experiment at mountain altitude. Facilities for the experiment were made available at the cosmic ray research station at La Marmolada (altitude 2040 metres) in the Italian Dolomites, through the generosity of Professor Rostagni of Padua University, and the directors of the Societa Adriatica di Electricitta.

Since 1953 many advances have been made in the knowledge of the heavy charged mesons, especially since the advent of the artificially produced heavy mesons in America. New types of meson have been discovered and the decay schemes and lifetimes have been elucidated. The present position will be summarised in a later chapter.

Section B - The Wilson Cloud Chamber.

The Wilson Cloud Chamber, since its invention by

C.T.R. Wilson in 1912, has proved to be an exceptionally fruitful tool in many fields of nuclear physics. In recent years, very many experiments, using some form of cloud chamber, have been carried out in the field of cosmic radiation. The cloud chamber utilises the principle that, in a volume which is supersaturated with vapour, condensation of the excess vapour can only occur if nuclei, upon which the drops can grow, are present. In normal circumstances, any volume of gas contains numerous dust particles, many of them too small to be seen, and these dust particles form the required condensation centres. It is possible to remove all such dust particles, by repeatedly producing condensation on them, and allowing them to be carried to the foot of the volume by the falling drops. In such a "clean" gas, it is difficult to cause condensation when a supersaturated condition is produced.

The supersaturation condition is produced by cooling a mass of gas, saturated with some suitable vapour, by an adiabatic expansion. In the fundamental experiments carried out by C.T.R. Wilson between 1897 and 1899, it was shown that condensation could occur even in a "clean" gas. He showed that there were two critical values of supersaturation, corresponding to two different types of condensation centre. At the lower critical value, described by Wilson as "the limit

of rain-like condensation", condensation took place on gaseous ions as nuclei. Whether the vapour condensed on the positive or on the negative ions at this limit depended upon the condensant used. If condensation occurred, say, on the positive ions, a slight increase in the supersaturation was necessary before condensation would occur on the negative ions as well. Under these conditions, the number of drops formed was small, and the drops were large enough to be seen individually. At the higher critical value - the limit of cloud-like condensation - the condensation nuclei are uncharged aggregates of gas molecules.

If the degree of supersaturation produced is such that condensation occurs only on charged ions, and if an ionising agent, such as an α-ray from a radioactive element, passes through the volume while the supersaturation condition persists, then ions will be formed in a very localised region near the path of the α-ray, and the resultant condensation on the ions will form a well defined track. If the conditions of the expansion are suitable, this track will stand out clearly, against the background of rain-like condensation, and may be easily photographed.

In any volume of gas and vapour, used in this way, gaseous ions will be formed constantly, whether there is a supersaturation condition present or not. In the

absence of condensation, such nuclei can diffuse well away from the position at which they were formed. At any subsequent establishment of supersaturation, condensation will occur on such nuclei, as well as upon well defined tracks. Since they have diffused away from the trajectory of the original ionising agent, no information can be obtained from them, and they merely contribute to the background condensation. Such "old" nuclei are removed by an electrostatic field - the clearing field.

After an adiabatic expansion, and the production of condensation on tracks, nuclei which are efficient condensation centres, even at low degrees of supersaturation, are found to be present. These are generally considered to be drops of the original condensation, which have re-evaporated to such a size that they cannot be seen by eye. These drops will be slow to fall out due to their small radii, and are removed by subsequent non-adiabatic expansions, known as slow or cleaning expansions.

The commonest type of cloud chamber is the volume defined chamber. In this the adiabatic expansion is produced by the movement of a piston in a geometrically defined manner. At each expansion, a definite volume change is produced. The degree of supersaturation produced is related to the <u>expansion ratio</u> of the

chamber. This is defined as the ratio of the volumes of the gas-vapour mixture, before and after the expansion.

Many types of chamber have been operated successfully. The particular chamber used in the present work will be described in the next chapter.

Chapter II.

THE HIGH PRESSURE CLOUD CHAMBER.

The high pressure chamber occupies a position between the conventional chamber, and the nuclear emulsion. The higher density of the gas gives an increased probability, as compared to the atmospheric pressure chamber, of a nuclear interaction occurring in the gas, while retaining the advantage of being able to see the full details. The chamber used for the experiment at La Marmolada was operated with argon, filled to a pressure of 75 atmospheres. Under these conditions the density of the gas is 0.135 gm./c.c. This is to be compared with the density of the nuclear emulsion which is approximately 4 gm./c.c. While this density, and consequently the probability of an interaction, is much higher, the labour of scanning for interactions is very great in the emulsion. This offsets to some extent the advantage of the high density.

The large thermal capacity of the gas filling gives the high pressure chamber a long sensitive time - approximately 2 seconds. This makes it possible to photograph each expansion twice. The additional scanning time of the random cosmic ray beam thus available has made it possible to examine the single scattering of high momentum cosmic rays as a side product of the

primary, penetrating shower, experiment. Other characteristics of the high pressure chamber are the much greater ionisation, causing even minimum ionisation tracks to be continuous; the lower expansion ratio that is necessary - due to the change of surface tension, and the ratio of specific heats of the condensant with pressure; the long recovery time of the chamber, which is of the order of 12 minutes, the reasons for this being discussed in Chapter VII; and the length of time necessary to make the expansion.

The chamber used at La Marmolada is a volume defined chamber, in which the expansion is made by the movement of a thin rubber diaphragm whose two extreme positions are defined by brass plates in which a large number of small holes are drilled. Since this chamber has previously been described in detail[13] only a short description will be given here. The chamber is made of non-magnetic stainless steel and is cylindrical in shape. The internal diameter is 20 cm. and the depth is also 20 cm. The walls are 5.5 cm. thick. Illumination for photography is provided through two small ports of 2.5 cm. thick armour plate glass. The photograph is taken through a window of the same material, of diameter 11.0 cm. and 3.5 cm. thick.

In order that events could be reconstructed in space, they were photographed stereoscopically. The

stereoscopic angle was 15°, and the lenses used were Dallmeyer Anastigmats, of focal length 35 mm. Due to the small window through which the photograph was taken, it was necessary to place the camera close to the chamber, otherwise a large part of the useful volume was not photographed. In order to obtain the necessary depth of focus, the maximum aperture that could be used was f/11, and the majority of photographs were obtained with this aperture.

It was found necessary to control the temperature of the surroundings to a high degree. The laboratory was thermostatted, but, since there was no provision for the extraction of heat, during the day, the temperature frequently rose above the set temperature. A fibre board hut was built round the chamber, and this was thermostatted separately. Heat was continuously extracted from the enclosed volume, by circulating water at 4°C through a radiator, through which air was drawn by a fan. The thermostat was a mercury thermometer with an electric contact built through the glass which controlled the operation of a heater. The temperature of the hut could be maintained stable to within 0.5°C and the necessity of changing the expansion ratio as the temperature changed was completely avoided. The usual temperature at which the chamber was operated was 15°C.

The control circuits were reconstructed by Mr. P. Baxter of University College, London. These circuits, on receipt of a pulse from the counter selection circuits, expanded the chamber, removed the clearing field, and after suitable delays took two photographs of the expansion. The repumping operations, cleaning cycle, winding on of the camera between expansions and the resetting of the chamber at the end of the recovery period were carried out manually by the operator.

The chamber was controlled by Geiger counters. Various selection systems were used. In the main, two trays of Geiger counters were used, one immediately above the chamber and the second some distance below the chamber. Lead could be placed above the top tray of Geiger counters and it was intended that the selection system would bias in favour of nuclear interactions occurring in this lead block. For the greater part of the experiment the thickness of this block was 10 cm. The disposition of the lead was as shown in the diagram. For short runs, thicknesses of 5 cm. and zero cm. were used for the top block.

The circuitry associated with the Geiger counters was very flexible, and was completely redesigned and built by Mr. A.J. Metheringham of University College, London. These circuits were assembled and tested at the mountain by various members of the group. Each

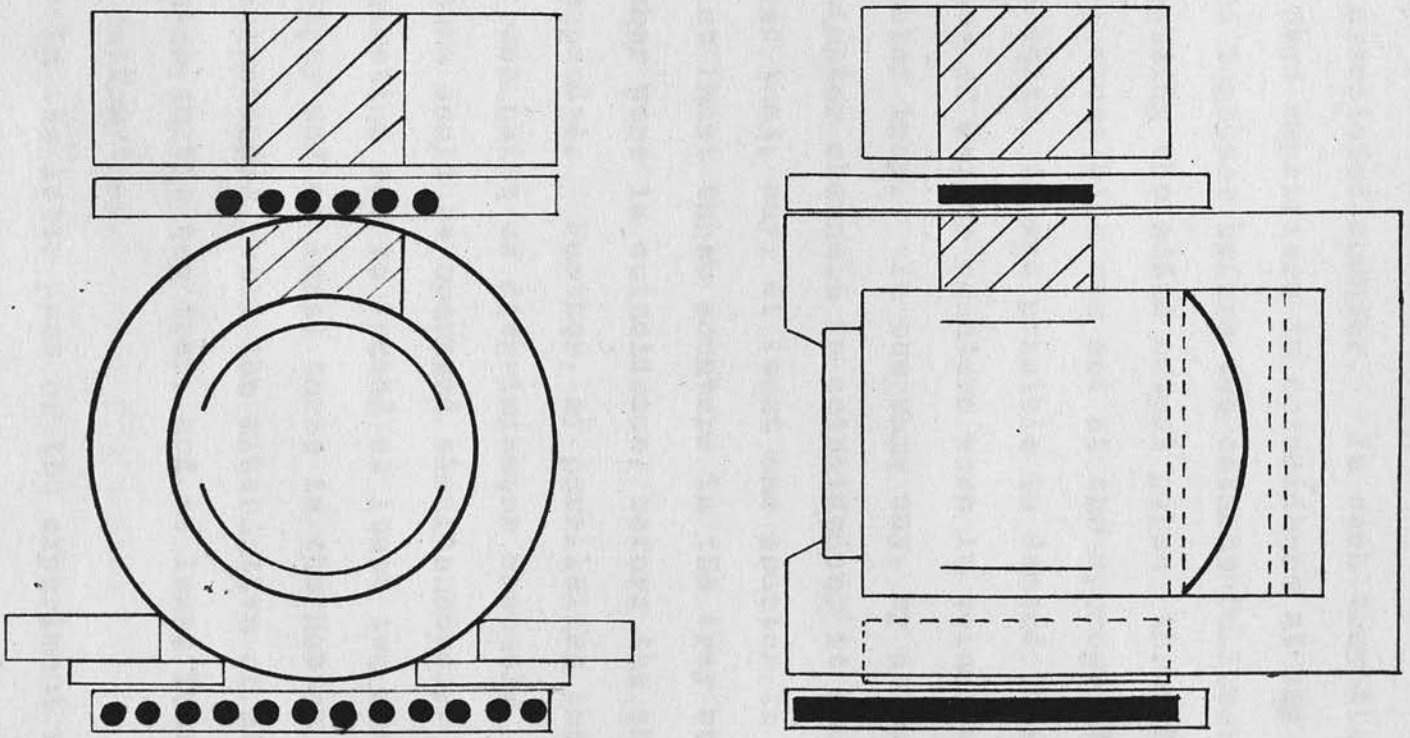

Figure 1. Diagram of the disposition of the lead and Geiger counters during the greater part of the Marmolada experiment. Scale 1 cm. = 5 cm.

counter had a separate head amplifier which gave a square pulse of amplitude 5 volts at each pulse from the associated counter. In each tray the pulses from all head amplifiers in coincidence at any instant were added together before the cathode-follower output stage. By passing the added output pulse through a discriminator, whose bias was set at the appropriate multiple of 5 volts, it was possible to demand that a given number of Geiger counters were in coincidence, in any selected tray. In the same way, by using two discriminator channels in coincidence, it could be required that, say, at least one counter in the top tray and at least three counters in the tray below the chamber were in coincidence, before the chamber would be expanded. Further, by paralleling the inputs of two such pairs of discriminator channels, two selection systems could be operated simultaneously. A common combination was to demand at least two counters in the top tray and at least three in the bottom tray to be in coincidence, with the alternative of at least one counter in the top tray, and at least four counters in the bottom tray.

In the later part of the experiment an even more flexible system was introduced, in order that information as to the merits of various counter selection systems could be obtained more quickly. The pulses

from the two trays were fed into a pulse adding amplifier, before being connected to the discriminator. By using three discriminator channels in coincidence, the chamber could be triggered by any five-fold coincidence, provided that at least one counter had counted in each tray.

The Geiger counters used were made at University College, London. They were of the external cathode type. This type of counter has the advantage that the length of the counter may be easily varied, and it was intended that Mr. A.J. Metheringham's investigation of counter selection systems should include the effect of varying the length. The counters were of diameter 2 cm. Those used in the top tray were 6 in. in length in the early work, and 4 in. in the later work. The counters used below the chamber were 9 in. long.

It will be seen that the selection system used was, in its general principle, very similar to that used by other workers in the field, who were using chambers at or near atmospheric pressure.

It was decided by Dr. G.R. Evans and the writer that this type of selection system was not adapted to the special case of this high pressure chamber. Owing to the massive steel walls of the chamber, it is not possible to concentrate the greater part of the star producing material in a position from which the

particles of the star are likely to pass into the useful volume of the chamber. Reference to figure 1 will show that the most favourable position for a star to be produced is in the shaded volume. For the dimensions shown, this gives a mass of approximately 41 kgm. within the favourable volume, as opposed to 84 kgm. elsewhere. Even these figures are too optimistic, since the useful volume of the chamber does not extend for the full depth of 20 cm. In addition the mass of steel and brass forming that part of the chamber behind the diaphragm has not been included in the calculation, even though stars produced there might set off the selection system.

Apart from interactions in the lead block above the chamber, there are three main types of event which can trigger the selection system used.

(a) Interactions in the "wrong" part of the distributed mass; i.e. those stars whose geometry make it unlikely that many particles will be seen in the chamber.

(b) Electron showers produced in the lead above the chamber. The particles of these showers will be stopped by using a sufficient thickness of lead (the radiation length in lead is 0.52 cm.). However, the stopping of the electrons will create many γ-rays by the brehmsstrahlung process. These γ-rays are difficult to absorb (absorption coefficient $\simeq$ 0.4/cm.) and

may trigger the Geiger counters below the chamber. That this type of event does occur is shown by photographs which contain no penetrating, counter-controlled particles, but many photoelectrons, Compton electrons and electron pairs (see figure 2a).

(c) Knock-on showers produced by fast μ -mesons (see figure 2b).

Clearly (b) might be remedied by placing much more lead above the chamber. This would also make the solid angle subtended by the chamber very much smaller, with respect to the desired type of interactions, taking place high up in the lead. It was considered that it was not worth putting more than 10 cm. of lead above the chamber. It would also be possible to reduce events of type (b) by putting more lead below the chamber, but only at the cost of increasing the number of events of type (c). Since a large proportion of those photographs, which do not show evidence of a nuclear interaction near the chamber, contain only one counter-controlled penetrating particle, events of type (c) are already numerous.

It was thought that it might be possible to use the different geometrical development of the various types of events to distinguish between them. Even in a nuclear disintegration of high energy the angular divergence of the star particles from the direction of

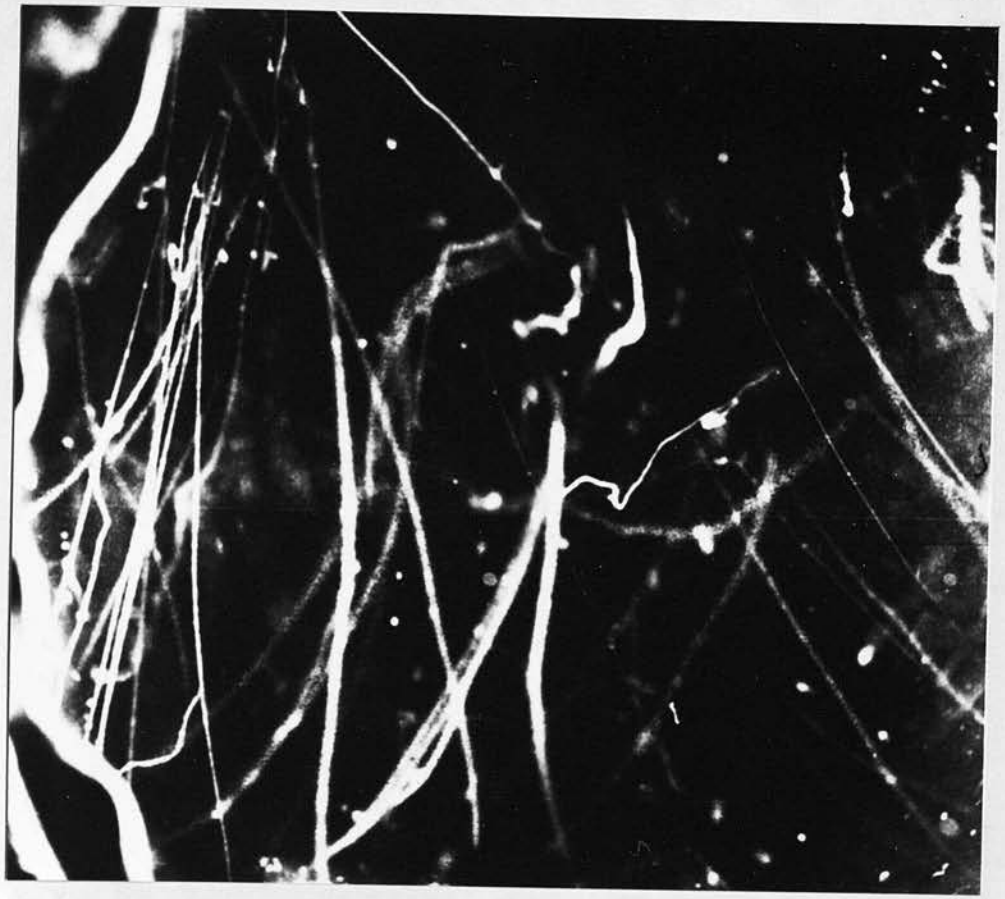

Figure 2a. Example of a knock-on shower which has triggered the selection system.

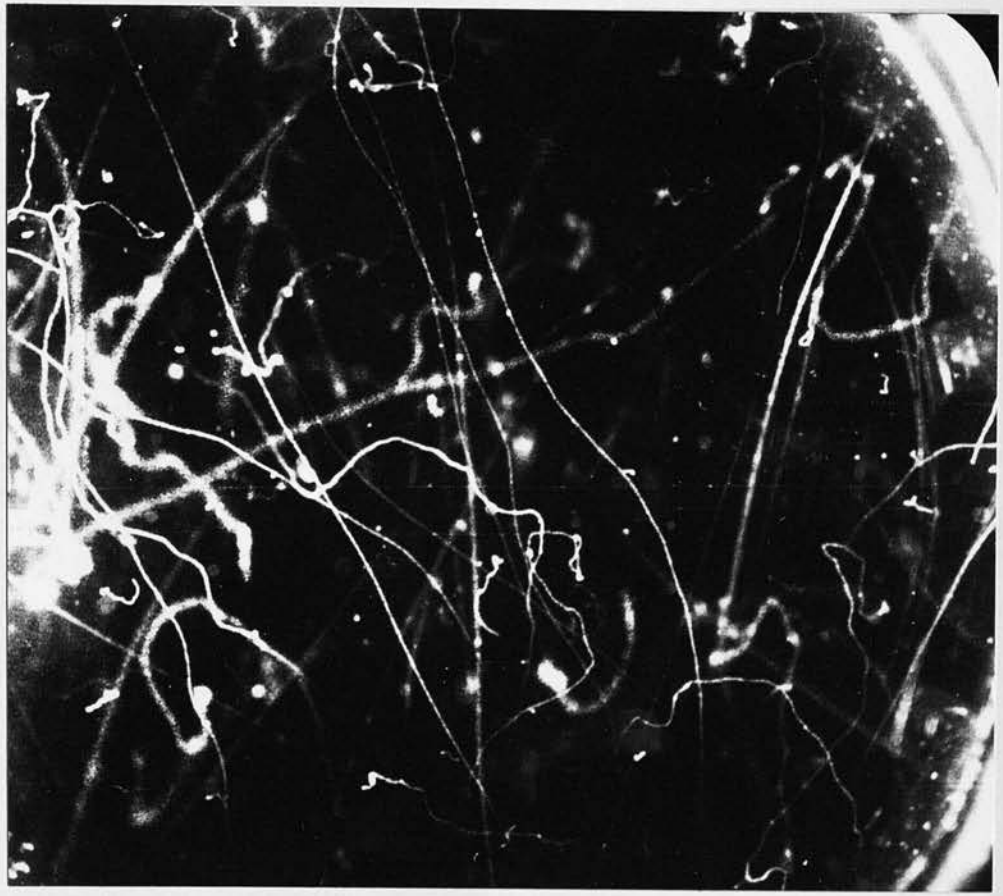

Figure 2b. Example of an event where the Geiger counters below the chamber have been triggered by γ-rays.

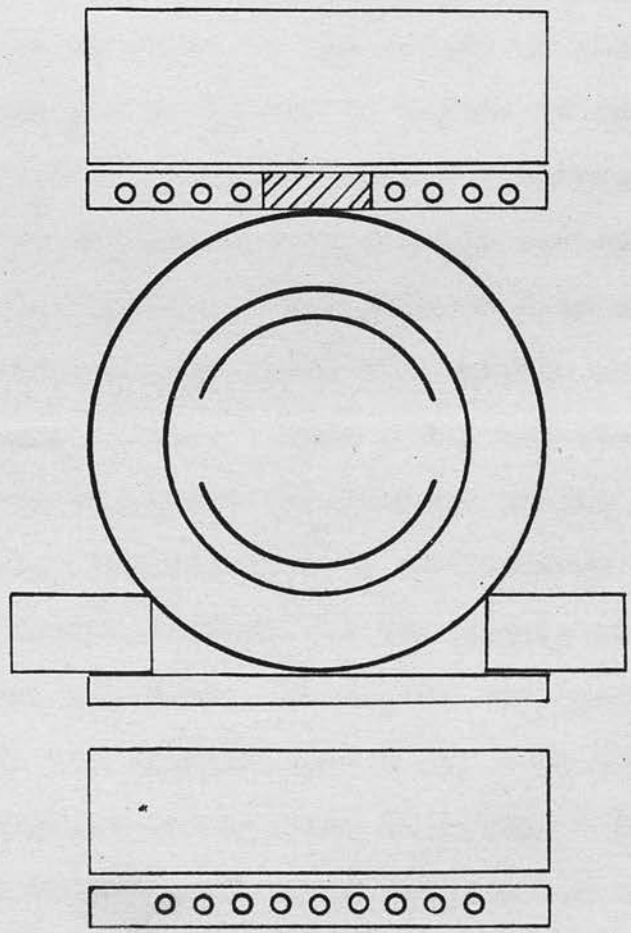

Figure 3. Disposition of lead and Geiger counters for the "split-tray" selection system. Scale 1 cm. = 5 cm.

the incident primary particle may be large, for example see figure 13. In general a small knock-on shower follows the direction of the primary particle quite closely. If, therefore, the selection system demands that an event shall trigger counters in two trays, each on the same horizontal level, that horizontal level being close to the origin of the interaction, there should be a bias in favour of the greater angular spread of the desired nuclear interaction.

The counter system finally devised is shown opposite in figure 3. Two sets of four 4 in. long counters, were placed above the chamber on the same horizontal level. Each group had its own output circuit and was quite independent of the other. In order to reduce the probability of knock-on showers giving coincidences between the two groups they were separated by 7 cm. of lead. To ensure that particles passed through the chamber nine 8 in. long counters were placed below the chamber as shown. The selection system demanded at least one counter from each of the three groups to be in coincidence. In all, 277 photographs were obtained with this system. The analysis of these photographs is compared below, with that of the same number of photographs taken on the more conventional system.

In the "Events" column have been tabulated the

Table 1.

Selection System used	Locally produced penetrating showers	Electron Showers	Blank Photographs	Photographs containing 1 counter-controlled penetrating particle	Events
"Split Tray"	31	26	74	66	8
"Conventional"	27	15	45	81	8

number of stars in the gas, plus the number of decays of all varieties.

Comparison of the two sets of figures show that the new system is no better than the old. As was to be expected, the number of photographs containing only one counter-controlled penetrating particle has decreased significantly in the new system. These photographs are presumed to be examples of triggering of the chamber by knock-on showers and, to this extent, the arguments behind the new system appear to be sound. This decrease is compensated by an increase in the electron shower, and "Blank" categories. The "Blank" photograph is presumed to be one where the counters have been triggered by γ-rays, and most of the electron showers observed must have also triggered the tray of Geiger counters under the chamber in this way, since the electrons would have to pass through 7 cm. of lead and 5.5 cm. of steel in order to reach the counters. The figures suggest that, of the various types of event which can satisfy the counter selection system, only a very small proportion is of the type desired. In this case it would be impossible to devise a selection system, using Geiger counters only, which would be much more efficient than the conventional penetrating shower detector. Additional information, such as would be provided by scintillation counters, proportional

counters, or Cerenkov counters, would be necessary, if a more efficient system were to be devised.

Unfortunately, it is not possible to compare the number of penetrating showers detected per hour, by the two selection systems. During the taking of the 277 photographs with the split tray system, there was an intermittent fault in the power pack supplying E.H.T. to the Geiger counters. This had the effect of putting the Geiger counters out of operation during parts of the sensitive period and, consequently, the true average counting rate with this system cannot be determined. It is suspected that the average counting rate was less than that of the conventional system. If this is so the split-tray system was less efficient than the other.

Chapter III.

METHODS OF ANALYSIS.

In all the work done with the photographs taken at La Marmolada, measurements have been made on a reprojection apparatus. This was designed by Dr. G.R. Evans and built in the workshop of the Department of Natural Philosophy, Edinburgh.

The film is placed in a reprojection head, which is an exact replica of the camera in which the photograph was taken. The film is illuminated from behind, through a plate of ground glass. In order to improve the intensity of illumination, the rear part of the camera was cut away, leaving only the lenses and the film gate. To prevent distortion of the film, because of heating from the lamp illuminating it, a fluorescent tube dissipating only 15 watts was used. This was found to be quite satisfactory.

The film was held flat in the film gate by pressing a plate of ground glass, cut to a suitable shape, against it by means of a spring clip. In the original camera in which the photograph was taken, this was replaced by an ebonite pressure plate. The lenses in the reprojection head were a matched pair of Dallmeyer, 35 mm. focal length, lenses. This pair was also matched to the pair used in the camera. It would have

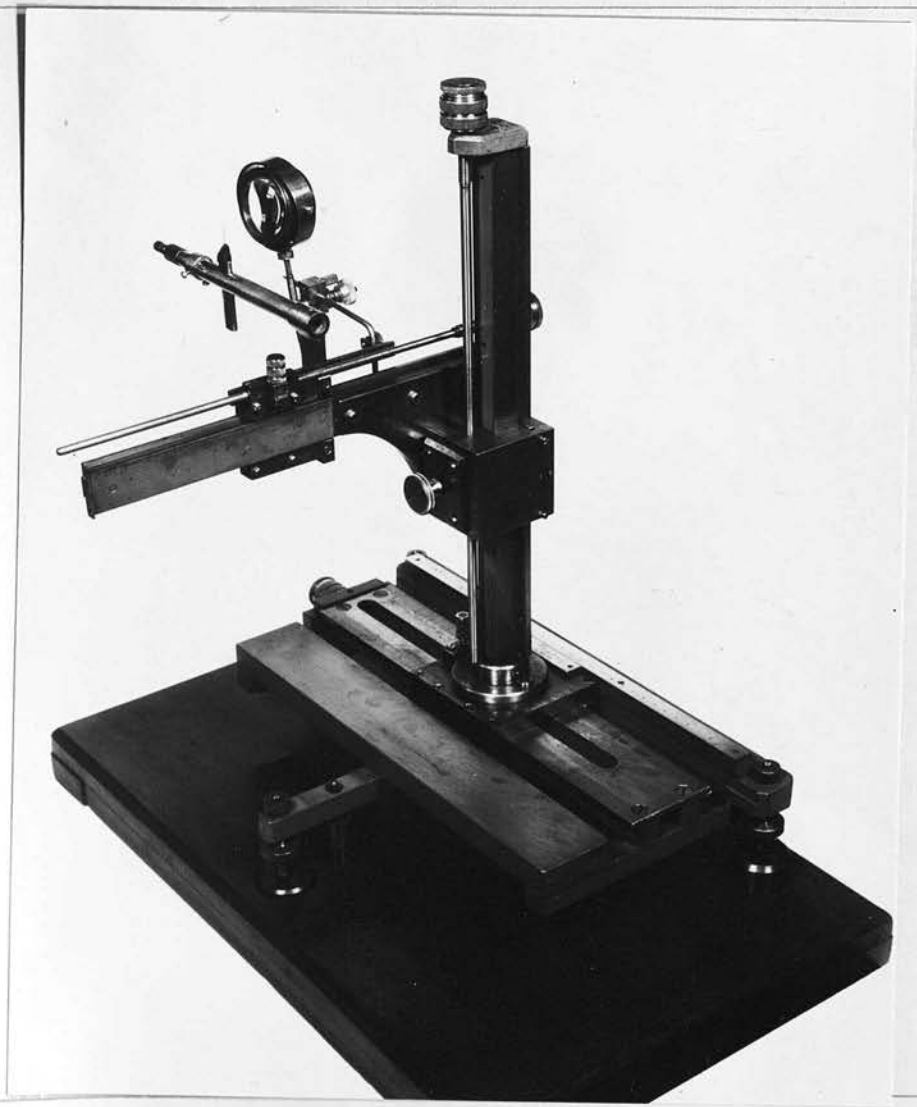

Figure 4a. The reprojection apparatus (the reprojector).

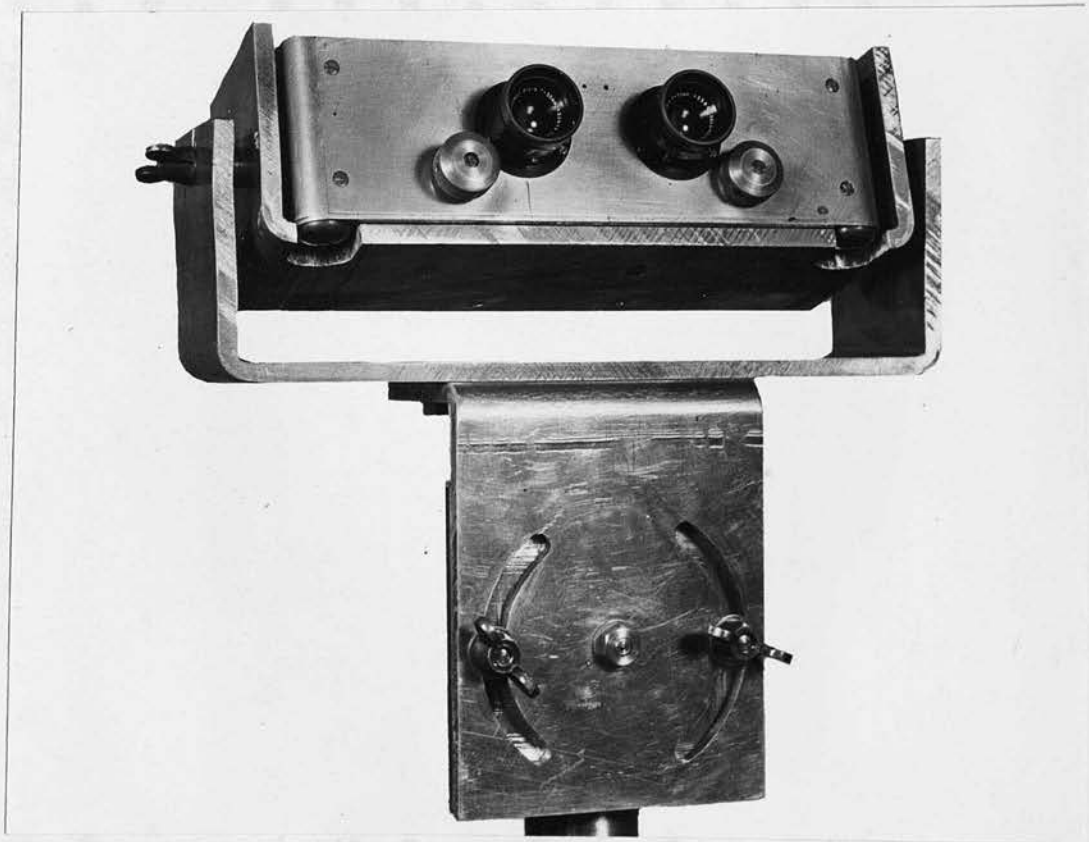

Figure 4b. The reprojection head, showing the independent rotations of the camera.

produced by the stereoscopic pair.

Before measurements could be taken, it was necessary to replace the film in the same position, relative to the lenses, as it had occupied when the photograph was taken. This was done by selecting some prominent point, such as the end of a stopped track or a δ -ray, and attempting to set the pin on it. If the film was not correctly placed, it would be found that the best position obtainable was one in which the pin coincided with the point in one image and appeared to be vertically above or below it in the other. The film could then be raised or lowered slightly, until the pin coincided with the chosen point in both images. When this was achieved, the film had been replaced in its original position.

This reprojector is very accurate and easy to use. To test its accuracy, a piece of perspex, with some straight lines ruled on it, was photographed and the lengths of the lines and the angles between them measured on the reprojector, and compared with the original. It was found that the ranges agreed to 0.01 cm. and the angles to 10 minutes of arc. The perspex had been deliberately photographed under poor illumination conditions and slightly out of focus, so that it would represent measurements on a track in the most difficult part of the chamber. When the pin was

repeatedly set on some fixed point, the x- and y-coordinates were reproducible to within 0.003 cm. and the z-coordinate to within 0.005 cm. The average value of a number of such settings was reproducible to within 0.001 cm. and 0.002 cm. respectively. If the film were removed from the camera and then replaced, the absolute values of the coordinates changed by quite large amounts, but ranges and angles were the same as before, within the accuracy of measurement.

In analysing an event, two types of information can be obtained. The first is the geometry of the event, i.e. the angles and ranges involved. This in general is used to detect the association of the event with any other tracks in the photograph, though in favourable cases the range may be used as a measure of energy, and the angles must be known for checking the consistency of an event with, say, a neutral decay. The events of interest are frequently produced in penetrating showers. In favourable cases, i.e. those which are produced fairly near the chamber, the point of origin can be accurately determined and, where applicable, coplanarity of the event with the origin established to within 0.5°.

The second type of information required is that leading to knowledge of the momentum and velocity, and hence the identity of a particle. If a particle stops

in the chamber, its range can be used as a measure of its energy. In general this is not available and the momentum is measured by means of multiple scattering. This can be measured directly from the film, allowing for the change in magnification with position, and for the effect of the conical projection of the lenses[14]. This procedure is both long and tedious, and a method of multiple scattering in space was developed instead. The mounting of the reprojector head was modified so that it could be rotated independently about the x- and z-axes of the reprojector, and the mounting of the fluorescent lamp was also altered so that it could rotate about the z-axis. This ensured that the film could be adequately illuminated in any position.

When the film had been correctly placed in the reprojector, the track, whose momentum was to be measured, was brought to a vertical position in space, by suitable rotations of the reprojector head. When this had been done, the pin, once it had been set on the track, would automatically follow the track in space, by simply moving it up and down the vertical y-axis (apart from small deviations due to the multiple scattering considered). One lens was then covered up. The line joining the pole of the remaining lens to the x-y plane was not, in general, perpendicular to that plane. The position of the reprojector head as a

whole was adjusted until it was perpendicular. This arrangement gives the maximum sensitivity (see figure 5). Since rotation of the reprojector head about the x-axis would raise or lower the position of any given point on the track with respect to the pin, and perhaps would remove it from the range of positions available to the pin, the stand supporting the reprojector head was made of adjustable height. The pin mount also carried a micrometer screw by which the pin could be moved a total distance of 0.5 cm. parallel to the x-axis.

When the track had been brought to the desired position in space, as described above, the x-coordinates of points on the track, separated by a fixed vertical interval (usually 0.25 cm.), were recorded. The momentum was calculated from the second differences of these coordinates, using the method developed by Fowler[15].

The relation connecting the multiple scattering and the momentum was derived by assuming that the relation given by Williams, and extended by Moliere[16], can be applied to the gas of the chamber. This yields that the mean projected deflection $\overline{\phi}$ in traversing a thickness t is

$$\overline{\phi} = \delta \times \lfloor \qquad \text{——————} (1)$$

where for argon at 75 atmospheres and 0°C

$$\lfloor = 1{\cdot}45 + 0{\cdot}80 \left(\log_e \frac{285\, t}{\beta^2 \cdot 0{\cdot}056} \right)^{1/2} \qquad \text{——————} (2)$$

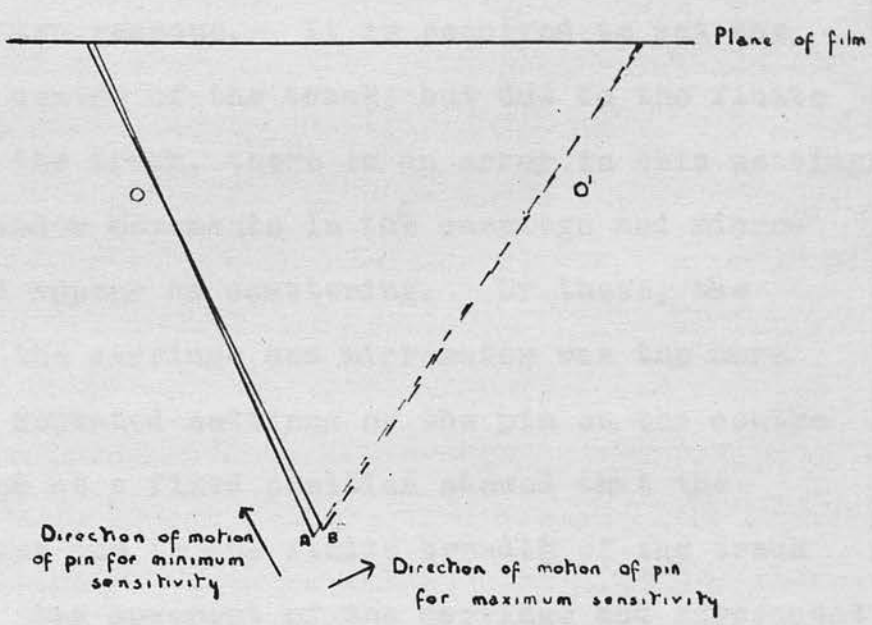

Figure 5. Diagram illustrating the condition for maximum sensitivity in making multiple scattering measurements in space. O and O' represent the poles of the stereoscopic pair of lenses, and A and B are the edges of the track in question. The diagram is not drawn to scale and is drawn assuming lens Oisto be used in the measurements.

and $$\delta = \frac{0.233\, t^{1/2}}{p\beta} \qquad \text{(3)}$$

where t is in cm., $p\beta$ in MeV./c and βc is the velocity of the particle.

In practice, it is not possible to measure $\overline{\phi}$ directly. The result calculated from the coordinates is a superposition of the true mean deflection and a spurious mean deflection due to "noise". This noise arises for two reasons. It is required to set the pin on the centre of the track, but due to the finite breadth of the track, there is an error in this setting. Secondly random movements in the carriage and micrometer would appear as scattering. Of these, the "noise" in the carriage and micrometer was the more serious. Repeated settings of the pin on the centre of the track at a fixed position showed that the average noise due to the finite breadth of the track was 12μ. Any movement of the carriage and subsequent resetting to the original position raised the noise level to 30μ. Since the carriage must be raised or lowered between readings on successive points, this noise could not be avoided. That this noise should exist is not surprising. The reprojector was not originally designed for this work, and the location of the carriage on the rails, upon which it slides, is not kinematic.

The upper limit to the momentum that can be

usefully estimated is set by this noise level. The noise is eliminated from the calculation in the usual manner. If the errors are distributed normally, it is easily shown from equations (1), (2) and (3) that the true mean square scattering angle for unit cell length is given by

$$\overline{\phi^2} = \frac{\overline{D_2^2} - \overline{D_1^2}}{t_2^3 - t_1^3}$$

where $\overline{D_2^2}$ and $\overline{D_1^2}$ are the mean square second differences, for cell lengths t_2 and t_1 respectively. Also the noise ε is given by

$$2\varepsilon^2 = \overline{D_1^2} + \overline{D_2^2} - \frac{(\overline{D_2^2} - \overline{D_1^2})(t_1^3 + t_2^3)}{(t_2^3 - t_1^3)}$$

17 It has been shown by Biswas, George, and Peters[17] that the best choice of cell length is such that the signal-to-noise ratio $\nu = \frac{\overline{D^2} - \overline{\varepsilon^2}}{\varepsilon^2} = 5.8$. In this case, the standard error in the root mean square second difference is $0.9/N^{\frac{1}{2}}$ where N is the number of independent cells in the length of track measured. If overlapping cells are used, as was done in this work, this becomes $0.78/N^{\frac{1}{2}}$.

It was assumed that at small cell lengths such as 0.25 cm., the measured scattering was entirely due to noise. A cell length giving a signal-to-noise ratio of $\simeq 6$ could then be selected, and the true mean square scattering angle calculated. In order that formula (1)

should apply, two corrections must be made. The right hand side must be multiplied by $\sqrt{\frac{\pi}{2}}$ since the root mean square scattering angle is used, not the mean scattering angle. Secondly since the scattering angle has been found as the mean angle between successive chords, instead of that between successive tangents, the right hand side of (1) must be multiplied by $\sqrt{\frac{2}{3}}$. Corrections for any deviations of temperature and pressure from those used in the calculation of (1) were also made.

With a counter-controlled track, it was possible to measure momenta equivalent to a value of $p\beta$ = 150 MeV/c. This gave a standard error of 30%. With post-expansion tracks it was possible to reach values of 300 MeV/c. As in emulsion work, a "cut-off" is applied so that all differences greater than four times the mean are taken to be four times the mean.

The methods described here are much more rapid than the measurements made directly off the film. A typical time for the whole process from inserting the film in the reprojector to the final calculation of $p\beta$ and the associated error is ninety minutes, as opposed to some four hours using the direct method. The accuracy of the two methods is comparable due to the larger relative effect of a small error in the film measurements.

To identify a particle, the velocity as well as

the momentum must be known. It is possible to estimate the velocity from the number of δ -rays on a track. The average number of δ -rays per cm. of track is given by $N = \frac{c}{\beta^2}\left\{\frac{1}{E_{min}} - \frac{1}{E_{max}}\right\}$ where c = 0.0172 under the conditions used. If the δ -ray count is done visually, care must be taken in deciding what is to be accepted as a δ -ray. Due to this, and the poor statistics in the track length available, this is not a reliable method for calculating β . It is of value, however, in distinguishing between fast and slow tracks. This will be used in the discussion of a particular event later (see page 60).

A much more reliable method is that of track width. Blackett, and later, Valley and Vitale, have deduced the equation

$$\frac{\omega^2 - \omega_0^2}{16D\tau} = \log_e \frac{I}{I_0}$$

where ω and ω_0 are the track widths at ionisations I and I_0 respectively. D is the diffusion coefficient of ions in the gas, and τ is the expansion time.

This technique has been applied successfully to
18 tracks in the high pressure chamber by Williams[18] who has discussed the difficulties of the method. The measurement of the width is carried out in space, so as to avoid the difficulty of change of magnification with depth in the chamber, using the reprojector previously described.

It is also possible to calculate the velocity β of a particle from the range and angle θ of ejection of a δ -ray from

$$\beta \cos\theta = \frac{pc}{E + mc^2}$$

where p and E are the momentum and total energy of the δ-ray and m is the mass of the electron. The above equation holds if the energy of the incident particle is much greater than mc^2. It is not easy to use this, since to measure the angle accurately at least 2 mm. of track is required and even in this length multiple scattering is appreciable.

In the next chapter, the methods described above will be used in the analysis of the photographs.

Chapter IV.

ANALYSIS OF THE PHOTOGRAPHS.

In all, 8993 counter controlled photographs were taken with the chamber at La Marmolada. Each one of these photographs was scanned by the present writer. The following details were recorded.

(a) The number of counter-controlled, unscattered tracks.

(b) Presence or absence of a shower, and of which type (when present).

(c) The number of high-momentum tracks, entering the chamber after the expansion.

(d) The presence of single scatterings in a high-momentum track.

(e) Interesting events such as stars in the gas, decays or unusual materialisation processes, for example direct pair production by a charged particle.

(f) Any event which could not be explained by one of the previous categories.

The more obvious fields of analysis, i.e. interactions in the gas[19], neutral decays[14], and electron pair distributions[20], had already been investigated by other members of the group. In the remaining part of this chapter the investigations of the following fields will be presented.

(1) The distribution of single scatterings of fast μ-mesons in the gas.

(2) The low-energy end of the μ-meson decay spectrum.

A. The Single Scattering of Fast μ-Mesons.

In recent years a considerable amount of work on this problem has been carried out. The original experiments of George, Redding and Trent[21], suggested that the μ-meson was scattered through large angles, more frequently than was predicted by coulomb scattering formulae. It was suggested that the increased scattering was due to the superposition of a nuclear scattering component, on to the coulomb scattering. Since previous experiments[4] with stopped μ-mesons had established that the μ-meson did not have a strong nuclear interaction, when at rest, this implied an interaction, strong only at high energies. Subsequent work showed that the "excess" scattering was not so great as previously suggested.[22, 23, 24, 25] The measured scattering distribution agreed well with that expected from a point nucleus (Rutherford scattering, corrected for screening of the nucleus). All these experiments were carried out underground, to filter out all penetrating particles other than μ-mesons. In most experiments the scattering took place in metal plates - mainly lead plates but later, experiments

were repeated using iron plates[24]. Because of this, it was not possible to examine the single scattering directly. The validity of the scattering law was tested by examination of the multiple scattering distribution in the plates at large angles. The distribution of multiple scattering under the assumption of a point nucleus has been calculated by Moliere[26], and that for a nucleus of finite size and uniform, spherical, charge distribution by Olbert[27]. The latter distribution is only a crude approximation since Olbert assumes that the nucleus scatters as if it were a point charge, up to a certain critical value of the angle of scattering, and that angles of scattering greater than this do not occur. Later in the work, theories for various charge distributions, including the case of the uniform sphere, have been given by Rose[28]. Since evidence from other methods shows that the charge is not concentrated at a point, it was reasonable to expect that multiple scattering distributions calculated on this basis would agree better with experiment, than that of Moliere. It was concluded that there was no evidence for excessive nuclear scattering of the μ - meson, but that there was a discrepancy between theory and experiment in the coulomb scattering and that this discrepancy was due to the lack of a sufficiently exact theory.

It was thought that the possibility of checking the true single scattering, available in the high pressure chamber, should be examined.

Since the primary, penetrating shower experiment was carried out at mountain altitude, some method of selecting μ-mesons was necessary. This was afforded by the long sensitive time of the high pressure chamber and the double flash system introduced to estimate distortion.

Particles in the photographs, which have entered the chamber later than those particles which triggered the counter selection system, are easily distinguished by their incomplete condensation, or in many cases, by their appearing only on the second photograph. With the delay times used, the reception time for such random tracks was approximately 600 milliseconds per expansion. In consequence, many such tracks are available for examination. Even at the altitude of the laboratory, the hard component of the random cosmic ray beam will be very largely composed of μ-mesons. A track was considered to be that of a μ-meson if it satisfied the following criteria.

(a) The track must be random, and must occur after the expansion.

(b) The track must show no sign of multiple scattering. This is equivalent to a value of $p\beta \geqslant$ 200 MeV./c.

(c) The track must not be associated in space with any other post-expansion track.

(d) There must be no sign of post-expansion electrons.

In all, 8805 such tracks were counted in the scanning of the photographs. The average length of random tracks in the chamber is 8.2 cm. This value was obtained from measurements on 100 tracks.

In order to calculate the expected scattering distribution, the momentum spectrum of the μ-meson beam must be known. Since no magnetic field was available with the high pressure chamber, the only other method for measurement of momentum is multiple scattering in the gas, and under condition (b) this could not be used. The momentum spectrum used in the calculation of the scattering distribution was obtained in the following way. The momentum distribution of μ-mesons at sea-level is known through the work of Blackett[30], J.G. Wilson[31] and others[32]. The momentum spectrum of the particles inside the high pressure chamber was deduced from that of J.G. Wilson, by correcting each momentum interval for the average energy loss in the atmosphere between sea level and altitude 2040 metres, and in passing into the chamber through the lead absorber and steel walls. The detailed steps of the calculation are as follows.

The range-energy relation for μ-mesons in air was

33 calculated, using the Bethe-Heitler formula[33], corrections being made for the variation of atmospheric pressure between sea level and the altitude of the laboratory, and for an assumed average temperature of 10°C. The average path length traversed was calculated from a knowledge of the variation of intensity with
34 zenith angle[34]. Then the energy lost, by particles in a particular momentum band, due to traversing this average thickness of atmosphere, was read off from the range-energy relation and hence the new momentum, corresponding to the considered interval of particles was found. In this way the momentum spectrum <u>outside</u> the cloud chamber was built up. The loss of μ-mesons by decay in flight, between the laboratory and sea level, may be neglected. In the time of flight, approximately 5% of the μ-mesons of energy 1 GeV would decay and correspondingly less for higher energies. The calculated peak outside the cloud chamber occurred at a momentum of 1400 MeV./c and consequently the major part of the spectrum will decrease in intensity by less than 5% due to this cause. In addition, μ-mesons will be created by the decay in flight of π-mesons, and this will offset to some extent the previously mentioned loss. The contamination of π-mesons in the random cosmic ray beam is estimated, from considerations presented later, to be 2%. The

momentum spectrum of μ -mesons thus created between sea level and La Marmolada is not known, and so no accurate correction for decays in flight can be made. It is considered that the net result will be small.

The calculation of the energy loss in passing through the 10 cm. lead absorber and the 5.5 cm. thick steel wall is more complicated, since the cylindrical shape of the walls of the chamber, makes the average path length of the μ -meson in the steel a function, not only of the angle the particle's trajectory makes with the vertical, but also of the horizontal distance from the centre of the chamber at which the path intersects the walls (see figure 6). Using the notation of the diagram, the average path length in steel is clearly given by

$$\bar{y} = \frac{\int_{\phi_1}^{\phi_2}\int_{\psi_1}^{\psi_2} \frac{y}{\cos(\psi+\phi)} \cos^2\phi \, d\phi \, d\psi}{\int_{\phi_1}^{\phi_2} \cos^2\phi \, d\phi \int_{\psi_1}^{\psi_2} d\psi} \qquad (1)$$

The first section of the double integral may be evaluated exactly

$$\int_{\phi_1}^{\phi_2}\int_{\psi_1}^{\psi_2} \frac{y}{\cos(\psi+\phi)} \cos^2\phi \, d\phi \, d\psi = y\int_{\phi_1}^{\phi_2} \cos^2\phi \, d\phi \int_{\psi_1}^{\psi_2} \frac{d\psi}{\cos(\psi+\phi)}$$

$$= \tfrac{1}{2} y \int_{\phi_1}^{\phi_2} \cos^2\phi \left[\log_e \frac{1+\sin(\psi+\phi)}{1-\sin(\psi+\phi)} \right]_{\psi=\psi_1}^{\psi=\psi_2} d\phi$$

This last integral was evaluated numerically using Simpson's Three-Eighths Rule with the interval of integration divided into twelve sections.

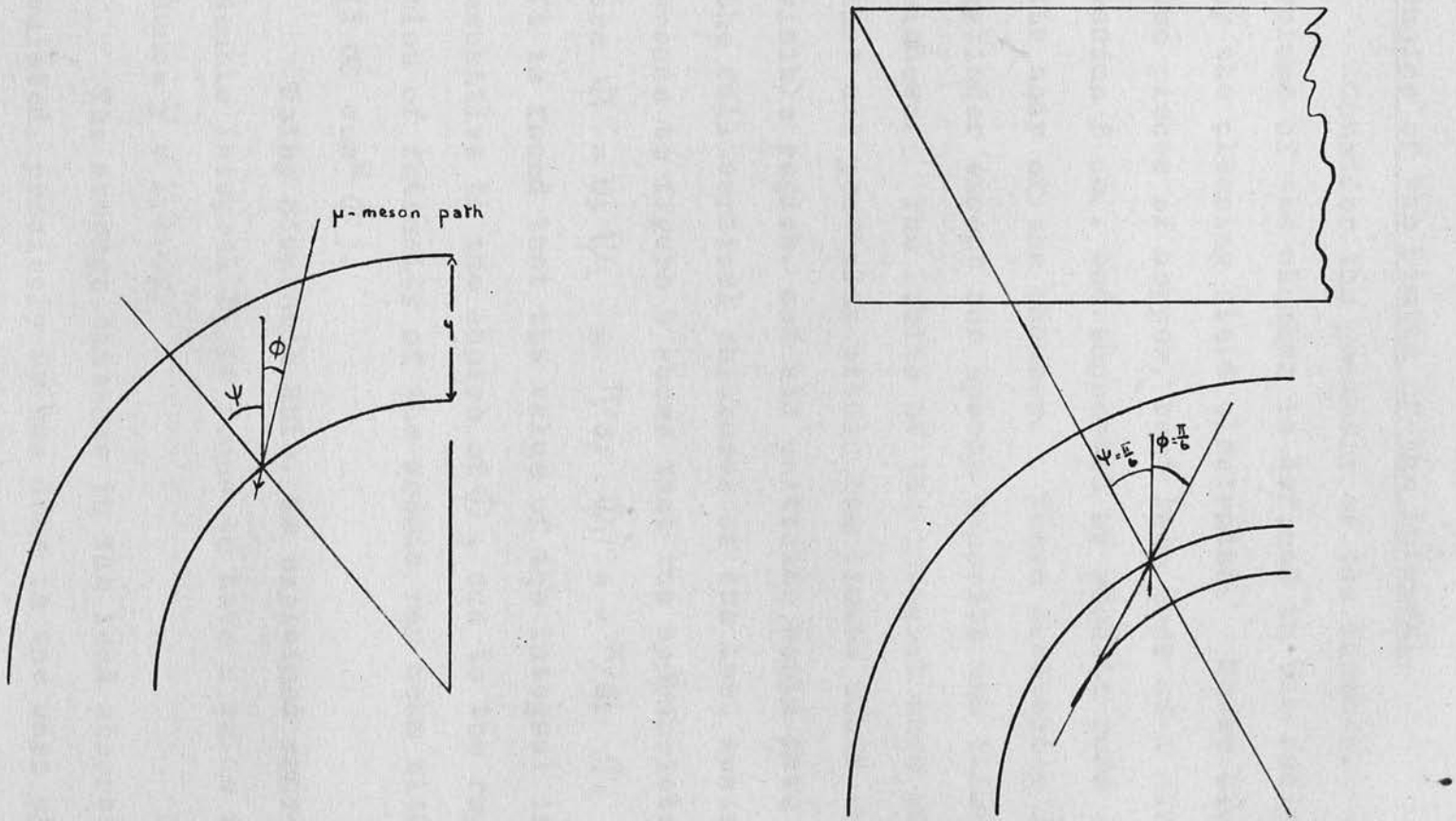

Figure 6. Diagram illustrating the dependence of average path length of μ-mesons in steel on the position of intersection of the meson trajectory with the chamber, and showing the choice of limits for the integral. Scale 1 cm. = 2.5 cm.

Choice of the Limits of the Integral.

Consider the geometry of the chamber. The useful volume of the chamber is defined in the radial direction by the clearing field electrodes. These consist of two pieces of copper, bent into arcs of a circle of radius 8 cm., and supported by ebonite rods screwed to the body of the chamber. These electrodes form a full cylinder except for spaces opposite the illumination windows. The limits of the integral were chosen so that all particles within the limits would enter the visible region, and all particles would have traversed the full vertical thickness of the lead absorber. Reference to figure 6 shows that the appropriate limits are $\psi_1 = 0$; $\psi_2 = \pi/6$; $\phi_1 = -\pi/6$; $\phi_2 = +\pi/6$. It is found that the value of the integral is not very sensitive to the choice of ϕ, due to the rapid variation of intensity of the cosmic ray beam with ϕ ($I \propto \cos^2 \phi$).

Using Simpson's Rule, as explained above, the double integral I_1 is found to have a value $2I_1 = 1.11y$. Hence $\bar{y} = 1.105y$.

The average distance in the lead absorber was calculated, precisely as was done in the case of the atmosphere. If the vertical thickness of the lead block is t cm. then the average path length is given by

$$\bar{t} = \frac{\int_0^{\frac{\pi}{6}} \frac{t}{\cos\phi} \cos^2\phi \, d\phi}{\int_0^{\frac{\pi}{6}} \cos^2\phi \, d\phi} \qquad \text{(2)}$$

The energy loss of the μ-meson beam in traversing these average distances was calculated from range-energy relations as previously explained.

The effect of multiple scattering in the lead block is treated as follows. Since the tracks considered are completely random, there is no loss of particles due to their being scattered away from the chamber. On average, as many will be scattered into the chamber as are scattered out. However, the extra path length in the lead and steel, will produce an extra energy loss, and this may distort the shape of the spectrum.

The mean angle of scattering suffered in traversing the lead and steel is

$$\bar{\Theta} = \frac{14960}{p\beta} \text{ degrees} \quad \text{where } p\beta \text{ is in MeV/c}$$

For $p\beta$ = 500 MeV/c $\bar{\Theta} \simeq 30^{\circ}$.

This corresponds to an extra path length of the order of 3 cm., and the energy lost because of this is approximately 30 MeV. In view of the assumptions

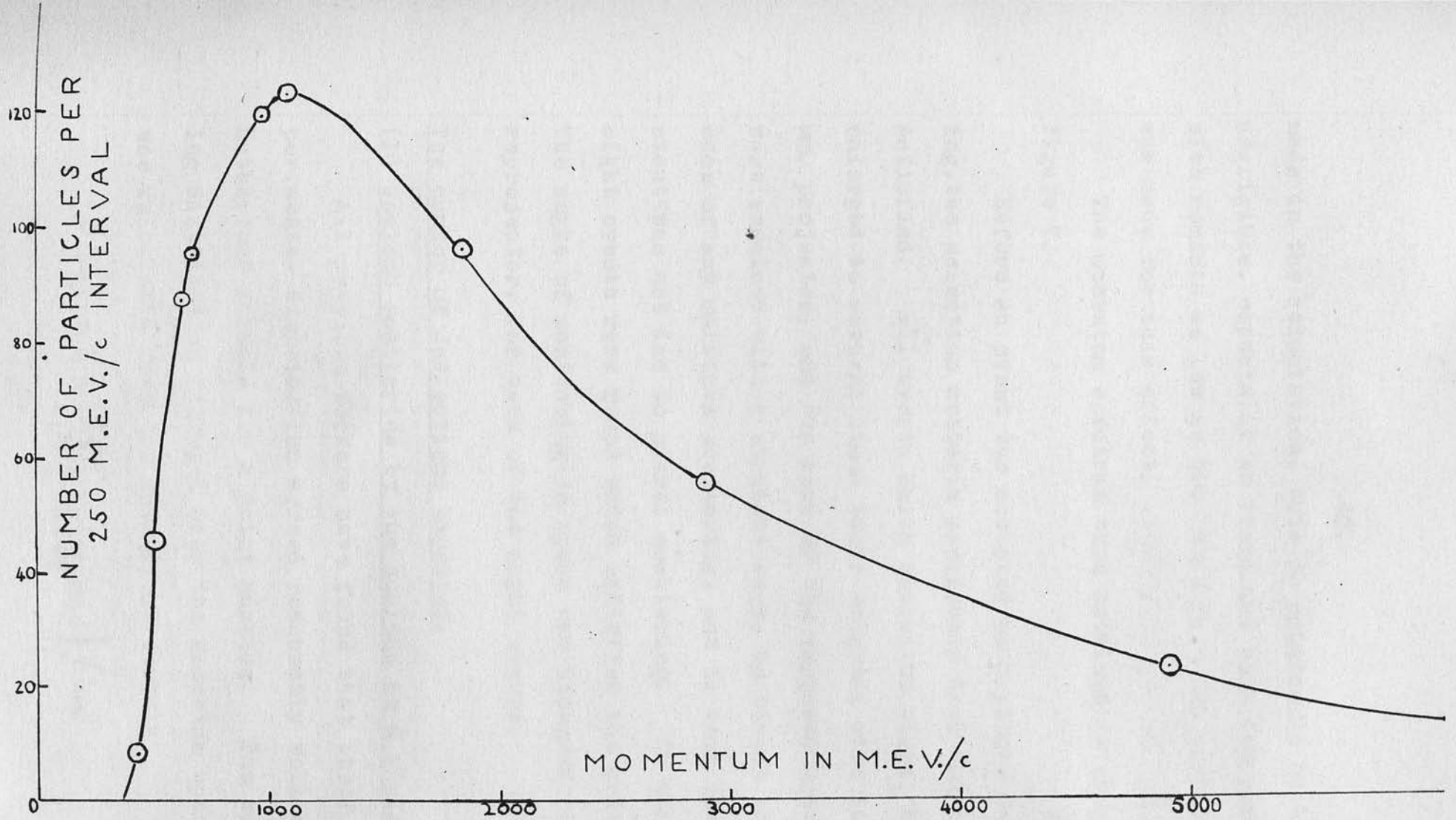

Figure 7. Momentum spectrum of μ-mesons inside the cloud chamber at La Marmolada. The curve is normalised to a total of 1400 particles for all possible momenta.

made in the calculation, this is considered to be negligible, especially as there are very few particles with momenta as low as 500 MeV./c. No correction was made for this effect.

The momentum spectrum thus obtained is shown in figure 7.

Before an event was accepted as a single scattering, the selection criteria previously used had to be satisfied. All events which satisfied these, were enlarged to several times their original size in a 35 mm. projector, and the arms of the supposed scattering were examined with a straight edge, to detect the presence of any multiple scattering, and to test that the event was not due to plural scattering. In all, eight events were found which satisfied the criteria. The angle of scattering in space was measured with the reprojector, for each of the eight events.

The number of deflections expected.

(1) Coulomb scattering by the nucleus as a whole.

All previous workers have found that their experimental distribution agreed reasonably well with the Rutherford formula for a point nucleus. The scattering distribution averaged over the momentum spectrum was calculated from the Rutherford formula

$$P(>\phi) = \pi N \left\{\frac{Ze^2}{p\beta c}\right\}^2 \left\{\frac{1}{\sin^2 \phi/2} - 1\right\} \Big/ \text{cm.}$$

where $P(>\phi)$ is the probability of there being a scattering through an angle $>\phi$; N is the number of atoms in 1 c.c. of the gas and $p\beta c$ is in MeV. In the conditions of this experiment, screening of the nucleus is negligible. Various corrections are necessary. There will be particles, other than μ -mesons, present in the random cosmic ray beam. By the selection criterion (d), it is considered that few high energy electrons will be included in the accepted particles. There will certainly be a small number of π -mesons and protons present. In scanning the 8993 photographs, there were found two stars, which were post-expansion, and produced by charged particles in flight. Taking the cross-section for star-production in the gas as 100 gm./cm.^{2} this corresponds to a total track length of interacting particles of 1480 cm. These particles are expected to have a lower momentum than the μ -mesons. The minimum value of $p\beta$ allowed by the selection criteria is 200 MeV/c. On the assumption that all the contamination particles have momenta = $\frac{200}{\beta}$ MeV/c, their scattering distribution was calculated as above, and the result added to the μ -meson distribution.

It is found from experiments on electron scattering[29] that the charge is not concentrated at a point, but is spread over a finite volume. The scattering

29

distribution from a nucleus, which is regarded as a uniformly charged sphere, can be calculated from that
28 of the point charge, by the relation given by Rose[28]

$$\sigma(\theta) = K\,\sigma_R \quad ; \quad K = \left[\frac{3}{(qR_0)^2}\left(\frac{\sin qR_0}{qR_0} - \cos qR_0\right)\right]^2$$

where $\sigma(\theta)$ is the differential cross-section at angle θ for the model considered, σ_R is the corresponding cross-section for a point nucleus, R_0 is the nuclear radius $= r_0 A^{1/3}$ where r_0 is taken as 1.2×10^{-13} cm. and $\hbar q$ is the momentum transfer.

The number of scatterings through an angle greater than 4^0 was calculated on this basis. It is considered that figures for angles less than 4^0 would be unreliable, due to the difficulty of efficient scanning below this angle, and due to possible effects of distortion.

(2) <u>The effect of scattering within the nucleus</u>.

There are several other possible contributions to the scattering distribution. Since the De Broglie wavelengths of the particles considered are of the order of, or less than, the mean distance between protons in the nucleus, there may be a contribution from coherent and incoherent scattering within the nucleus.
35 This problem has been treated by Amaldi and Gatto[35] for light nuclei. If their results are assumed applicable to the present case, the maximum contribution is $\left(\frac{1}{Z}\right)\sigma_R$. The coherent scattering may be estimated

by considering each proton, as an independent scattering centre, and this also yields a contribution $\left(\frac{1}{Z}\right)\sigma_R$. In both those processes, considerable momentum is imparted to the proton and one might expect to observe the track in the chamber. No such events have been found. This is not conclusive, both because of the small size of the effect and because the energy of the struck proton will frequently be spread throughout the whole nucleus, leading to evaporation of neutrons as in the case of μ-meson capture. In any event, the effect is small.

(3) The effect of decays in flight simulating deflections.

The decay in flight of a μ-meson, or a π-meson, may simulate a single scattering. Because of the relatively long life of the μ-meson, and the high momenta of those considered, the contribution from μ-meson decay is negligible. For π-meson decay, the effect depends on the assumed momenta of the π-mesons.

From the observed star production, it is estimated that there are 150 π-meson tracks included in the random cosmic ray beam scanned. This can only be a rough estimate and may be in error by a factor of two. If it is assumed that the momentum of all the π-mesons is that equivalent to $p\beta = 200$ MeV/c then 1.2 decays would be observed, and the apparent angles of scattering would be in the range 0° to 10°. As the assumed mo-

mentum rises, the observed number will drop fairly rapidly, due to the dilation of the lifetime. For the case of $\pi - \mu$ decays which simulate large angle scatterings, it should be noted that for the assumed momentum of the π-mesons the μ-meson would have a $p\beta$ value less than 200 MeV/c. It is doubtful whether small departures below the 200 MeV/c limit could be detected visually in scanning, especially if the path length of the μ-meson is small. This last consideration may not be important.

(4) <u>The effect of scattering by nuclear forces</u>.

There may also be a contribution due to nuclear scattering of π-mesons. The effect of this is difficult to estimate, since the distribution with angle depends strongly on the assumed momenta. The results
36 of Fermi and Anderson[36], on π-mesons scattered by protons, at an energy of 135 MeV, show a strong predominance of backward scattering. Their results are fitted by a form

$$\frac{d\sigma}{d\Omega} = a + b\cos\theta + c\cos^2\theta$$

where $\frac{d\sigma}{d\Omega}$ is the differential cross-section at angle θ, and Ω is the solid angle considered. Considering only the direct scattering, as opposed to the charge exchange scattering, and assuming equal numbers of positive and negative π-mesons, the integration of the above expression yields a prediction that only 0.14

scatterings would occur in the range 4^{o} to 13^{o}.

37 Recent work by Clarke and Major[37] on the scattering of 4.2 GeV π-mesons in emulsions shows that, for this energy, all the expected scatterings would lie in the range 0^{o} to 13^{o}. The total number of scatterings expected for a geometric cross-section is two.

In order to establish whether or not any such nuclear scatterings occurred, the deflections of penetrating shower particles were examined. Only showers consisting of a small number of particles were considered, since, in large showers, a small angle scattering would be difficult to detect. In all, 1034 tracks were scanned. Five examples of deflections were found, satisfying the criterion of no multiple scattering along the arms. In every case the angle of scattering was greater than 13^{o}, the smallest being 15^{o}. The apparent absence of coulomb scattering implies that the average momentum of the shower particles is given by

$$p \geqslant \frac{500}{\beta} \text{ Mev/c.}$$

If it may be assumed that the random π-mesons have the same momentum spectrum as the shower particles, the total absence of scatterings of less than 15^{o} implies that the coulomb scattering is negligible and that the nuclear scattering is predominantly large angle. If all the deflections found among those showers are assumed to be nuclear in origin, the resultant cross-

section is approximately one third of geometric, and the expected number of scatterings in 1480 cm. of track is 0.7. In addition, there is a high probability of the nuclear component being $> 13^{\circ}$. It would seem that the contribution from nuclear scattering is very small.

However the coulomb scattering and the possibility of decay cannot be neglected on the basis of this evidence. It seems unlikely that the momentum spectrum of the contamination particles is the same as that of the counter-controlled, shower particles. The contamination particles must be produced some distance away from the chamber, otherwise associated particles would be seen, and the loss of energy by absorption and the loss of low energy particles by decay will alter the average momentum. Without knowledge of the point of production it is difficult to estimate whether the average momentum will rise or fall.

(5) The effect of inaccuracy of the momentum spectrum.

It is also possible that there could be a gross underestimate of the number of low energy μ-mesons. In the 8993 photographs, 23 events have been interpreted as stopping μ-mesons, either by their characteristic decay or by their production of an Auger electron, when captured into an orbit round an argon nucleus. Mesons which are captured without producing such an

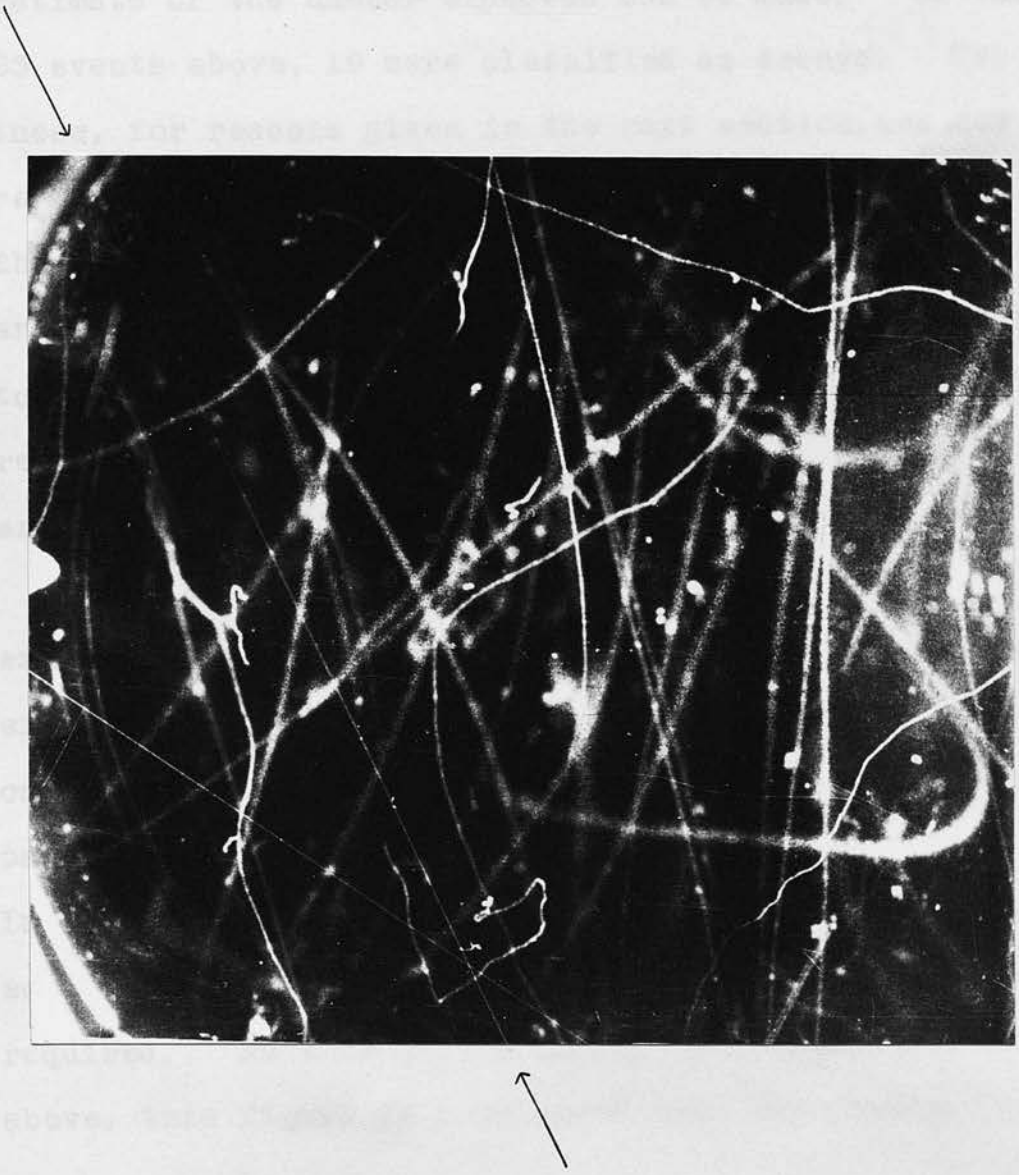

Figure 8. A single scattering of a fast μ -meson through an angle of 8^{o}.

electron, are not easy to detect, without the comparison of the multiple scattering against range. An estimate of the number expected can be made. Of the 23 events above, 19 were classified as decays. Two of these, for reasons given in the next section, are now regarded as nuclear capture processes. It is known that only 13% of stopped negative μ-mesons decay in argon. Since the positive excess is 20% it is possible to calculate the total number of stopping mesons. The result is 26, of which 16 are positively charged and 10 are negatively charged.

Of these, many are counter-controlled or pre-expansion events. There is only one case of a post-expansion capture process with an Auger electron, and one post-expansion μ-e decay. Therefore the total path length of very slow μ-meson track is $\simeq$ 40 cm. In order to add one scattering to the predicted value, some 1000 cm. of track of $p\beta$ = 200 MeV/c would be required. In view of the number of stopping tracks above, this figure is considered very improbable.

Discussion of the results.

The experimental results and the theoretical predictions are shown in Table 2. The number of scatterings due to π-meson phenomena might be twice as large as stated, owing to the uncertain method of estimating the number of π-mesons. In this case, the number of

Table 2.

Θ	4°	6°	8°	12°
No. of events observed greater than Θ	6	4	1	1
No. of events due to μ -mesons, predicted by point nucleus	0.99	0.44	0.25	0.11
No. of events due to μ -mesons, predicted by uniform nuclear model $R = 1.2 \times 10^{-13} A^{\frac{1}{3}}$ cm.	0.18	0.04	0.0	0.0
No. of deflections due to π -mesons ($p\beta$ = 200 MeV/c)	1.3	0.61	0.31	0.15
No. of deflections due to $\pi - \mu$ decays in flight ($p\beta$ = 200 MeV/c)	1.2	Total predicted by theory (uniform nuclear model) $\Theta > 4^\circ$		2.7
Total predicted by theory (point nucleus model)	3.5			

scatterings through angles greater than 4^{o} could be as high as 6. In this theoretical number, all scattering is that due to a point nucleus. With these results, it is clearly not possible to distinguish between the point nucleus and the uniform nuclear model, far less to establish the presence of an anomalous component.

It is unsatisfactory that so large a percentage of the observed deflections are accounted for by the 2% of contamination particles. It seems strange that to explain the observed number of scatterings all of the π-meson contamination must have values of $p\beta$ = 200 MeV/c. On the other hand, it is very difficult to see why more scatterings than are predicted by the point nucleus should be observed. If the excess were to be interpreted as an anomalous scattering, the cross-section would be so large that other workers such as McDiarmid would have found very many more scatterings than were observed. If the differences found by McDiarmid, between experiment and the physically more reasonable theory of the uniform nuclear model, were entirely due to a nuclear scattering, the cross-section so determined predicts only 0.5 scatterings for the conditions of the present work. It is unreasonable to expect a much greater cross-section in argon than in, say, lead.

It is hoped that this unsatisfactory position may be resolved in the future by developing a method of

multiple scattering, capable of reaching higher values of $p\beta$. It would then be possible to measure the momenta of the six scattered tracks and this would allow the assumptions, underlying the corrections, to be checked. It should be noted that if it were found that the $p\beta$ values of the deflections were much larger than 200 MeV/c, the agreement with the point nucleus model would not be destroyed. The decrease in the contribution from coulomb scattering of π-mesons, and from decays in flight, would be counter-balanced by the necessity to admit a contribution from scattering by nuclear forces.

At the present time no evidence for the existence of a nuclear scattering is afforded by the present work, though it may be possible to reach a more definite conclusion in the future. The maximum cross-section for anomalous scattering allowed by the present work is 2×10^{-28} cm.^{2}/nucleon.
This may be compared with the value derived by Kannanagra of $2.3 \pm 1 \times 10^{-28}$ cm.^{2}/nucleon.

B. The Low Energy End of the μ-Meson Decay Spectrum.

It is now well established that positive μ-mesons decay according to the scheme $\mu^+ \rightarrow e^+ + \nu + \nu$ where the positron may have an energy up to 55 MeV. Some of the negative μ-mesons at rest decay according to a similar scheme, while a proportion may be captured

by a nucleus of the material in which the meson stops. The probability of capture increases rapidly with the atomic number of the capturing nucleus. The capture mechanism is envisaged to be $\mu^- + p^+ \longrightarrow n^\circ + \nu$

The neutron created in this interaction receives part of the rest-energy of the μ-meson and the nucleus is put into an excited state. The de-excitation occurs through the emission of neutrons. These neutrons have
38 been detected by the work of Sard and his colleagues[38]. The de-excitation proceeds via the emission of neutrons, because the coulomb barrier inhibits the escape of protons.

The decay spectrum of the μ-meson is similar to that of a β-active element and the average value of the electron energy is 35 MeV. There are very few low
39 energy decay electrons, for example Leighton[39] reports that in 75 examples of μ-e decay, no example of an electron in the energy interval 0 - 5 MeV was found. Similar results are reached by Peyrou and Lagarique. These experiments were to some extent biased against observing low energy decays, since the cloud chambers were in both cases counter-countrolled. Similar results from workers in emulsions are also biased because of the difficulty of seeing electrons of this energy, and of clearly associating them with the end of the μ-meson track. It seems well established, however, that low energy, i.e. $<$ 5 MeV, decay electrons

are rare.

In the photographs scanned, 19 examples were found of μ-e decays at rest. Of these, two were low energy decays. In one case the electron stopped in the chamber. Amongst photographs taken in the same chamber at University College, Wales, a further seven examples of μ-e decays were found. One of these was also a low energy decay. In this event a magnetic field of 6000 gauss was operated, and the μ-meson is known to be negatively charged. The sign of the two other examples is not known. In one case the whole sequence is $\pi \longrightarrow \mu \longrightarrow$e, but from the measured range of the μ-meson this example must be a decay in flight of the π-meson. The dynamics of the decay are satisfied if the velocity of the π-meson is 0.188. Details of the three events are given in Table 3.

It seems most unlikely that such a large proportion of the available decays are of such low energy. Previous experiments have agreed well with theory on this point. The only other possibility is that they arise from the capture of negative μ-mesons by the argon nucleus. The observed electrons cannot be Auger electrons - compare the photograph of event 4418 with that of 7767 which shows an Auger capture process. The range of the Auger electron is 0.75 cm. as opposed to 15 cm. in the "decay" event. Wheeler[40] has calculated that the energy of the μ-meson bound in a 1s state

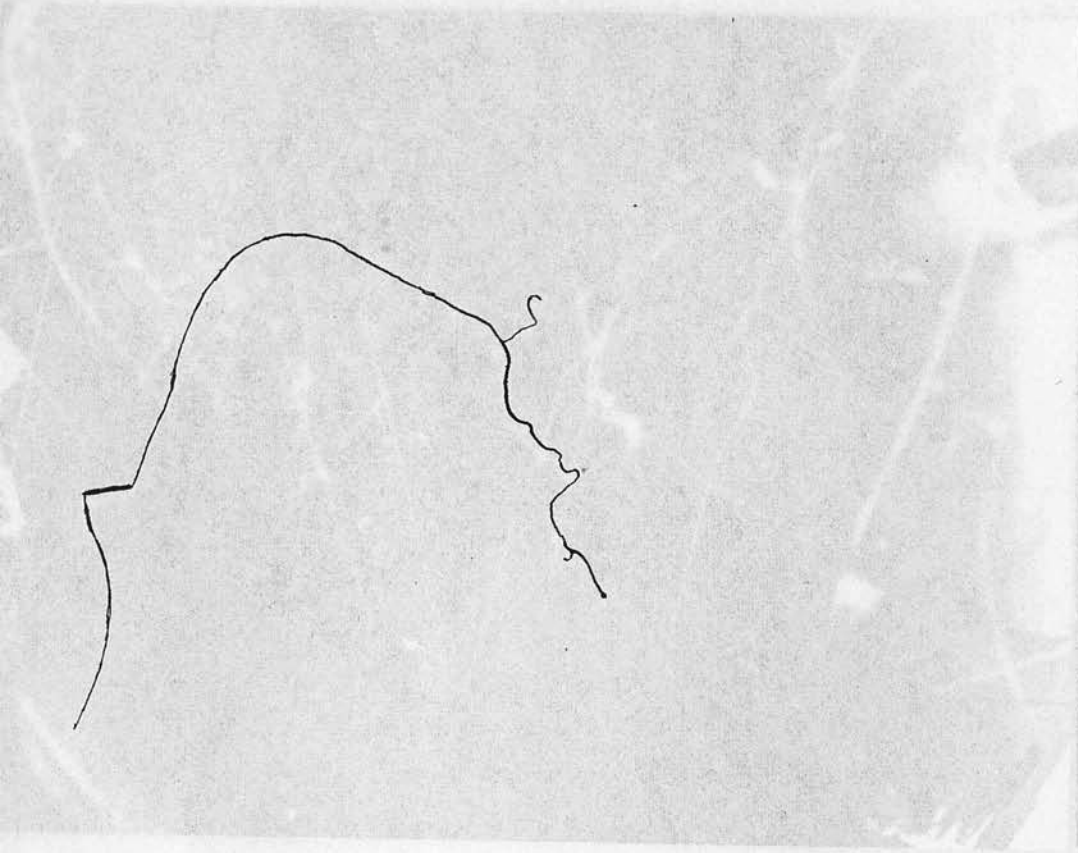

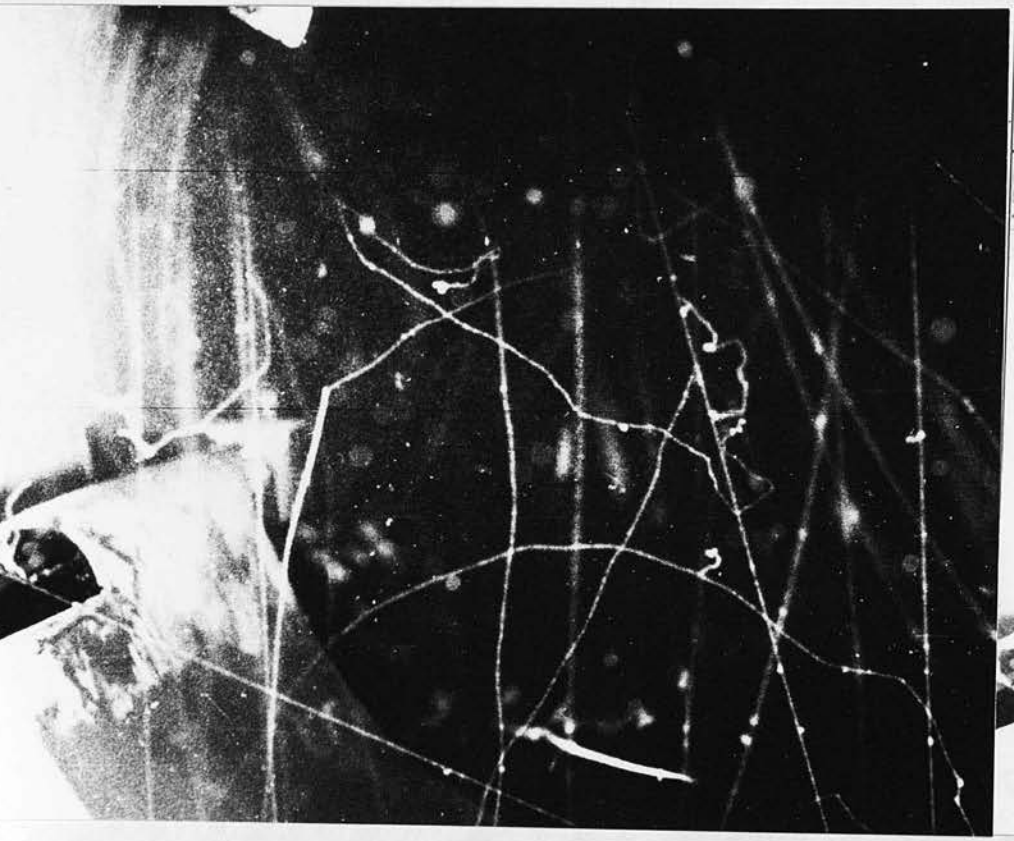

Figure 9a. Photograph number 4122
(see text, page 51).

Figure 9b. Photograph number 4418
(see text, page 51).

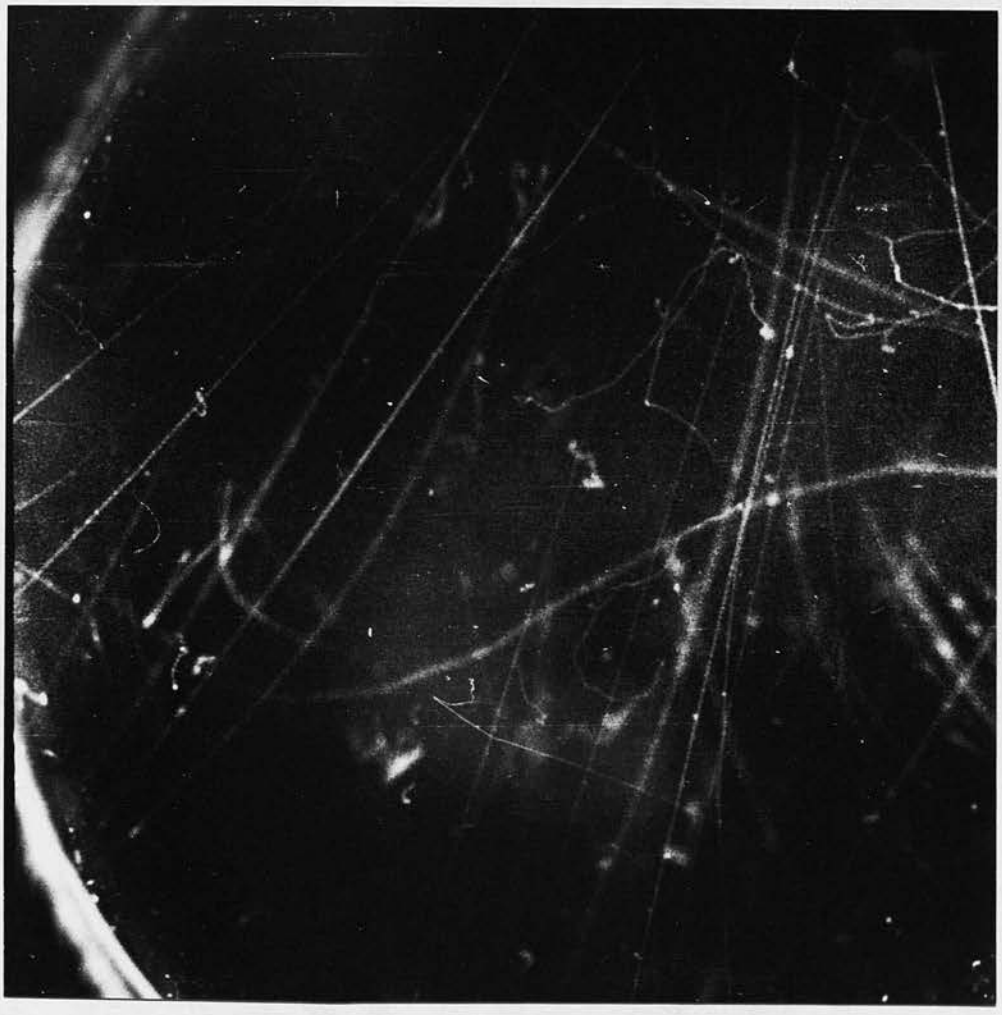

Figure 14. Probable example of the capture of a negative μ-meson by an argon nucleus. The electron is an Auger electron and is of energy 300 K.e.v.

of an argon atom is approximately 1 MeV. This gives an upper limit to the energy available for ejection of an electron. The lowest value of Z, for which the observed energies could be produced is 37. It might be argued that small amounts of heavy material contamination, in the gas filling, would have a large effect due to the Z^4 variation of the capture cross-section. The only contaminations feasible in sufficient quantities would be those caused by the rare gases krypton and xenon. Since these could not be present in proportions greater than occur in the air, the magnitude of this effect may be estimated. Using the figures given in Kaye and Laby's Tables, it is found that the ratio of capture in krypton to that in argon is not greater than 2×10^{-4} and the corresponding ratio for xenon is approximately the same.

Since all three events are consistent with the μ-meson carrying negative charge, the most likely explanation is that the effect is attendant upon nuclear capture of the μ-meson. In argon, the capture process is frequent. Of all negative μ-mesons which stop in the chamber, only 13% survive to decay in the normal way. The process of de-excitation of the capturing nucleus, by the emission of neutrons, will proceed until the remaining energy of excitation is less than the binding energy of a neutron in the residual nucleus. The remaining energy, of the order of 10 MeV, can only

be dissipated by the emission of β -rays or γ -rays. As yet it has not been definitely established that such β - or γ -emission does exist, owing to the presence of such radiation, in the same energy region, consequent on orbital changes of the electrons. It is unlikely that the observed electrons could be produced by the internal conversion of γ -rays emitted in the de-excitation process, since for these energies the conversion coefficient is very small. It would therefore appear that the most probable explanation is that of direct emission of β -rays.

It is possible that more than three of the stopping μ -mesons exhibit this mode of de-excitation. Subtracting the above two events from the 19 μ -e decays found yields a final value of 17 μ -e decays. These 17 examples will be made up of all the positive mesons and 13% of the negative mesons. Using a positive excess of 20% this yields, to the nearest integer, that the total number of stopped μ -mesons is 26, of which 16 are positive, and 10 are negative. Of the 10 negative mesons, one will decay and the remaining 9 will be captured. Four examples have been found of capture into an extra-nuclear orbit with the emission of an Auger electron. This suggests that five should have been captured into a Bohr orbit without the ejection of an Auger electron. The two examples of "low-energy decay" found in the Marmolada photographs are presumably

of this type. However for argon the capture with γ - emission is more probable than that with Auger emission. For $Z = 20$ the transition rate for the meson from a 2p state to a 1s state by radiative emission is 2.15×10^{16} per second, while, for the corresponding transition by Auger emission, it is 3.1×10^{11} per second. This suggests that some of the events classed as Auger emission may be examples of nuclear emission of β -rays. It is not possible to prove or disprove this suggestion since the energies involved are of the same order as could be produced by the Auger process.

It is difficult to understand why a negative electron should be emitted. If the nucleus were imagined to be excited to a definite level, some 3 MeV above the ground state, and if both the ground state and the supposed level were of spin 0, then the direct γ -ray emission would be forbidden, and the observed electrons might in this case be internal conversion electrons. This would require that the electrons be emitted with a definite energy. Reference to Table 3 shows that this is possible. However it seems strange that the statistical process of boiling off neutrons should result in the establishment of a sharp level. It may be that either the capture process $\mu^- + p^+ \longrightarrow n^\circ + \nu$ is not adequate to explain the results, or that the models used in the discussion are not completely applicable.

Chapter V.

ANALYSIS OF INDIVIDUAL EVENTS.

In a total of 8993 photographs, there have been found 29 events interpreted as neutral decays (Λ^o or Θ^o), 233 interactions in the gas of the chamber, 19 μ-e decays and numerous electron pairs. The V^o events, the stars and the electron pairs have been treated by other members of the group, and some aspects of the μ-e decays have been dealt with in the previous chapter. In this chapter, four events of particular interest will be discussed.

(1) Events numbers 7204 and 7559 (see figures 10a and b).

Both these events ~~(see the photographs opposite)~~ are examples of interactions in the gas, where one of the secondary particles appears to emit a low energy β-ray at the end of its range. Both stars are counter-controlled. The faint nature of event 7204 is due to it being in a region of very poor illumination. The β-ray emitted by the secondary of event 7559 appears to be post-expansion in origin, but due to the poor illumination of 7204 it is not possible to decide whether that β-particle is counter-controlled or not. Event 7559 also shows the apparent emission of a β-ray, directly from the interaction. This aspect will be

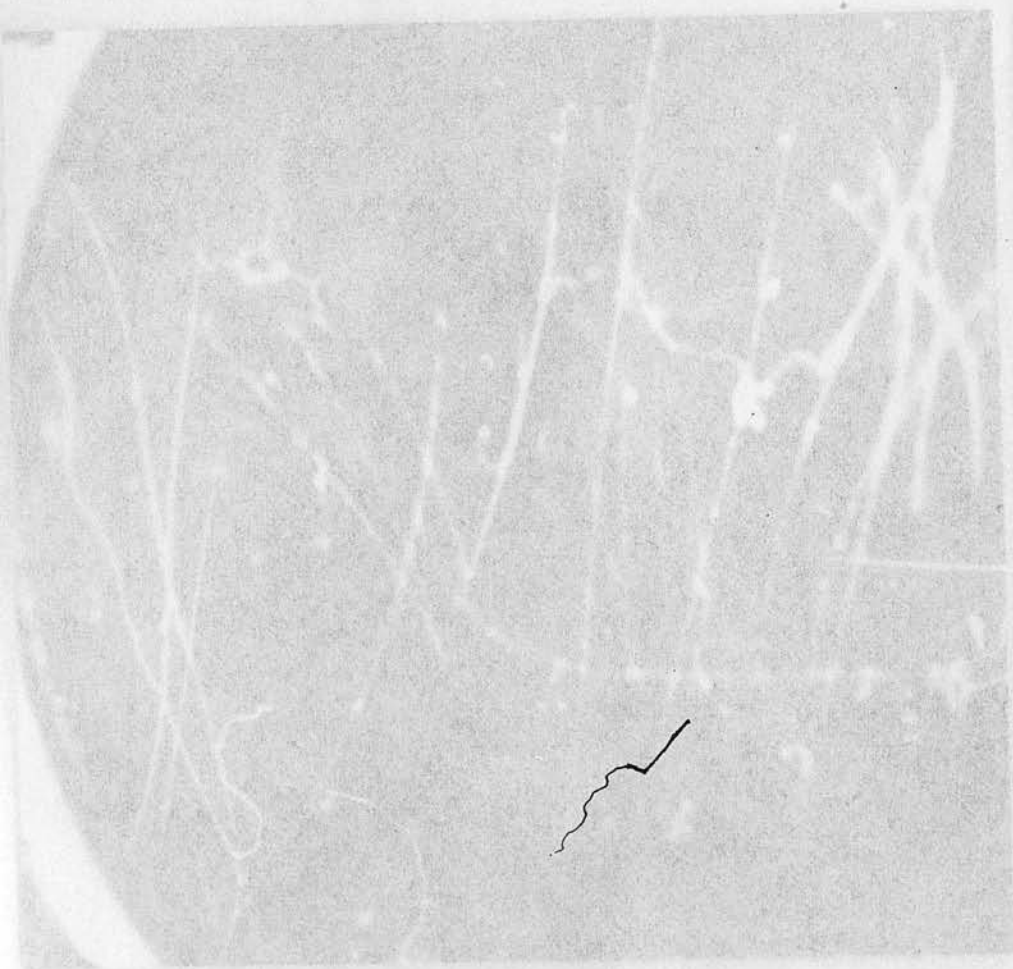

Figure 10a. Photograph number 7804.
A radioactive fragment, identified as Be^8, is emitted and decays.

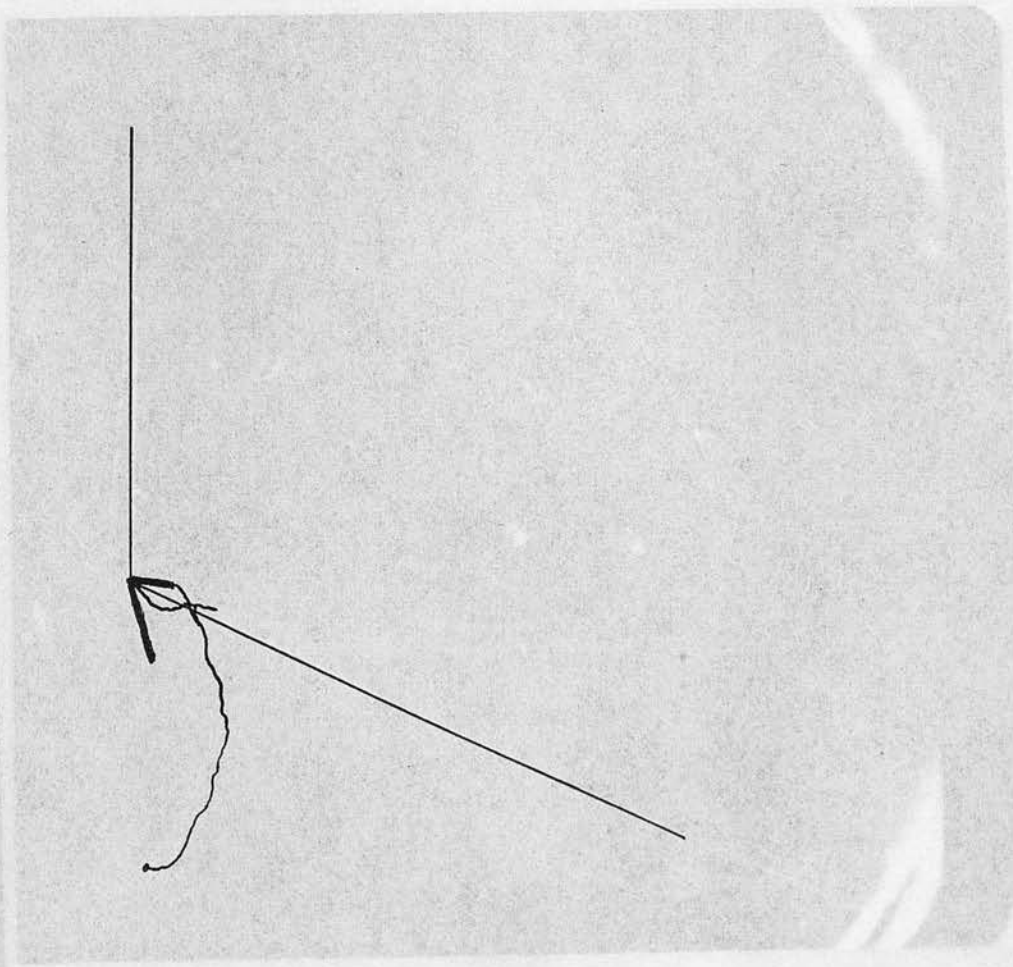

Figure 10b. Photograph number 7859.
A second example of the emission of a Be^8 fragment from a star.

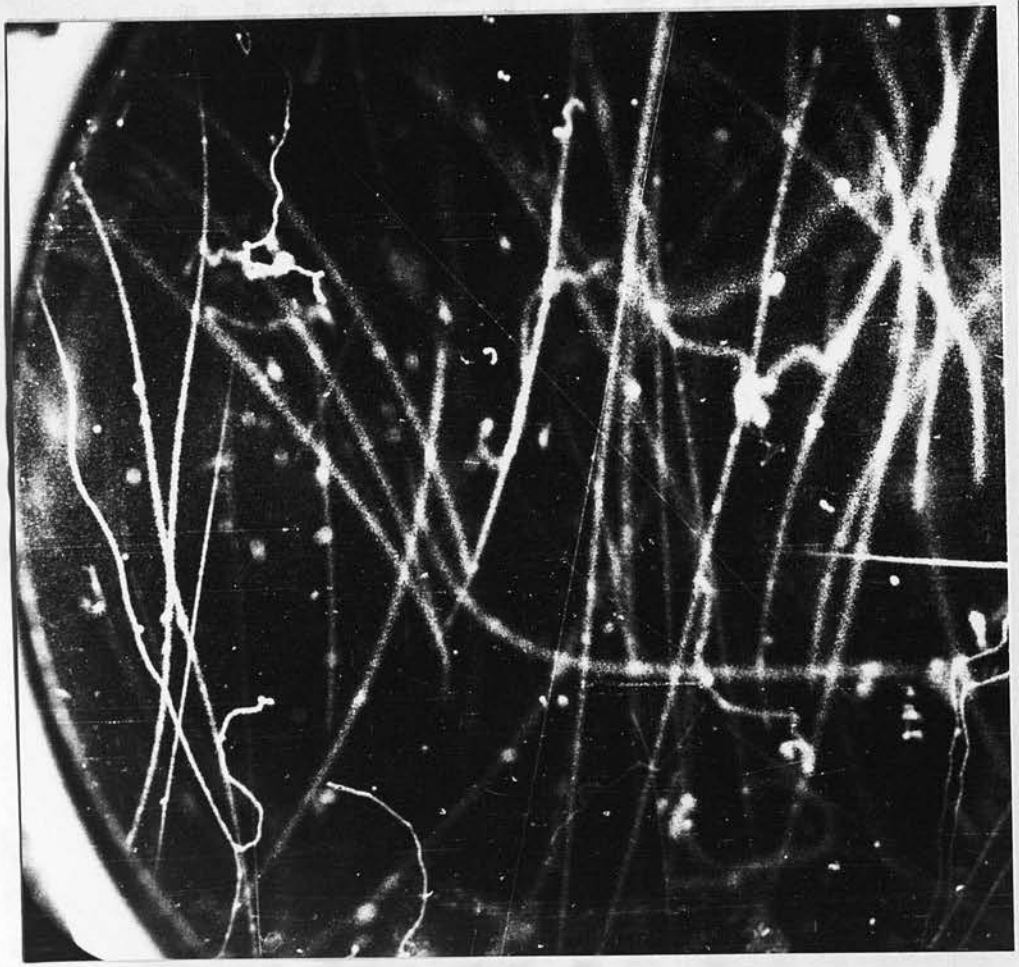

Figure 10a. Photograph number 7204.
A radioactive fragment, identified as He^6, is emitted and decays.

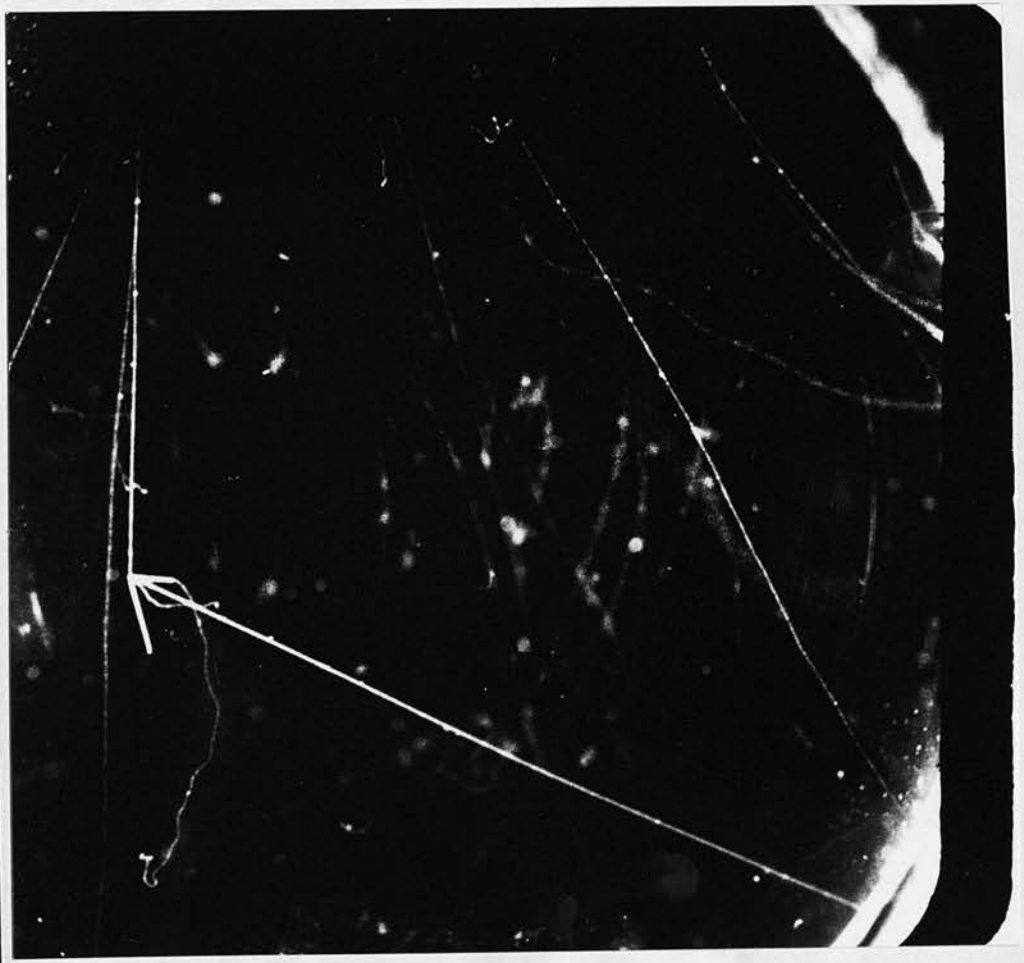

Figure 10b. Photograph number 7559.
A second example of the emission of a He^6 fragment from a star.

treated separately. In both cases the full event appears on the first, as well as the second, flash.

The most reasonable explanation is that these photographs show the decay of a radioactive fragment. Clearly the decay must be one with a very short half-life. The energy of the β-ray in event 7204, as measured by its range, is 0.65 MeV, while the energy of that in 7559 is 1.05 MeV. The stars must represent the disruption of a nucleus of argon. Examination of "Nuclear Data" yields the possible identities of the decaying fragment as P^{29}, Si^{27}, Al^{26}, N^{16}, N^{17}, N^{12}, B^{12}, Li^{8} or He^{6}. Their properties are as shown in Table 4. Those elements, with half-lives greater than 4 seconds, can be ruled out since, from the appearance of the decay particles, they have both appeared within 200 milliseconds of the expansion, and cannot have appeared later than 400 milliseconds after it. The probability that two decays would be observed within this period is only 0.5%. Of those with short half-lives, Li^{8} can be immediately ruled out since the end product of the decay would be Be^{8} which decays to two α-particles with a half-life of the order of 10^{-16} seconds. These α-particles would certainly have been observed in the second flash at least. Of the remaining three possibilities, viz. N^{12}, B^{12}, He^{6}, the last is the most probable.

Table 4.

Element	Half-Life (seconds)	Decay Product	Maximum Energy of Decay Product
Phosphorus 29	4.65	β^+	3.6 MeV
Silicon 27	4.9	β^+	3.6 MeV
Aluminium 26	6.3	β^+	2.6 - 3.4 MeV
Nitrogen 17	4.13	β^-	3.7 MeV
Nitrogen 16	7.3	β^-	3.8 MeV
Nitrogen 12	12.5×10^{-3}	β^+	16.6 MeV
Boron 12	0.027	β^-	13.43 MeV
Lithium 8	0.88	β^-	13.0 MeV
Helium 6	0.82	β^-	3.23 - 3.7 MeV

In event 7559, the radioactive fragment is similar in appearance to track D, which is a typical α -particle. Since the rate of loss of energy by collision increases with the square of the charge of the colliding particle, the identification of the fragment with nitrogen or boron would mean that the energy taken by it was very large. This is considered unlikely since recoil nuclei are seldom seen in stars in the gas, and when seen are of short range.

It is therefore concluded that the most probable interpretation is that both photographs represent the decay of He^6 fragments, though the possibility that one or both represent the decay of either N^{12} or B^{12} cannot be ruled out.

The second β -particle in event 7559 may be explained in two ways. Identifying the other secondaries of the star visually, as a proton and an α -particle, and assuming that the primary is also a proton, the equation of the reaction might have been

$$A_{18}^{40} + H_1^1 \longrightarrow He_2^6 + He_2^4 + H_1^1 + 3n_0^1 + Si_{14}^{27}$$

assuming that as many neutrons as protons and α -particles were emitted. Silicon 27 is β^+-active with a half-life of 4.9 seconds. It is therefore possible that the second β -particle may be the decay product of silicon 27. The probability of observing this decay is not greater than 5%.

Alternatively, it may have been a δ -ray produced by the primary very near the star. If the δ -ray were produced within a millimetre of the star, its origin could not be distinguished from the star. It does not seem possible to distinguish between the two possibilities.

(2) Event number 986.

This event is shown in figure 11. The angle ABC is 6° and there is a 16° single scattering at C. Multiple scattering measurements on the arm BA yield a value

$$p\beta = 123^{+52}_{-31} \text{ MeV/c}$$

while $$p\beta_{AC} = 96^{+82}_{-33} \text{ MeV/c}$$

and $$p\beta_{CD} = 110^{+100}_{-33} \text{ MeV/c}$$

The track BCD is therefore taken to be that of a single particle and the resultant value is

$$p\beta = 107^{+54}_{-26} \text{ MeV/c}$$

The event cannot be an electron pair. The prominent δ -ray on BA is projected forward. If the incident particle had been an electron, even for an angle of ejection of 30°, the energy of the δ -ray would be 3 MeV and it would have had a range in the chamber of 15 cm. Secondly an electron of the measured momentum would be a relativistic particle and the tracks would have fewer δ -rays (for $\beta \simeq 1$, the average number of δ -rays of energy greater than 40 keV is 1 per 4 cm. of track). The direction of projection of the δ -ray

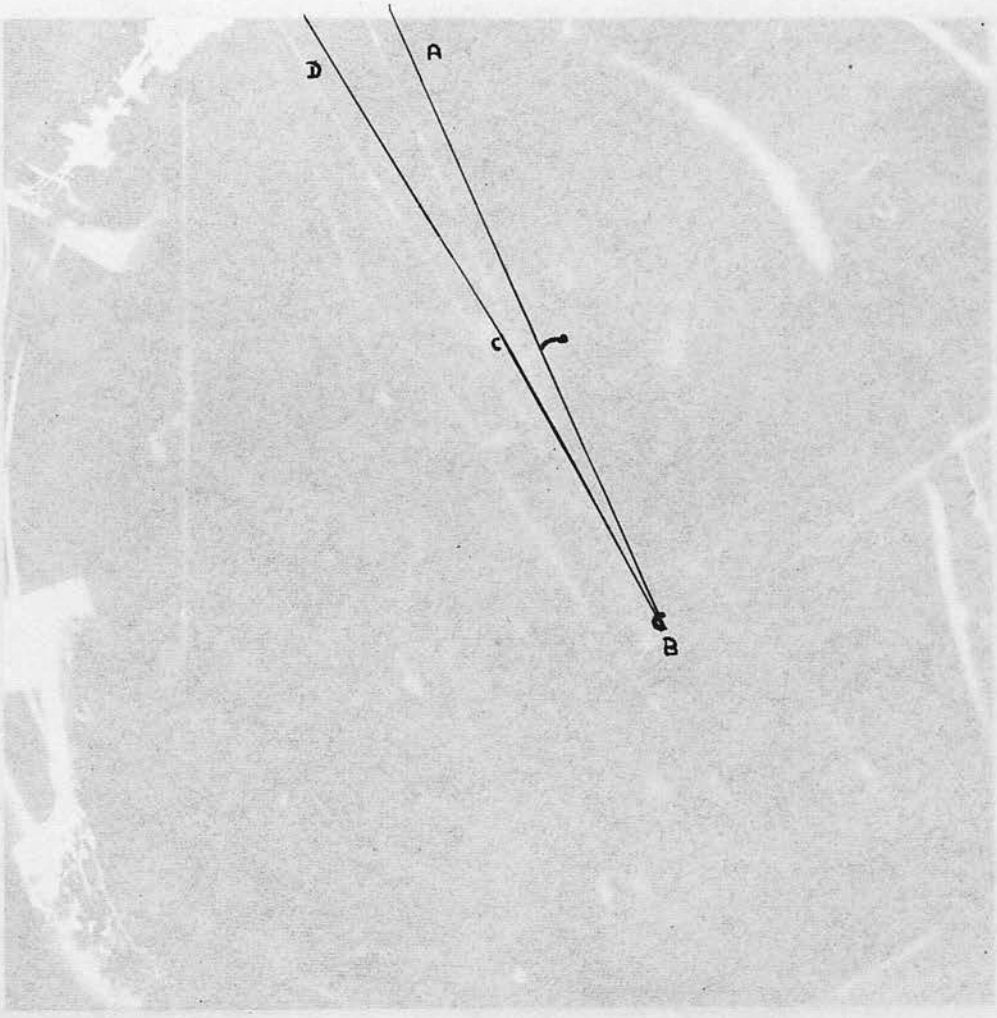
D
A
C
B

Figure 11. An event which is tentatively identified as an example of the decay mode $K^{\circ} \longrightarrow \pi + \mu +$ neutral.

indicates that the particle causing track AB travels from B to A. The direction of DB cannot be directly determined. If it were $\vec{DB}$ then the only possible explanation is that the event is a scattering by nuclear forces, since none of the known charged meson decay processes are consistent with the dynamics of the event. For example, if it were a K_{μ_2} decay, the decay product would have stopped in the chamber, the velocity of the μ-meson in the laboratory system being 0.27. It is not possible to rule out the interpretation of a scattering; however, if the direction of projection of the δ-ray on BA is accepted it would also require that the momentum of the arm BD was as high as that of BA. From the $p\beta$ values and the associated error limits quoted above this is quite possible. Track width measurements show that track BA is somewhat broader than BD. This implies that the collision would be inelastic with an energy loss of approximately 10 MeV. This would require that the $p\beta$-value of track BD was in fact greater than that of track BA. If the direction of the δ-ray is rejected, because of the possibility of scattering, then the momenta are consistent with the interpretation as a scattering by nuclear forces, but the track widths are not. Examination of photographs containing penetrating showers shows that large angle scatterings are not infrequent. In 1034

shower particle tracks 30 deflections were found. The majority of these were large angle deflections, i.e. through angles greater than 20°. In no case was the angle of scattering greater than 90°, though five examples were scattered through angles of the order of 90°. This evidence is not conclusive, since the results of Anderson and Fermi for π -meson scattering near this energy show a strong predominance of backward scattering, and the energy of the shower particles examined may not be the same as the event considered here.

If the direction of the arm BD were from B to D, the event must be either a neutral decay, or a neutral-induced two prong star. The latter possibility is not likely, since a proton of the measured $p\beta$ values would ionise at 4 times minimum. Comparison of the track width with that of the prominent δ -ray, which is at minimum ionisation for the greater part of its length, excludes this. A K-meson would ionise 3 times minimum and is likewise rejected. It is considered unlikely that a two prong star should consist of two light mesons.

Track width measurements indicate that track BD is slightly thinner than track BA. There is no other counter-controlled track on the photograph and so it is not possible to measure the velocities accurately. It

is estimated that an upper limit to the ionisation is twice minimum. The number of δ -rays shows that the particles are relatively slow. On arm BD there are estimated visually to be 6.5 ± 0.5 δ-rays of energy greater than 40 keV, as opposed to the expected value of 2 if $\beta \simeq 1$. If both arms were light mesons, their ionisations would be 1.16 minimum for μ -mesons and 1.28 minimum for π -mesons. The best interpretation would seem to be that the tracks are those of two light mesons.

It is not possible that the event is a Θ^{o} decay since the $p\beta$ -values and the angle of 6^{o} are not consistent with the decay scheme. Since the ionisation evidence rules out the possibility of a Λ^{o}, the event must be at least a three body process.

The combination of the multiple scattering with the track widths suggests that particle BD is lighter than particle BA and leads to the decay scheme

$$K^{o} \longrightarrow \pi + \mu + \text{neutral.}$$

Such decay schemes have been previously reported by
41 Evans, Evans, Griffiths and Muller in 1951[41], and by
42 Lederman et al. in 1957[42].

The possibility that the track BD is that of an electron is not excluded, but it is considered unlikely in view of the δ-ray evidence.

It is not possible to distinguish definitely

between the interpretation as a scattering by nuclear forces and the interpretation as a neutral decay. It is considered that the decay is the more probable of the two, since to accept the other requires the rejection of some of the evidence, either that of the δ -ray or that of the scattering, but this conclusion must be considered as tentative.

It is therefore tentatively concluded that the event represents the decay mode

$$K^{o} \longrightarrow \overline{\Pi} + \mu + \text{neutral}$$

with the possibility that it represents

$$K^{o} \longrightarrow \Pi^{+} + \Pi^{-} + \text{neutral}$$

and the alternative interpretation is that it represents a Π -meson scattered through an angle of 174^{o}.

(3) Event number 6163 (see figure 12).

This event is a three prong star in the gas. One arm, ADE, is appreciably scattered and, on visual inspection, this track appears to be associated with a second, counter-controlled track, coming from the walls of the chamber. It is found on reprojection that they are not in fact associated. Owing to the appreciable scattering of track ADE in the gas, this is not conclusive, since a much greater degree of scattering will occur in the wall, and this would be expected to have destroyed any evidence of spatial association. Multiple scattering measurements were carried out on the

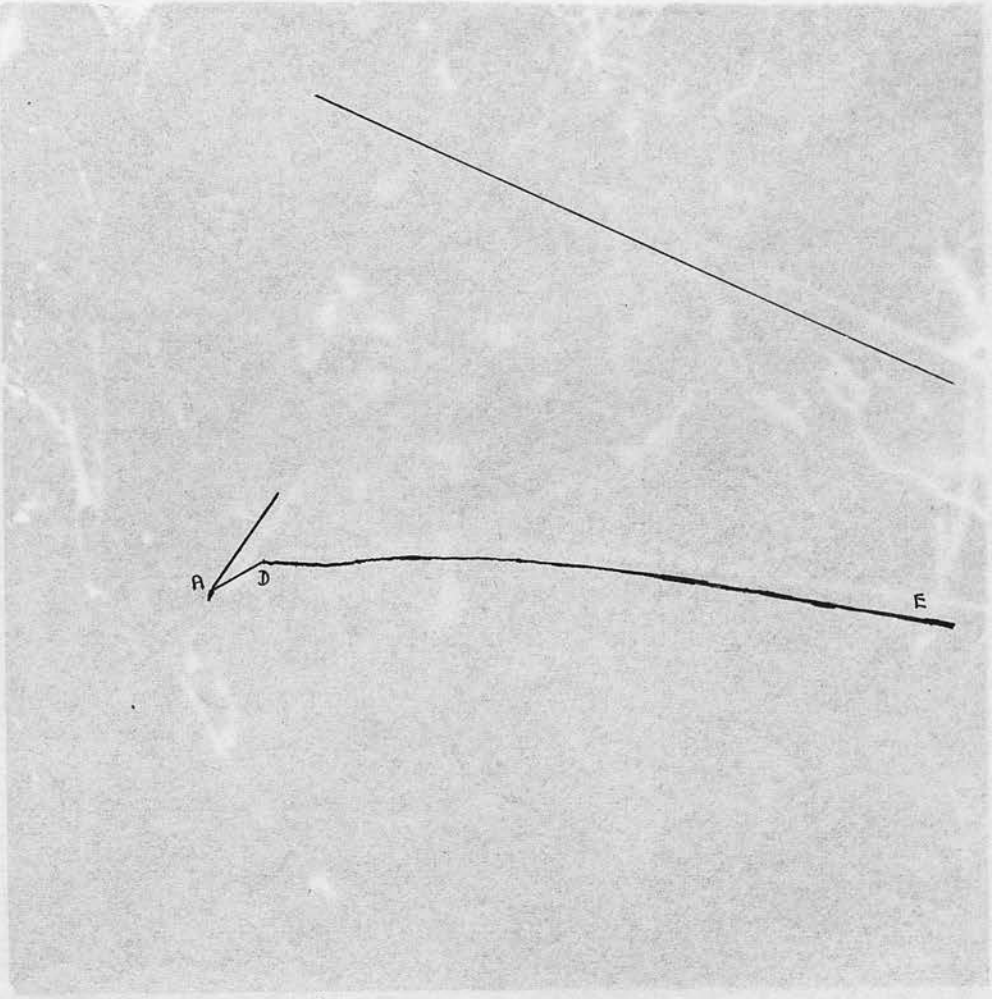
A
D
E

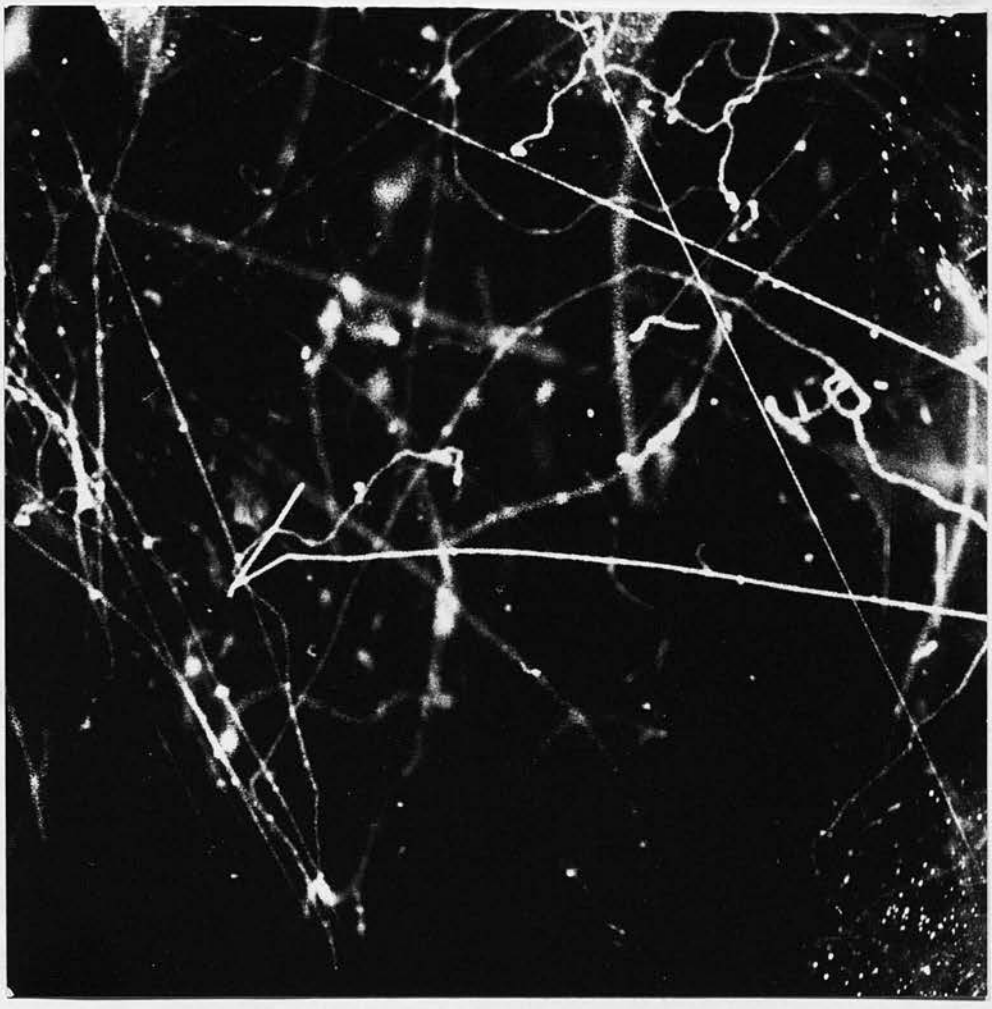

Figure 12. A nuclear interaction caused by the capture of a negative K-meson.

section DE and yield the result

$$p\beta = 26^{+8}_{-5} \text{ MeV/c.}$$

Since the velocity of the particle may well have varied in the length of the track, this value is the value of $p\beta$ at the half-distance, i.e. 3.75 cm. from point D. In addition, the scattering increases as one goes from E to D (this is clearly shown in the print). If this evidence is valid (the path length upon which it is based is very small) the direction of motion of particle ED is established as from E to D, and is therefore the primary of the star. Combining the multiple scattering with the residual range, the mass of the particle is found to be

$$1000^{+300}_{-200} \; m_e$$

and is therefore identified as a K-meson.

At D there is a single scattering of $34^{\circ}42'$. For a $p\beta$-value of 26 MeV/c one would expect to see one scattering, through an angle greater than 30°, in 1140 cm. of track. That portion of the track between the single scattering and the star appears to be less scattered than the previous part of the track. Owing to the length (0.7 cm.) of this portion, this lack of scattering is not reliable, but the possibility that the K-meson decays at D and that the star is produced by the secondary particle must be considered. If this is so, the K-meson is then identified as a $K^-_{\pi_3}$ since the secondary

of the K_{π_2} has a much higher velocity than the observed particle.

There also seems to be a change in the thickness at the point D, that portion between A and D being thinner than the portion beyond D. The points A, D and the small single scattering beyond D all lie in a plane at right angles to the optic axis and therefore any changes of thickness along these parts of the track are due solely to changes of velocity, and are independent of out of focus effects etc. This is evidence for a decay in flight of the K-meson, but it cannot be regarded as conclusive.

If the highly scattered particle were, in fact, travelling outwards from the star, it cannot be heavier than a light meson. A proton of the observed $p\beta$ would stop in the chamber, and while a K-meson would just escape, the part of the track at the edge of the photograph does not appear to be that of a particle so near the end of its range (for example there is no thickening up of the track).

But a π -meson of $p\beta$ = 26 MeV./c would not produce such a thick track. The second long prong of the star is 1.45 cm. long and if it is a proton has a velocity β = 0.142 and would ionise 29 times minimum. A π -meson of 26 MeV./c has a velocity β = 0.426 and ionises at 4 times minimum. The track of the "proton"

is no thicker than that of the "π-meson" and consequently it seems unlikely that the scattered track is a π-meson.

The most probable interpretation is that the star is produced by the capture of a negative K-meson, with the slight possibility that the K-meson decays in flight according to

$$K^- \longrightarrow \pi^- + \pi^\circ + \pi^\circ$$

with the π^- being captured to form a star. Since the existence of the negatively charged K_{π_3} meson has not been definitely established, the above possibility would have been important, if it could have been established.

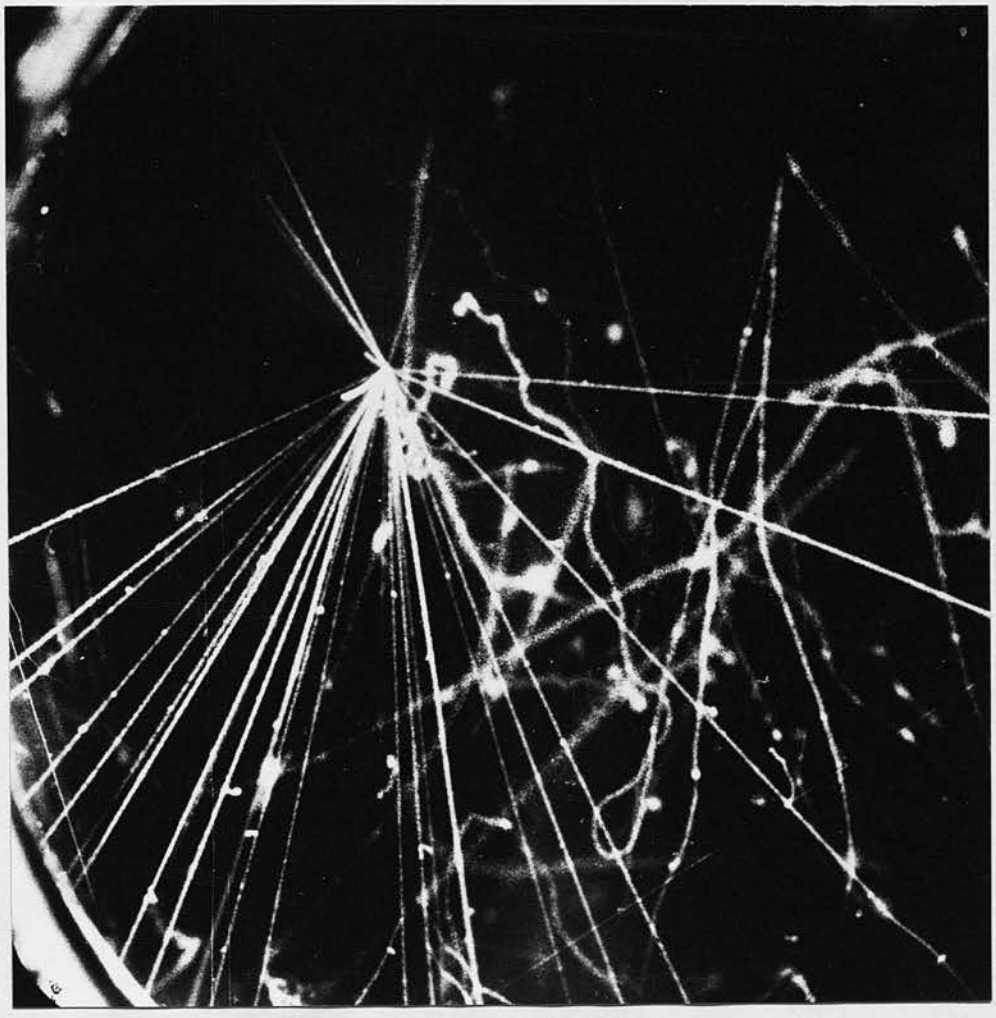

Figure 13. A nuclear interaction in the gas in which 31 charged particles are involved.

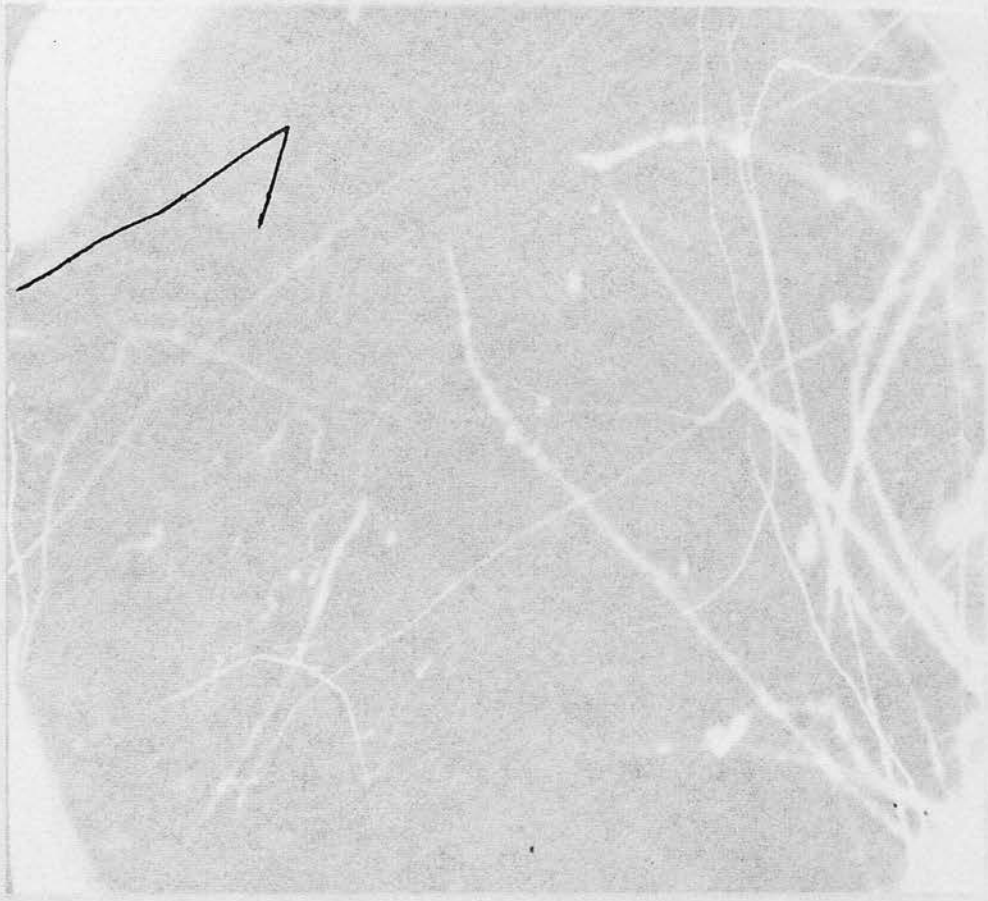

Figure 15. An example of the annihilation in flight of a positron.

Figure 15. An example of the annihilation in flight of a positron.

Chapter VI.

CONCLUSIONS AND PRESENT DAY POSITION.

The experience gained in the operation of the high pressure chamber at La Marmolada has shown that, in certain circumstances, it can be a research tool of value. The cooperation between the University of Edinburgh and University College, London, is to be continued in the field of particle physics, using high pressure cloud chambers. The work leading up to this possibility, and the series of experiments which have been planned will be described in the remaining chapters of this thesis.

It is felt that the results obtained, and the experience gained, have justified the carrying out of the work. The experiment suffered from the difficulty that a full team of personnel, trained in the operation of cloud chambers, and the interpretation of cloud chamber photographs, was not available. At the start of the work only Dr. G.R. Evans had had previous experience in these fields. The delay for the members of the group to acquire the necessary experience and for the preliminary experimental difficulties to be overcome led to the loss of valuable time. In consequence results were obtained which were frequently only confirmation of previous results reported by other

groups. Further, the relatively low rate of photography, on average 30 photographs a day, reduced the number of events found, though this was compensated by the much greater equivalent path length of a track in the high pressure chamber.

Since the start of the experiment in 1953 many advances have been made and this section of the thesis will be concluded by a statement of the present day position.

The particles known as mesons are divided into three groups. The first is that consisting of the light or L-mesons. The L-mesons are of two types, the μ-meson and the π-meson. The μ-meson has a mass of 206.7 electron masses and has a half-life of 2.22×10^{-6} seconds, decaying into an electron and two neutrinos. This meson exists in two charge states - positive and negative. The π-meson has a mass of 273.1 electron masses for the positively and negatively charged types. These have a half-life in vacuo of 2.54×10^{-8} seconds and decay according to the mode

$$\pi^{\pm} \longrightarrow \mu^{\pm} + \text{neutrino.}$$

There also exists an uncharged π-meson which decays into 2 γ-photons with a half-life of $\simeq 10^{-15}$ seconds (it has recently been reported at the 1957 Rochester Conference that it may be shorter than this). This meson has a mass of 264.3 electron masses. The family

of π -mesons is believed to be closely connected with nuclear forces, and they have a strong interaction with nuclei.

The second group, known as the K-mesons, is very complex. Members of this group have all an identical mass, within experimental error, of 965 electron masses. A large number of decay modes have been observed and are listed below.

Mode	Decay scheme	Half-life (seconds)
τ^+	$\longrightarrow \pi^+ + \pi^- + \pi^+$	1.27×10^{-8}
τ^-	$\longrightarrow \pi^+ + \pi^- + \pi^-$	1.27×10^{-8}
θ°	$\longrightarrow \pi^+ + \pi^-$	1.3×10^{-10}
$K^+_{\pi_2}$	$\longrightarrow \pi^+ + \pi^\circ$	12.1×10^{-9}
$K^+_{\pi_3}$	$\longrightarrow \pi^+ + \pi^\circ + \pi^\circ$	$\simeq 10 \times 10^{-9}$
$K^+_{\mu_2}$	$\longrightarrow \mu^+ + \nu$	$\simeq 10 \times 10^{-9}$
$K^+_{\mu_3}$	$\longrightarrow \mu^+ + \pi^\circ + \nu$	$\simeq 10 \times 10^{-9}$
$K^+_{\beta_3}$	$\longrightarrow e^+ + ? + ?$	$\simeq 10 \times 10^{-9}$

In addition, there is some evidence for the existence of $K^-_{\pi_2}$ and $K^-_{\beta_3}$ modes of decay, and possible the $K^-_{\pi_3}$ and $K^-_{\mu_2}$. The negative K-mesons are much rarer than the positive mesons, and in a similar way to the negative π -meson are difficult to observe due to their strong nuclear interaction. It is not known whether this group consists of more than one type of particle. In recent months, the consideration of this problem has

led to the discovery that certain symmetry properties known as the conservation of parity are not fulfilled in the weak interactions, such as K-meson decay. There is also evidence for a long lived component of the neutral K-meson group. This was predicted on theoretical grounds by Gell-Mann, and experimental evidence
42 has been obtained by Lederman [42] that these exist and have decay schemes

$$K^0 \longrightarrow \pi + \mu + \text{neutral}$$

$$K^0 \longrightarrow \pi + e + \text{neutral}$$

and possibly $K^0 \longrightarrow \pi^+ + \pi^- + \text{neutral}$

The meson decay described earlier in this work is presumably of this type.

The third group consists of mesons heavier than the proton - the hyperons.

Particle	Decay	Mass	Half-life (seconds)
Λ°	$\longrightarrow p^+ + \pi^-$	2181.5 m_e	3.7×10^{-10}
Σ^+	$\longrightarrow p^+ + \pi^\circ$	2326.9 m_e	3.4×10^{-11}
	$\longrightarrow n^\circ + \pi^+$		
Σ^-	$\longrightarrow n^\circ + \pi^-$	2326.9 m_e	$\geq 3.4 \times 10^{-11}$
Σ°	$\longrightarrow \Lambda^\circ + \gamma$?	2326.9 m_e	$\ll 10^{-10}$
Ξ^-	$\longrightarrow \Lambda^\circ + \pi^-$	2586 m_e	$\simeq 10^{-10}$

43 It is possible that heavier hyperons exist[43], but evidence is not conclusive. The hyperons may, in some

respects, be regarded as excited, virtual states of nucleons.

Present day theories of the elementary particles predict that for every particle there exists a corresponding antiparticle. The antiparticle has the same mass as the particle, where applicable the antiparticle has the opposite charge to the particle, and the particle and antiparticle have opposite magnetic moments. Examples of this are the electron and its antiparticle, the positron, and the positive π-meson and its antiparticle, the negative π-meson. It is also concluded that neutral mesons have antiparticles. An example of the antiparticle to the θ^o-meson has been reported by
44 Alvarez[44]. The identification as an antiparticle, rather than as the particle, follows from the "conservation of strangeness" according to the Gell-Mann
11 scheme[11].

There are many puzzling features in the physics of elementary particles at the present time. The principal one is the apparent identity of the masses and lifetimes of the τ-meson and the θ-meson, while their parities are opposite. This has led to the discovery that parity is not conserved in the "weak" interactions, such as β-decay. The evidence on this point does not shed any light on the parent τ - θ puzzle and the solution, alternative to that of non-conservation of parity,

put forward by Lee and Yang, of "parity doublets" is being tested at the time of writing. It was proposed that particles such as the τ - and θ -mesons were members of a doubly degenerate parity state, this degeneracy being removed by the "weak interactions". Gatto[45] has shown that if only the "weak" interactions are concerned, then the mass difference between the τ - and θ -mesons could be as low as 10^{-5} eV and would be quite undetectable. If this suggestion were true, it follows that both the Λ^{o} and Σ^{o} would also be parity doublets. At the present time no evidence has been found for this[44] and the situation is still unclear.

Chapter VII.

INTRODUCTION TO THE EXPERIMENTS ON FAST RECOMPRESSION.

The operation of the high pressure chamber at the mountain altitude of La Marmolada in the Italian Dolomites showed that if there was to be a useful field for it, either in cosmic ray work or with the particle accelerators, some means would have to be found of reducing the recycling time. The factors which determine the recycling time of a cloud chamber are
(1) the time necessary to remove from the gas any condensation nuclei produced by the previous fast expansion. This will be referred to as the deposition time.
(2) the time necessary for the chamber to reach thermal equilibrium. In conventional working of a cloud chamber, the gas in the working volume acquires heat from the body of the chamber while in the expanded state, and after it has been recompressed to its original volume, it is at a higher temperature than the body of the chamber. Any subsequent, slow, cleaning expansions increase this temperature excess. Due to the low conductivity of the gas, this excess is slow to disappear.
(3) the time necessary for the condensant to diffuse through the volume and resaturate it.

In recent years, two techniques have been developed

to reduce the recycling times of cloud chambers. The first is the overcompression technique, developed
46 originally by Gaerttner and Yeater[46] and used since by other workers. In this system, after the fast expansion, the piston or diaphragm is returned to a position forward of the original, so that the gas in the working volume is overcompressed. This operation is generally carried out as quickly as possible, though Goldwasser
47 and Nicolai[47] used a slow overcompression when working with a heavy ionisation cycle.

The piston or diaphragm is left in the overcompressed state for some time and is then slowly returned to the original, pre-expansion position. This slow expansion serves to clean the chamber by depositing condensation nuclei.

In the work of Gaerttner and Yeater, it was hoped that the overcompression would evaporate the charged drops to such a size that their mobilities would be of the same order of magnitude as those of the ions. This would allow the clearing field to sweep the drops away.

In principle, by the correct timing of the various parts of the cycle, it should be possible to arrange that the gas gives up as much heat to the surroundings, when it is above equilibrium temperature, as it receives from them when it is below it. Thus the chamber should be at its working temperature as soon as the

slow expansion is completed.

The other method available to reduce the recycling time is that of fast recompression, first described by
48 Emigh[48]. In this, the piston or diaphragm is returned to its original position as fast as possible, after expansion. This is obviously similar to the overcompression method. It is, in fact, the overcompression system with an overcompression ratio of zero (the overcompression ratio is defined as the difference between the overcompressed and equilibrium volumes, divided by the equilibrium volume).

It is found that neither in the overcompression nor the fast recompression case is it possible to re-evaporate the drops completely. Barford reports that overcompression ratios of up to a half do not succeed in this. The overcompression technique does, however, allow a significant reduction in the time required for thermal equilibrium to be attained. A recycling period of 30 seconds has been achieved by Barford and French using a rectangular chamber of dimensions 30 x 40 x 20 cm., while for a smaller chamber,
49 diameter 9 in. and depth 2 in., Walker[49] has reached a recycling time of 10 seconds without difficulty. Gaerttner and Yeater, with a very shallow chamber, could recycle at 2.5 seconds.

It is generally agreed in the literature that the

overcompression cycle is the better of the two. The disadvantages of the fast recompression cycle are (1) it is not possible to make any cleaning expansions. (2) it is not possible, even in principle, to operate with a balanced heat cycle. There must always be a net gain of heat. Walker reports that, when operating his chamber on a fast recompression cycle, it was necessary to increase the expansion ratio above that required for the overcompression system, in order to prevent the loss of tracks, and that this was due to a gain of heat in the cycle.

Emigh agrees that this is so, but points out that the fast recompression system is mechanically simpler to construct and operate. Recently, however, simple overcompression systems have been demonstrated by Barford and French for a piston chamber, and by Walker for a diaphragm chamber. Barford in his review of the subject states that fast recompression is unlikely to be worth while in chambers where the deposition time (which depends on the vertical dimension of the chamber) is longer than the time for the conventional slow recompression.

The work done, and the conclusions drawn from it, which has been discussed in the previous section, has been applied only to chambers of near atmospheric pressure. In considering the application of one or

other of these techniques to the special case of the high pressure chamber, several points must be considered. While it may be possible to use the over-compression cycle with no net gain or loss of heat, there must also be considered the distribution of temperature within the working volume.

Consider the way in which supersaturation is destroyed in the main body of the gas (in conventional working of a cloud chamber). Williams[50] has treated this problem. He gives for the sensitive time τ of a cloud chamber, the expression

$$\tau = 0{\cdot}77 \frac{\rho s}{k(\gamma-1)^2}\left(\frac{V}{S}\right)^2\left(\frac{\delta r}{r}\right)^2$$

where ρ is the density, s the specific heat at constant pressure, k the thermal conductivity and γ the ratio of the specific heat of the gas. V and S are respectively the volume and surface area of the working volume of the chamber. δr and r are connected to the expansion ratio. The expansion ratio just necessary for track formation is 1 + r while the expansion ratio at which the chamber works is $1 + r + \delta r$.

If this theory is applied to the high pressure chamber used at La Marmolada, it predicts a sensitive time of the order of 200 seconds, as opposed to the measured value of 1.9 to 2 seconds. It is suggested that the discrepancy arises in the following way.

The time τ is that required for supersaturation in the body of the gas to be destroyed by conduction of heat from the walls into the thin layer of gas nearest to the walls. This layer expands, and the compression of the central mass that ensues is the principal method of heating it. However, after a period of the order of two seconds, convection currents arise, due to the difference in temperature between the thin layer nearest the walls and the main body of gas. These convection currents have the effect of carrying heat into the gas much more quickly than can be done by the Williams mechanism, and the supersaturation is quickly destroyed. In atmospheric chambers of normal size, the sensitive time is much shorter and the Williams mechanism will be able to destroy the supersaturation before the convection currents occur.

The convection currents have a second, very important, effect. The hotter gas will be carried to the top of the chamber, and the cooler gas to the bottom. Once the chamber is restored to its original volume, this distribution of temperature will be relatively stable and the gas as a whole will be at a higher temperature than the walls. The time which will be required to give up the excess heat may be estimated in the following way.

Temperature measurements have been made by Duff

and Morris[51] in a high pressure cloud chamber identical in all essentials to the chamber at Edinburgh. The results show that the gas at the top of the chamber is approximately 2°C above equilibrium temperature, while the gas at the bottom is near equilibrium temperature. The distribution of temperature across the vertical diameter of the chamber is not uniform. There is a small, nearly uniform temperature gradient between the foot of the chamber and a position approximately three quarters of the total height. Above this the temperature is greater.

For the treatment of the recovery time of the chamber, it will be assumed that at the beginning of the recovery time the gas is at the wall temperature over the whole volume of the chamber, except for a volume consisting of that part of the chamber above a plane, drawn parallel to the axis of the cylindrical volume at a height of three quarters of the internal diameter of the chamber. (For the purpose of comparison with Duff and Morris, the height used is that of the larger chamber at Edinburgh, i.e. 9 inches).

The change in temperature $d\theta$ in time t due to the Williams mechanism is given by

$$-d\theta = (\gamma - 1)1{\cdot}14 \frac{S}{V}(\theta - \theta_2)\left\{\frac{K}{\rho s}\right\}^{1/2}\sqrt{t} \qquad (1)$$

where γ, S, V, K, ρ, s have been previously

defined, θ is the temperature of the main body of gas and θ_2 is the temperature of the walls (assumed constant). It is assumed in the Williams expression that $d\theta$ is small compared to $\theta - \theta_2$. This is always valid in the case of the calculation of the sensitive time of a chamber, but is not valid in this case where we wish $d\theta$ to be nearly equal to $(\theta_1 - \theta_2)$, where θ_1 is the temperature of the gas considered after pumping operations cease. It is necessary to integrate (1) to give

$$\log_e \frac{\delta}{\theta_1 - \theta_2} = -(\gamma - 1)\left\{\frac{\kappa}{\rho s}\right\}^{1/2} 1{\cdot}14 \frac{S}{V}\sqrt{t} \qquad (2)$$

where δ is the temperature excess remaining after time t seconds, i.e.

$$\frac{\delta}{\theta_1 - \theta_2} = \exp\left(-c\sqrt{t}\right)$$

where

$$c = (\gamma - 1)\left\{\frac{\kappa}{\rho s}\right\}^{1/2} 1{\cdot}14 \frac{S}{V}$$

If only the Williams mechanism is operative, this expression will give the variation of the temperature gradient with time. Reference to figure 16 will show that the temperature gradient dies away more quickly than can be explained by the Williams mechanism. Since the gas configuration considered is relatively stable, the only other means by which the gas loses heat is by direct conduction. The calculation of the temperature drop by the combination of the expansion of the hot gas

and the conduction of heat directly, is complicated. It is required to solve rigorously the differential equation of heat conduction with an "adiabatic" term added. The solution of this equation is not known for the temperature distribution considered, though
52 Kluyver and Endt[52] give a solution for a cylindrical volume of gas with a given temperature distribution. The evaluation of the expression they give involves at least three tedious numerical integrations, and it is considered that the following approximate treatment will be as accurate as assuming that the Kluyver and Endt formula may be applied to the present configuration of temperature.

If we assume that the gas layer next the walls is in thermal equilibrium with a constant temperature gradient, the rate of flow of heat into the central gas is given by

$$\frac{dQ}{dt} = \kappa S \frac{d\theta}{dx} \qquad (3)$$

where $\frac{d\theta}{dx}$ is the temperature gradient. This heat flow will cause a temperature rise in the central gas of

$$\frac{d\theta}{dt} = \frac{\kappa}{\rho s} \frac{S}{V} \frac{d\theta}{dx} \qquad (4)$$

where all symbols are as previously defined. Hence

$$\frac{d\theta}{dt} = \frac{\kappa}{\rho s} \frac{S}{V} \delta(t')$$

where $\delta(t')$ is the average temperature excess of the central gas over the walls during the interval dt. In

order to take into account the thermal lag by which the temperature of the central gas will rise a finite time after the application of the heat, $\delta(t')$ was taken to be the temperature excess at the beginning of the interval.

Clearly it will not be possible simply to add the changes in temperature given by equations (2) and (4). In general, their combined effect is very complicated. However, after the cooling process has reached the stage where the rate of change of temperature is small it should be possible to assume that the conduction process and the expansion process act independently. In this case the temperature changes may be added. This was done for that part of the curve to the right of the four minute ordinate. From the integrated expression for the temperature-time variation on the Williams model, the temperature at any time is read off. Using the corrected temperature excess at the beginning of the previous time interval, the temperature change in that interval, due to conduction, is calculated. This change is then subtracted from the previously read temperature to give the final temperature at that time. For the initial point on this corrected curve, the temperature excess for the conduction correction was taken to be the temperature excess measured by Duff and Morris at that time.

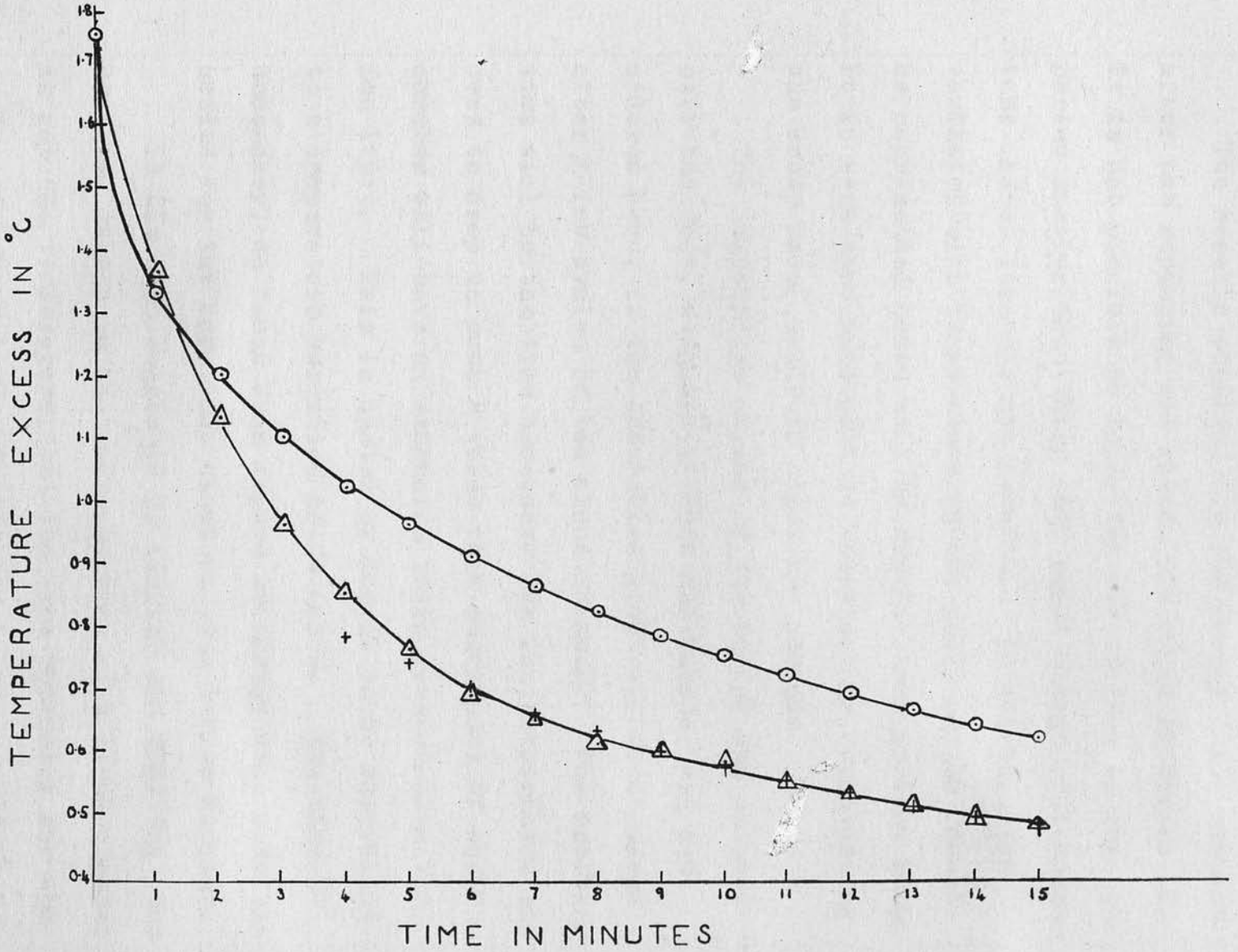

Figure 16. The variation of the temperature gradient across the chamber with waiting period.

Points △ are the experimental values of Morris and Duff.
Points ⊙ are calculated for the Williams mechanism alone.
Points + are calculated for the Williams mechanism corrected for conduction.

The results obtained for the period, four minutes after the repumping and later, are shown in figure 16. It is not possible to apply the calculation to the period earlier than this; the rapid change of temperature causes inconsistent results. In addition the variation with temperature in the early period should be represented quite well by the Williams process alone. It is seen that agreement is satisfactory (considering the crude model used) in these two periods.

The temperature excess of the top of the chamber over the foot, measured by Duff and Morris, and considered here, is the saturation gradient, established after a few cycles of the cloud chamber. The recovery time will be the time necessary for the temperature excess to drop to such a value that every part of the chamber will have an expansion ratio greater than the ion limit. This is quoted by Morris to be equivalent to a temperature variation of $\simeq 0.5^{\circ}C$. The time necessary, as found from figure 16, agrees well with that needed for the Marmolada chamber, viz. twelve minutes.

It has been suggested by Kluyver and Endt that the decisive factor in the recovery time of a cloud chamber is not the temperature, but the time necessary for the condensed vapour to resaturate the volume. They give an expression for the recovery due to this. The appropriate values to be substituted in their expression,

for the case of the high pressure chamber, are not readily available, but depending on the assumptions made their formula yields values between 10 and 20 minutes. It is known from the work at Marmolada that the chamber may be recycled at eight minutes with no evidence of incomplete saturation, though distortion is present. The reason for the discrepancy is probably that Kluyver and Endt neglected convection currents which would carry vapour much more quickly than the diffusion process. Kluyver and Endt were using a very small chamber, with a temperature recovery time of six seconds, and a vapour diffusion time of approximately twenty seconds. In these short times, convection is unlikely to affect matters to any great extent. It is therefore likely that the time necessary for the rediffusion of vapour is substantially less than the temperature recovery time.

The third factor which affects the recovery is the deposition time. In the chambers used, this is of the order of thirty seconds and may be neglected.

It seemed clear, on the basis of the previous discussion, that to reduce the recycling time significantly it was necessary to prevent the temperature gradient being set up. Clearly, the fast compression of the gas in the working volume would achieve this by reducing the time in which heat exchange took place

between the gas and the walls. However during the slow expansion of the overcompression cycle, a gradient would be set up in a way analogous to that occurring during the fast expansion. For this reason it was felt that the fast recompression system offered better prospects. This, in addition to the comparative ease with which the chamber could be adapted, caused fast recompression, not overcompression, to be selected.

In closing, it should be pointed out that in the case of the high pressure chamber it is, in practice, possible to work with no net gain of heat in the cycle.

Applying the Williams formula (1) to the interval between expansion and recompression it is found that the rise in temperature is $0.0997\sqrt{t}^{\circ}C$ in t seconds. For t = 0.7 second, this yields a temperature rise of $0.0834^{\circ}C$, which is quite negligible. This consideration will apply to any large chamber (except for multiplate chambers where $\frac{S}{V}$ is artificially large). For example in the previously mentioned chamber of Walker there is a temperature rise of $0.441\sqrt{t}^{\circ}C$ where t seconds is the time between expansion and recompression. Walker quotes t as 0.3 second, hence the rise in temperature expected is of the order of $0.25^{\circ}C$. This will clearly build up to some saturation value during a run of expansions made at regular intervals. This temperature rise will be the same throughout the main

body of the gas, since it occurs via the Williams mechanism. This will make it necessary for a higher expansion ratio to be used in the fast recompression system compared to that necessary when the gas reaches thermal equilibrium with the walls before the next expansion, and this is reported by Walker to be so. It is found with the Edinburgh chamber that with an argon filling (pressure 60 atmospheres) and pure ethyl alcohol as condensant the necessary expansion ratio on the fast recompression system is 1.05. This is the same as required for conventional working and is confirmation that no significant heat gain occurs over the cycle as a whole.

Chapter VIII.

THE EXPERIMENTAL SET-UP.

The cloud chamber used in the fast recompression experiments is very similar to that used in Italy. It is one of a pair designed by Mr. H. Tomlinson, of University College, London, who used the Marmolada chamber as a model. The new chamber is slightly larger than the old, being 9 in. in diameter and 9 in. deep. (See figure 17.) The walls of the chamber are 7 cm. thick and are constructed of "Weldanka P" non-magnetic, stainless steel. The walls are provided with openings for three small armour-plate glass windows, through which illumination is provided, two clearing field electrode leads, and a source plug, through which the beam from an accelerator may enter the chamber. The front window, through which the event is photographed, is much larger than that on the Marmolada chamber, being 21.5 cm. in diameter and 4 cm. thick. This allows a greater volume of the chamber to be photographed, and since the camera may be placed further away a greater depth of focus is obtained.

The chamber is volume-defined and the expansion is made by the movement of a rubber diaphragm between two perforated brass plates P_1, P_2. The perforationsof

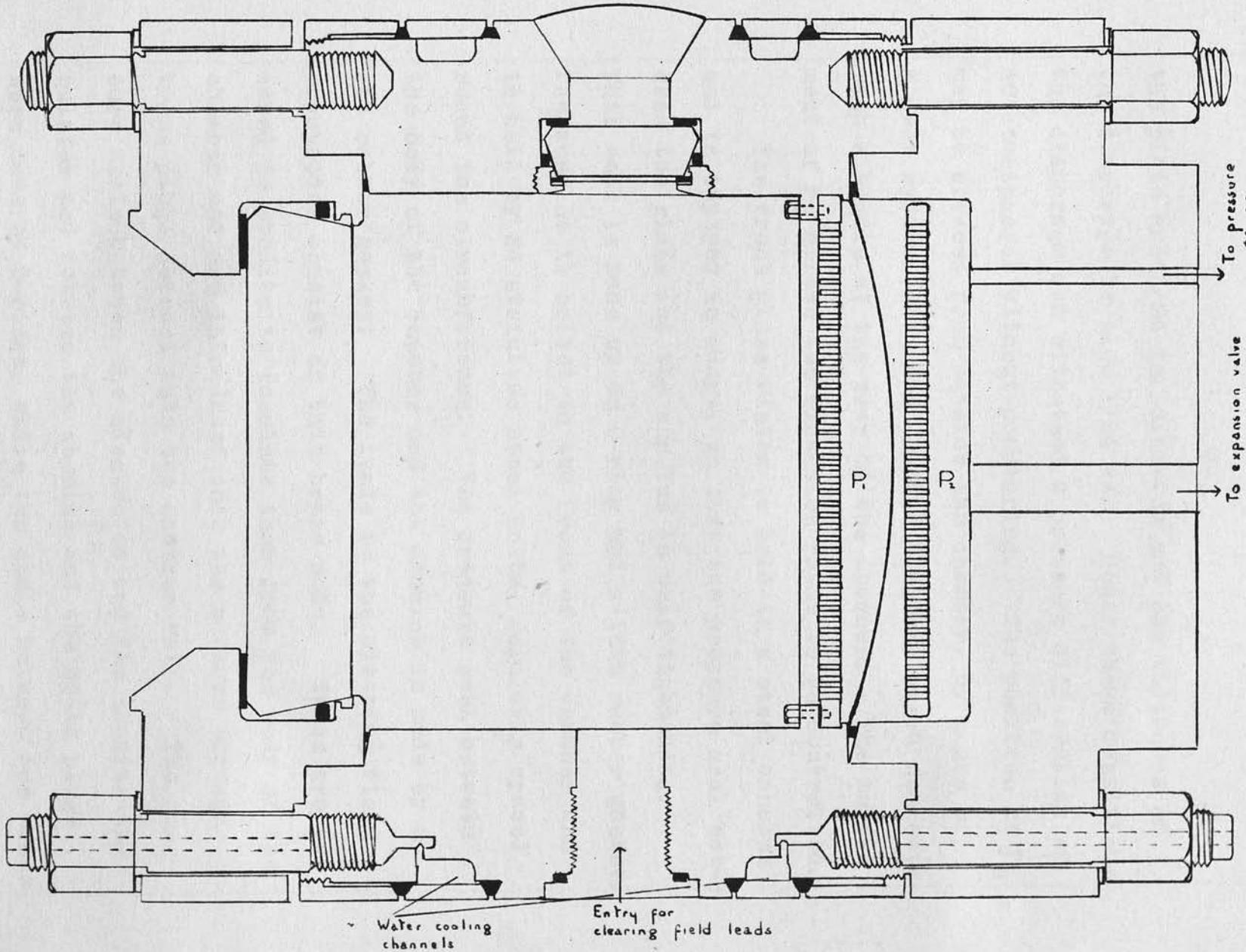

Figure 17. The cloud chamber used for the recompression experiments.

The scale is 1 cm. = 2.5 cm.

the plate are 1/24 in. diameter and the thickness of the diaphragm is also 1/24 in. Under these conditions the diaphragm can withstand a pressure differential of 40 atmospheres without puncturing. The position of P_2 may be altered from outside the chamber, by means of a gear system (not shown in the diagram) which connects with a handle at the rear of the chamber. The movement of P_2 allows the expansion ratio to be controlled.

The front glass window is held in a steel annulus and is tapered in shape, so that the pressure seal between the glass and the annulus is self tightening. This seal is made by an O-ring and a thin rubber gasket. The annulus is bolted to the front of the chamber and is held by 24 stainless steel bolts, regularly spaced round the circumference. The pressure seal between the body of the chamber and the annulus is made by a red rubber gasket. The leads to the clearing field electrodes consist of thin brass rods. These are encased in ebonite to insulate them from the body of the chamber and are introduced into the chamber through brass plugs screwed into the chamber wall. The pressure seals between the electrodes and the ebonite insulator and between the ebonite and the brass plugs were made by O-rings, while the seals between the brass plugs and the chamber wall were made by bonded seals.

A series of brass rods were mounted, parallel to

the axis of the chamber, between two ebonite rings of diameter slightly less than that of the chamber. They were divided into two groups, each of twenty-one rods. Electrical connection between members of a group was provided by soldering a piece of copper wire on to each rod in the group. This system formed the clearing field electrodes of the chamber. A positive electrostatic voltage was applied to one group, and a negative to the other, via the clearing field leads through the chamber wall. The chamber was normally operated with voltages of $\pm$ 800 volts on the electrodes.

A circular piece of black velvet, of the same diameter as the visible portion of the plate P_1, was mounted on a piece of fine mesh copper gauze, and placed a short distance in front of the plate. This served to make the gas flow laminar and it was also a suitable background for photography. The clearing field electrodes, the inside walls of the chamber and the outside of the metal annulus holding the front window were painted with an alcohol resisting, matt black paint, in order to prevent light being scattered into the camera lenses. To prevent light being reflected from the velvet surface, the inside of the illumination ports was partially blocked off by Apiezon Q-compound, in such a way that light did not fall on the velvet.

The various parts of the chamber were connected to

pressure gauges by means of $\frac{1}{4}$ in. copper piping. The connection between the front chamber and its pressure gauge was made via a needle valve. This valve was kept shut during the operation of the chamber. If this was not done, the large degree of over-expansion produced in the piping caused the formation of dense cloud which raised the level of the background condensation.

Two of the bolts securing the front annulus had holes drilled down their centres. These communicated with a channel running round the body of the chamber. Water could thus be made to flow round the chamber walls, in order to maintain the temperature steady. A similar water channel was present in the walls of that part of the chamber behind the diaphragm.

When the chamber was first assembled, it could not be made to work satisfactorily. The level of background condensation was such that tracks could not be properly distinguished. It was eventually discovered that the trouble arose whenever the diaphragm was allowed to touch the plate P_1. If the diaphragm was not allowed to do this, but was floated, good quality tracks were obtained. Similar trouble was experienced with a low pressure chamber in this department. This type of "dirt" had never been encountered in the Marmolada chamber, even though it contained the same

type of rubber. Towards the end of the experiment in Italy, this difficulty was experienced after replacing the old diaphragm with one made from red rubber, newly brought from Britain. It was found that a diaphragm made from rubber purchased in Italy worked satisfactorily. A supply was brought back to Edinburgh and used in the new chamber. Since then good quality tracks have been easily obtained.

The reason why the red rubber contaminated the chamber is not known. It was found to be a function both of the rubber and the metal plate. When the plate was half faced over with Tufnol, a definite improvement was noted. Good quality tracks could be obtained, but two cleaning expansions were necessary. With the Italian rubber no cleaning expansions were needed.

The Recompression System.

The recompression system is shown diagrammatically in figure 18.

The adiabatic expansion was made by establishing a pressure difference across valve V_1 and allowing V_1 to open suddenly. The sudden pressure drop in the volume behind the diaphragm caused it to move from its initial position of being pressed hard against plate P_1, to being pressed against the back plate P_2, with a consequent expansion of the volume in front of the diaphragm.

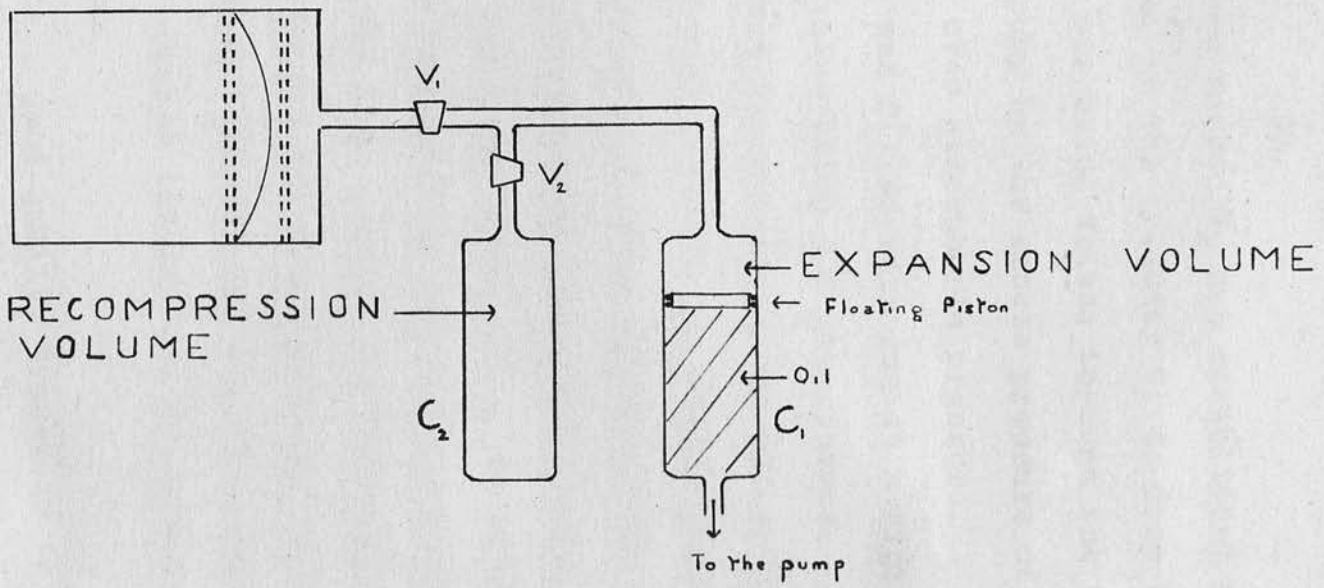

Figure 18. Diagram showing the recompression system.

Not drawn to scale.

The pressure difference across V_1 was established by allowing the oil level in the cylinder C_1 to drop by a suitable amount, the oil being driven through the solenoid valves of the pump by the excess pressure of the gas in the cylinder, over atmospheric pressure.

The cylinder C_2 was filled with gas at a high pressure, a typical value being 100 atmospheres. After the expansion, the fast recompression was accomplished by opening V_2. The high pressure gas passed through V_1 and pushed the diaphragm forward against plate P_1. V_1 was then shut, thus isolating the cloud chamber. The pump raised the oil-level in C_1 until the pressure in the two cylinders reached that necessary for the recompression. V_2 was then closed, and the oil in cylinder C_1 allowed to run out into the pump, until the pressure in C_1 was that required for the expansion. The system has then reached the initial state and the cycle may be repeated.

In order to obtain good quality tracks it is necessary that the expansion should be as fast as possible. The recompression must also be fast, to reduce the time that the gas in the front volume of the chamber is below wall temperature. A large mass of gas must pass through the valves, in the expansion and compression processes, and consequently the apertures of the valves must be as large as possible. The

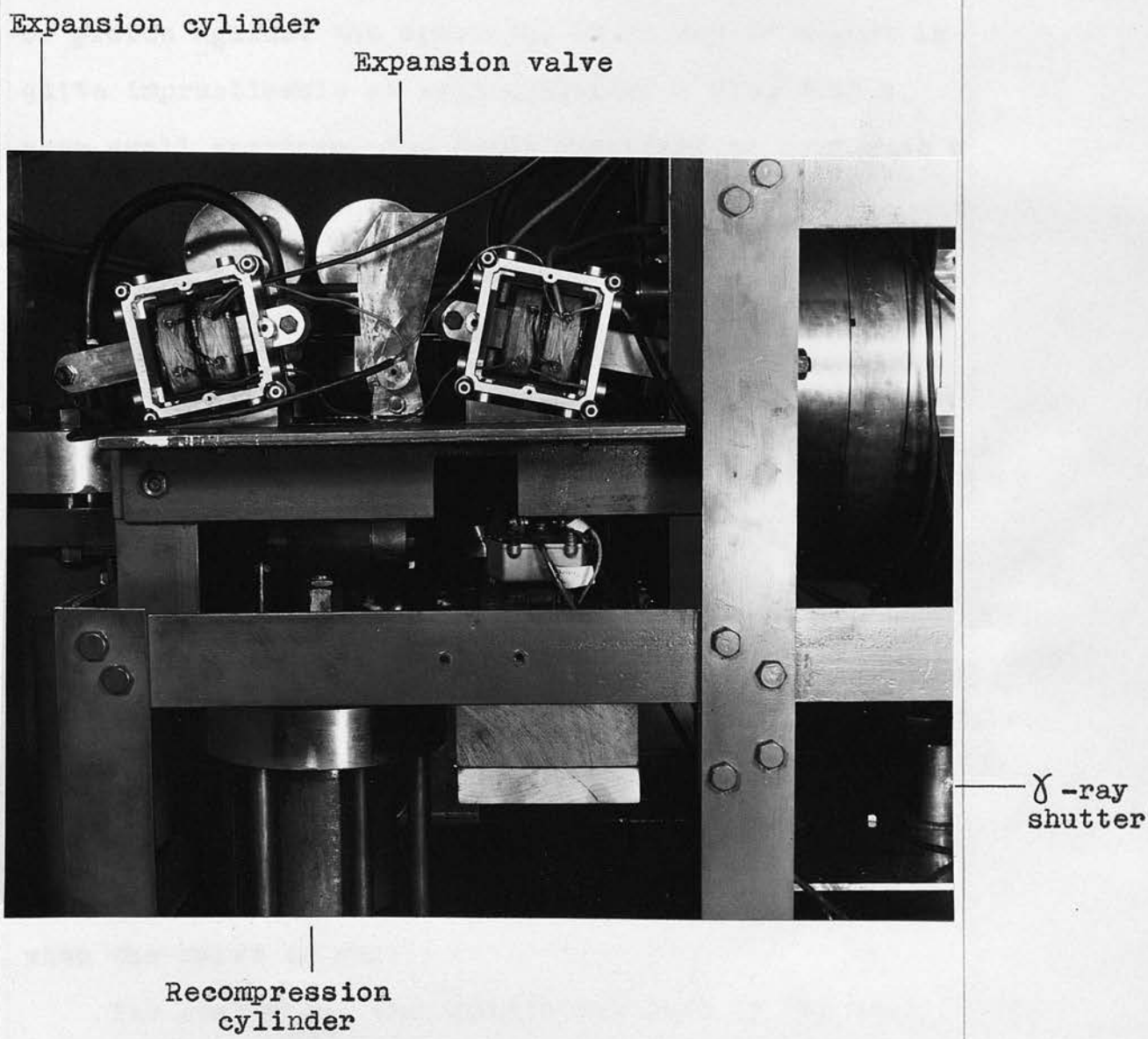

Figure 19. The cloud chamber showing expansion and recompression cylinders and valves, and the shutter for the γ -ray source.

conventional type of cloud chamber valve, in which the seal against the pressure is made by holding some sort of piston against the aperture, by an electromagnet, is quite impracticable at high pressure. Even with a very small aperture, the force necessary to hold such a valve shut is of the order of 200 lbs. weight. In the Marmolada chamber the valve was held shut by a steel screw, and the valve was opened by the rapid rotation of the screw by a spring. It was desired to use a larger aperture than that of the Marmolada valve. A new type of valve was designed by Dr. G.R. Evans and is shown in figure 20.

The seal is made by a metal cone against a metal seating. The spindle is made of stainless steel, and the body and seating of the valve are brass. Since both ends of the spindle are at atmospheric pressure, there is no net force on the spindle in any position (except for a very small force on the ring of contact when the valve is shut).

The seal along the spindle was made by two Gaco internal distributor seals, while the seals between the component parts of the body were made by Klingerit washers. The valve can be opened or shut by rotating a handle attached to one end of the spindle, through a quarter turn, by means of a large electromagnet.

This valve has proved to be completely satisfactory.

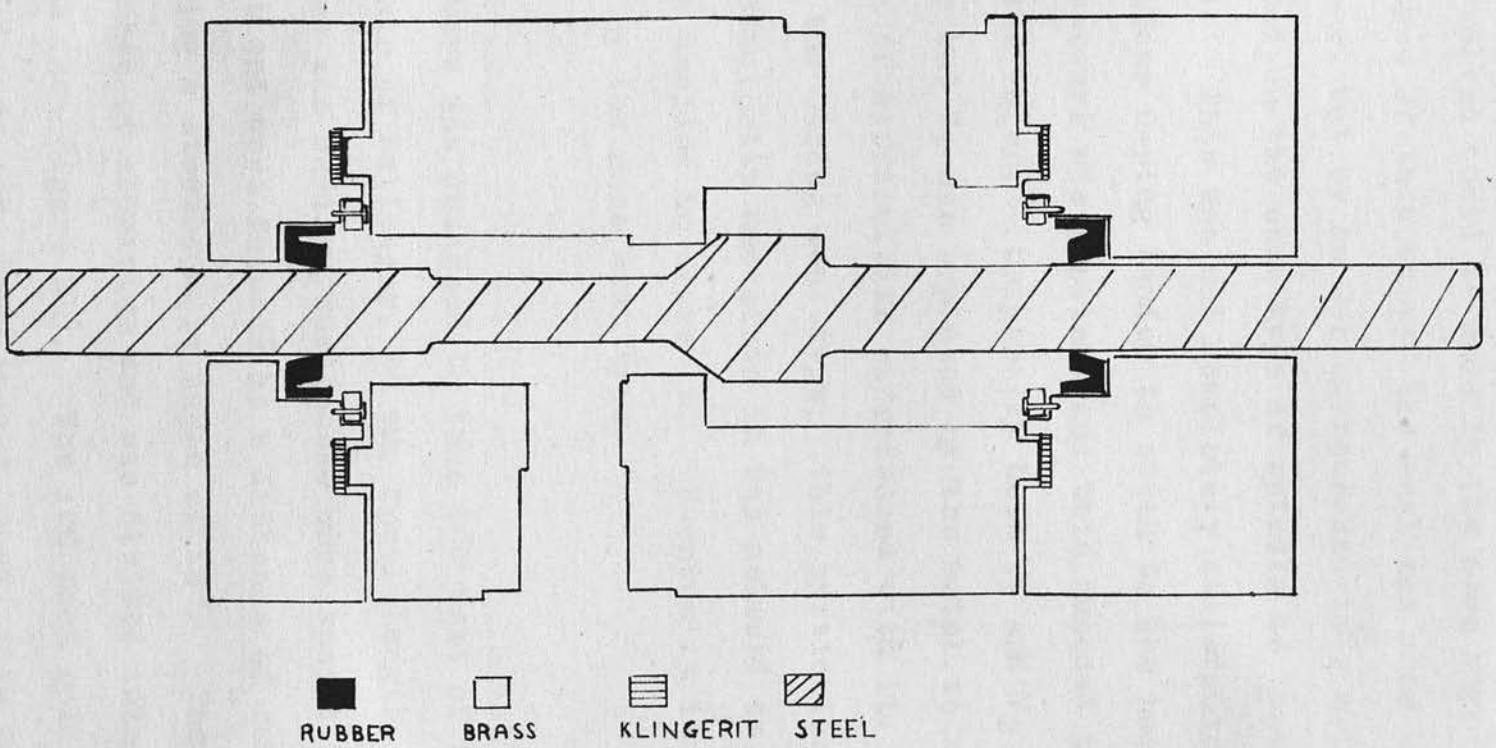

Figure 20. The expansion valve drawn full scale.

The aperture of the valves used is half an inch, but much larger valves could be made in the same way. In an earlier type of this valve, the seal was made not by the metal cone, but by an O-ring recessed into a flat piston mounted on the same type of spindle as that finally used. This was not completely satisfactory, since the rubber O-ring tended to stick to the brass face when pressure was applied, and this impeded the opening of the valve. Originally both V_1 and V_2 were of this type but V_1 was replaced by the metal to metal seal because of difficulties experienced with it. V_2 is still of the O-ring seal type; this particular valve worked satisfactorily and since it was awkward to remove, it was decided to leave it. Eventually it is to be replaced by the cone seal type.

The Camera.

The camera was designed to take 100 feet of film. A matched pair of Dallmeyer, 35 mm. focal length, anastigmat lenses was used. The lenses were spaced three inches apart and were focused at a distance of fourteen inches, giving a stereoscopic angle of 12°. The camera was made of aluminium and was divided into three compartments (see figure 21). The 100 foot roll of film was placed in one, four inches broad, five and a quarter inches long and three and a quarter inches deep. It passed between two ebonite rollers and through a

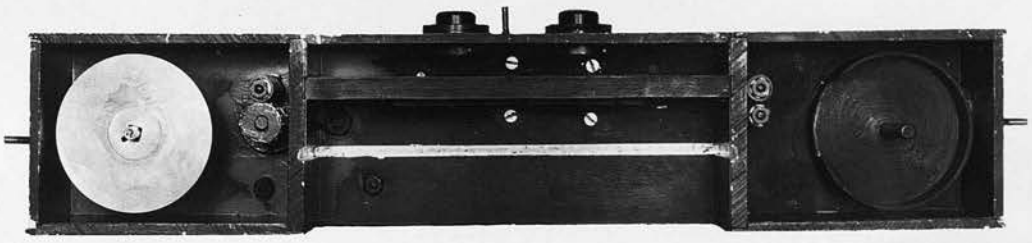

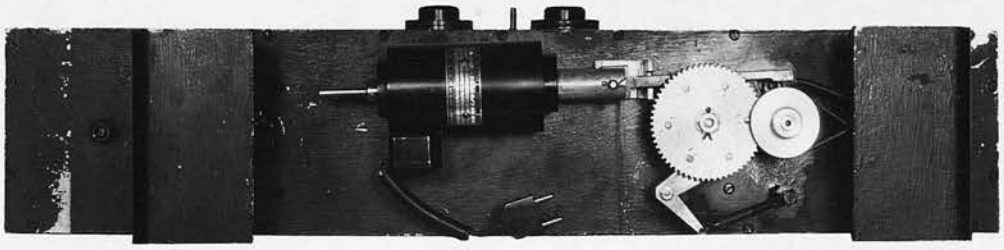

Figure 21. The camera used in the recompression experiments showing the general plan and the wind on mechanism.

slot into the camera proper. An ebonite panel had a shallow channel milled out, in which the film slid. Two long, rectangular slots were cut in the panel. The size of the image on the film was defined by two pieces of ebonite, each with a hole 2.7 cm. by 2.5 cm. cut in them. These pieces were mounted, one over each of the slots in the ebonite panel, so that their position in the horizontal direction could be varied. An ebonite spacer was inserted between them, in order to define their positions. In this way, the separation of the film gates could be easily varied. When adjusted, the separation was three and a quarter inches. The ebonite panel was mounted in slots cut in the aluminium walls separating the three compartments and was parallel to the front of the camera.

The lenses were mounted in front of the film gates, positioned so that the images of the cloud chamber could pass through them, and fall on the film. The focusing adjustment was obtained by mounting each lens inside a hollow brass tube, threaded on the outside. Suitably sized holes, to fit the tubes, were drilled in the front wall of the camera, and tapped to receive the tubes. The tubes were screwed into the aluminium wall, the distance of the lenses from the film gate, and hence the focusing, depending upon how far in they were screwed. The position of the lens mount was fixed by

screwing a brass collar over that part of it inside the camera, until it was hard against the aluminium wall. These also served to exclude light. The outer thread on the lens mounts is also used to screw on a brass cap. This protects the lenses during transit, and prevents light entering the camera when it is not being used.

The film was held flat against the film gates by an ebonite pressure plate pushed against the film by two springs. The plate was mounted on a rectangular piece of aluminium which slipped into slots cut in the dividing walls. It could thus be easily removed for the purpose of loading the film.

The film passed through a second slot into the third compartment. The perforations of the film were engaged in the teeth of a standard film sprocket, which was used to wind on the film. The take-up spool was mounted on a spindle with a ball-bearing, and was close to the sprocket. After the film was passed round the sprocket, it was threaded into a slot in the take-up spool. To facilitate this, the top flange of the spool could be unscrewed, so that the slot could be easily reached by the hands. The three compartments were closed on the top by slide lids which could be locked in position by nuts. The inside of the camera was painted black to prevent the reflection of light.

The wind-on mechanism was completely automatic.

A large gear wheel was mounted below the camera, and six pins were mounted regularly on its upper flat surface. The armature of a magnet was loosely jointed to a hook, which lay against whichever pin happened to be in the correct position. On the opposite side of the wheel, an L-shaped piece of brass fitted between two pins and was held in position by slight tension from a spring. When the magnet was energised, the hook pulled on the pin, and the rotation of the gear wheel moved the L-shaped cam from between its pins. When the magnet was de-energised, the spring pulled the cam back between the next pair of pins, while a second spring pulled the hook back behind its pin, the loose jointing allowing the hook to slide over the pin and regain its former position. The action was a positive one, since if the stroke of the magnet was slightly too great, or too small, the cam forced the gear wheel back to its correct position. At each stroke of the magnet, the gear wheel turned by exactly one sixth of a revolution.

The large gear wheel is enmeshed with a smaller, chosen to give half a revolution per stroke of the magnet. This gear is fixed on a shaft from the sprocket, so that the sprocket turns by half a revolution each time. A friction drive connects this shaft to that of the take-up spool. In this way the take-up

spool winds on until the film is taut and then stops.

The magnet is bolted to the underside of the camera. It is a Westool solenoid, rated at 110 volts D.C.. In this work it is run off 250 volts D.C. and a mains rheostat is placed in series with the coil to give an adjustment for the speed of the stroke. It is found that, if the film is wound on too quickly, the take-up spool does not revolve fast enough and the film lies loose in the camera. Two legs have been fixed to the base of the camera, so that the wind-on mechanism is clear of the surface the camera stands on.

The camera is mounted on an aluminium stand in front of the chamber. Two stops define the position of the camera and it can be locked in position by two wing nuts. The lenses are used at f/8. It is found that at this aperture, the depth of focus is quite satisfactory. The film used is Ilford 5G91. Up to 100 feet of film can be processed using the Kodak spiral film developer and drier.

As in the Marmolada experiment, the chamber is housed in a fibre board hut, the walls of the hut having an air space between them. The hut is thermostatted by a system similar to that previously described, and the hut is maintained at a temperature of 16°C.

Chapter IX.

THE CONTROL SYSTEM OF THE CLOUD CHAMBER.

(1) Operations required in the cycle.

The following operations are required in the fast recompression cycle.

(a) Open V_1 and short the clearing field to earth.

(b) Take the first photograph.

(c) Wind on the camera.

(d) Take the second photograph.

(e) Open V_2 to recompress the front chamber.

(f) Shut V_1.

(g) Repump the recompression cylinder and shut V_2.

(h) Let oil out from the expansion cylinder to preset level, wind on the camera, and restore the clearing field.

(i) After a suitable delay, reset the chamber for expansion.

The control system to be described was designed to carry out the above sequence of operations automatically.

(2) General.

Since the object of the fast recompression technique was to reduce the recycling time of the high pressure cloud chamber to such an extent that it could

be used as a particle detector with the new high energy accelerators, it was decided that the control circuitry must be very reliable in operation. For this reason, all parts of the control system were designed as simply as possible.

The cycle was controlled by a uniselector. This instrument has a number of fixed pins, arranged in banks (in this case two). A movable contact is associated with each bank and can make contact with each pin of the bank in turn. The movement of the rotating contact is effected by passing a current through the coil of the uniselector for a short period. The action of the uniselector is thus that of a many-position switch.

One bank of pins is used to switch appropriate values of resistance into the timing circuit, which controls the current to the uniselector coil. The second, separate, bank of pins controls the operation of a number of Post Office relays. These relays, in turn, control the various operations required in the cloud chamber cycle, either directly through their contacts or, where made necessary by virtue of the high voltages or currents requiring to be switched, by means of auxiliary, specialised, relays.

(3) <u>The Timing Circuit</u>. (see figure 22).

The timing circuit used is the simple thyratron timer. The discharge of the thyratron is prevented by

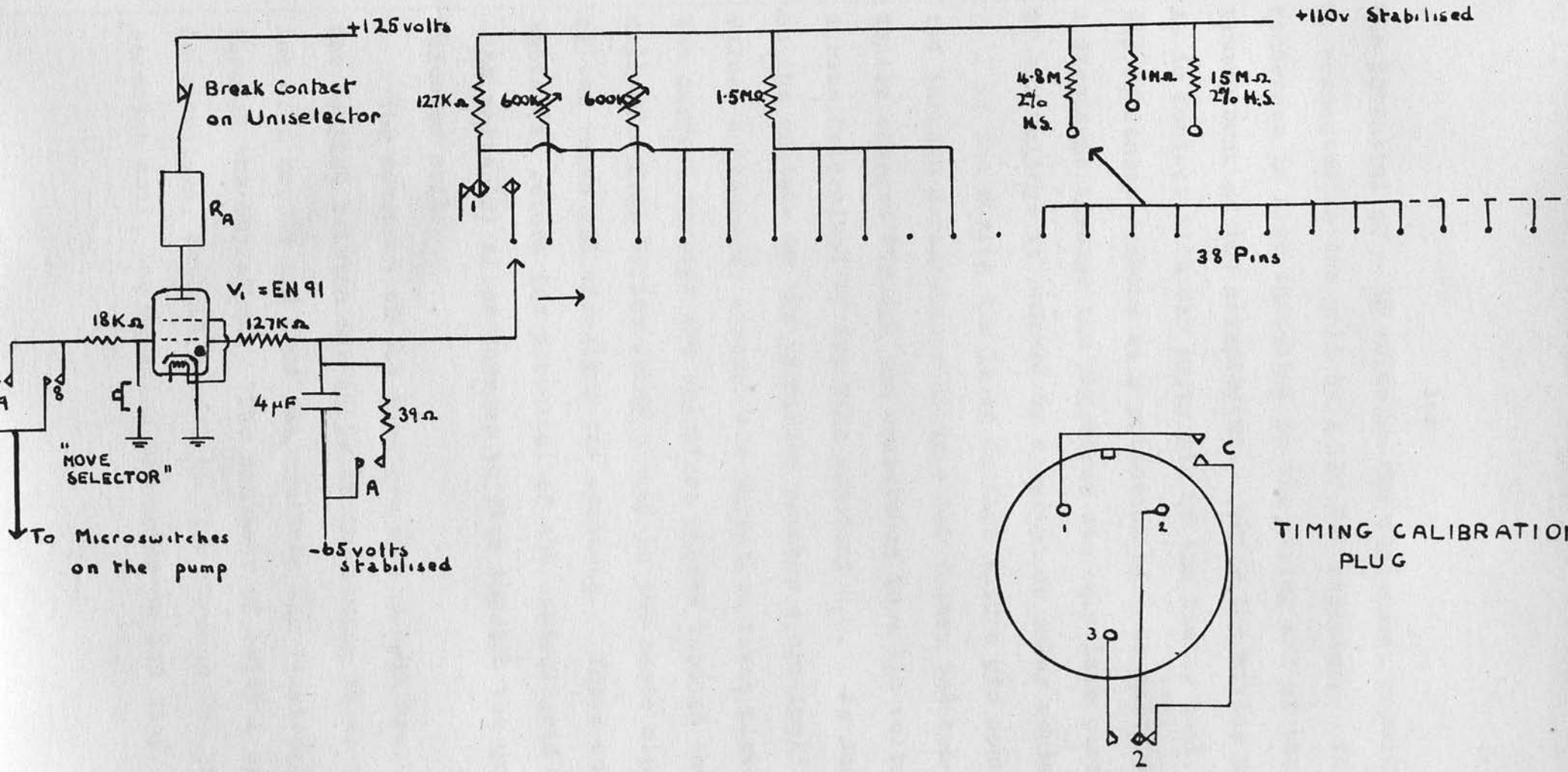

Figure 22. The timing circuit and connections for its calibration. The numbers refer to the relay to which the contact belongs.

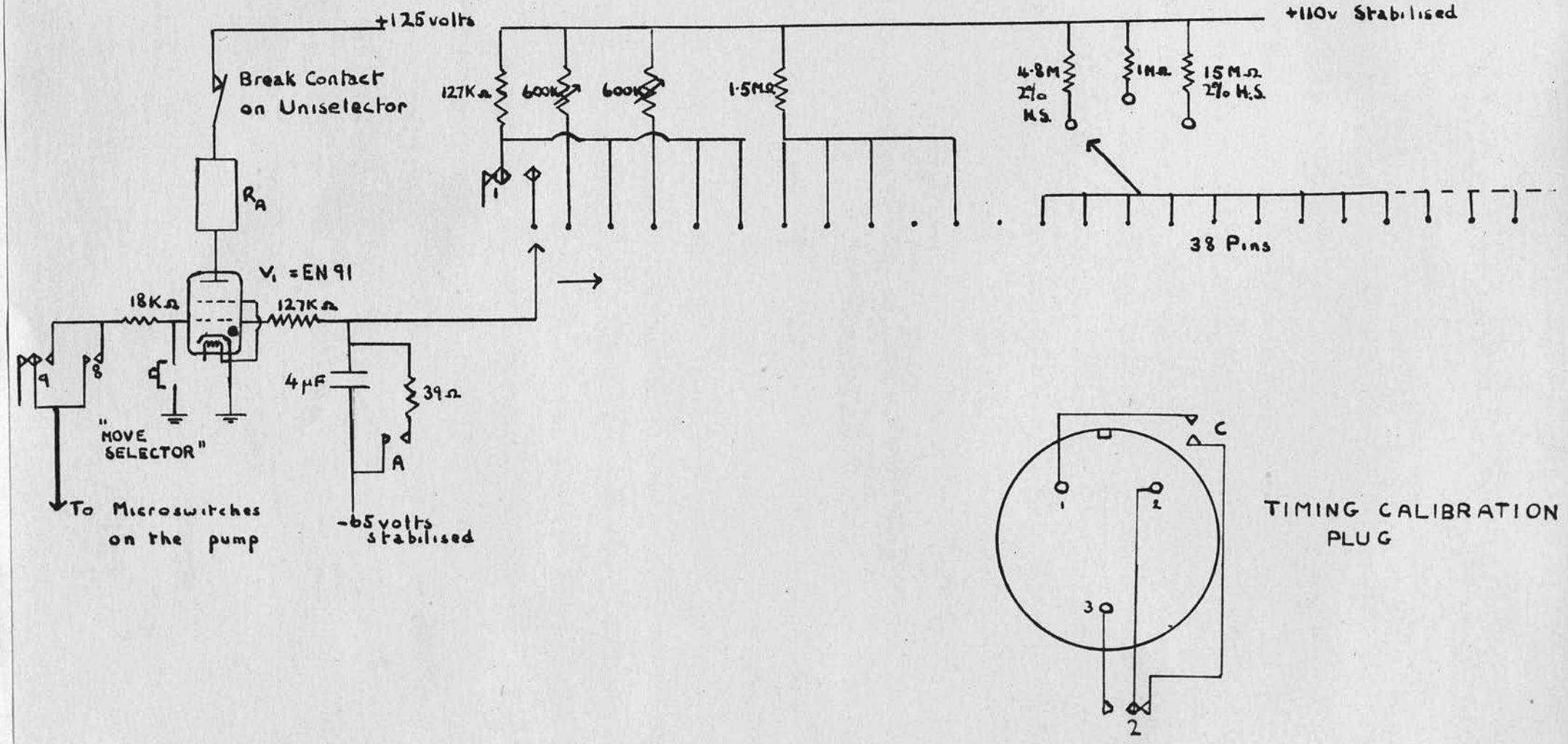

Figure 22. The timing circuit and connections for its calibration. The numbers refer to the relay to which the contact belongs.

the potential of - 65 volts on the condenser, capacity C, connected to the grid by a 127 KΩ resistor. This condenser is also connected to the moving arm of the timing bank of the uniselector. While the moving arm is in contact with the empty pin of the timing bank, the condenser remains at a potential of - 65 volts and a discharge through the thyratron can only take place if this voltage is removed by a switch or relay contact.

If the moving arm is in contact with a pin connected through a resistance R_1 to + 110 volts, the condenser charges through the resistance to + 110 volts at a rate determined by the time constant R_1C. As soon as the voltage on the condenser reaches a critical value, a discharge through the thyratron takes place. The current through the thyratron passes through the coil of a Post Office relay placed in the anode circuit of the valve and energises its contacts. These contacts (a) return the potential of the control grid to - 65 volts (b) allow current to flow through the uniselector coil.

The movement of the armature of the coil breaks the contact between the anode of the timing valve and the H.T. supply and thus extinguishes the discharge through the thyratron. The contacts of relay A are de-energised, current ceases to flow through the uniselector coil, the rotating arm moves on one step, and

the H.T. supply is reconnected to the anode of the valve, a further discharge being prevented by the negative potential on the control grid. The condenser charges up again at a rate determined by the new resistance R_2 and the whole cycle is repeated.

The accuracy with which this type of circuit operates depends on the constancy of the critical voltage on the control grid which will just prevent the discharge. Information sheets supplied by the manufacturer for this valve show that this voltage may vary by as much as two volts. The effect that this variation has upon the final accuracy of the circuit may be minimised by a suitable choice of the positive and negative voltages between which the timing condenser charges.

With the voltage used for the H.T. supply to the timing valve (125 volts), the critical voltage for discharge is of the order of - 2 volts. The rate of charging through a resistance of a condenser is small when the voltage on the condenser is nearly that towards which it is charging. In this case a small increase in the critical voltage, which the condenser is required to reach before the thyratron strikes, will entail a large error in the time at which the valve conducts. This would correspond to the choice of, say, earth potential for the upper voltage to which the

condenser charges.

If, however, the upper voltage is chosen to be much greater than the critical voltage, the critical voltage will be reached when the condenser is charging at a high rate and a small change in the critical voltage will entail a small error in the time of striking of the thyratron. For this reason the voltages between which the condenser charges were chosen as + 110 volts and - 65 volts. In addition these voltages were obtained from a stabilised power pack, using two 150B2 inert gas stabilisers in series across the output of the smoothing circuit.

The calibration of the timing circuit (discussed in the next section) shows that for delays of one second or greater the variation is less than one per cent. while for the shortest delays used (0.4 second) it was not greater than two per cent.

(4) Calibration of the Timing Circuit.

If a pulse generator is connected to a scaling unit through a relay contact, the scaler will record counts only if the relay contact is made. If the frequency of the generator is known, the total number of counts recorded is a measure of the time for which the contact was made. This principle was used to calibrate the timing circuit. A pulse generator and scaler could be connected via a plug at the side of the

uniselector chassis to relay contacts, as shown in figure 22.

By connecting the generator to pin 2 and the scaler to pin 1, the delay between the start of the cycle and the taking of the first photograph could be measured. The delay between the first photograph and the second photograph could be calibrated by transferring the scaler to pin 3.

The pulse generator was used at an average frequency of 6882 cycles/minute. This frequency was measured before the start of the calibration, between the calibration of the first and second flashes and after the completion of the calibration. The individual frequencies thus measured did not vary from the mean value by more than one per cent.

The two delays being considered were continuously variable. At each of ten settings in the range, six determinations were made of the counts recorded by the scaler. At settings near the maximum delay the standard deviation in the number of counts recorded was less than the variation in the frequency of the generator. At settings near the minimum delay, the standard deviation (as determined from the residuals of the six individual readings) was one per cent. Taking into account the variation of frequency of the generator, the overall accuracy of any point in the calibration is better

than two per cent.

The method used for the calibration allows the delays of the photographs in a run to be measured individually if desired. In addition it is simple to operate and is capable of higher accuracy than was required in the present work.

(5) The Triggering System. (see figure 23).

The cycle is started by the discharge of a second thyratron. This valve has two relays in its anode circuit. These relays open the expansion valve, remove the clearing field and start the uniselector cycle by connecting the grid of the timing thyratron to 110 volts via a 127 KΩ resistance. The remainder of the operations of the cycle are performed by the relays controlled by the uniselector.

The triggering thyratron may be fired by a positive pulse from the "COUNTER-CONTROL" input, by a switch on the front panel, for test purposes, or by a relay contact when the chamber is cycling continuously.

When the switch "COUNTER-CONTROL OR RANDOM AUTO" is open the grid is held at a negative voltage by the potential divider formed by the 10 MΩ and 1 MΩ resistors. When the timing circuit returns to the quiescent state, relay 11 is energised and the counter-control input is connected to the triggering circuit.

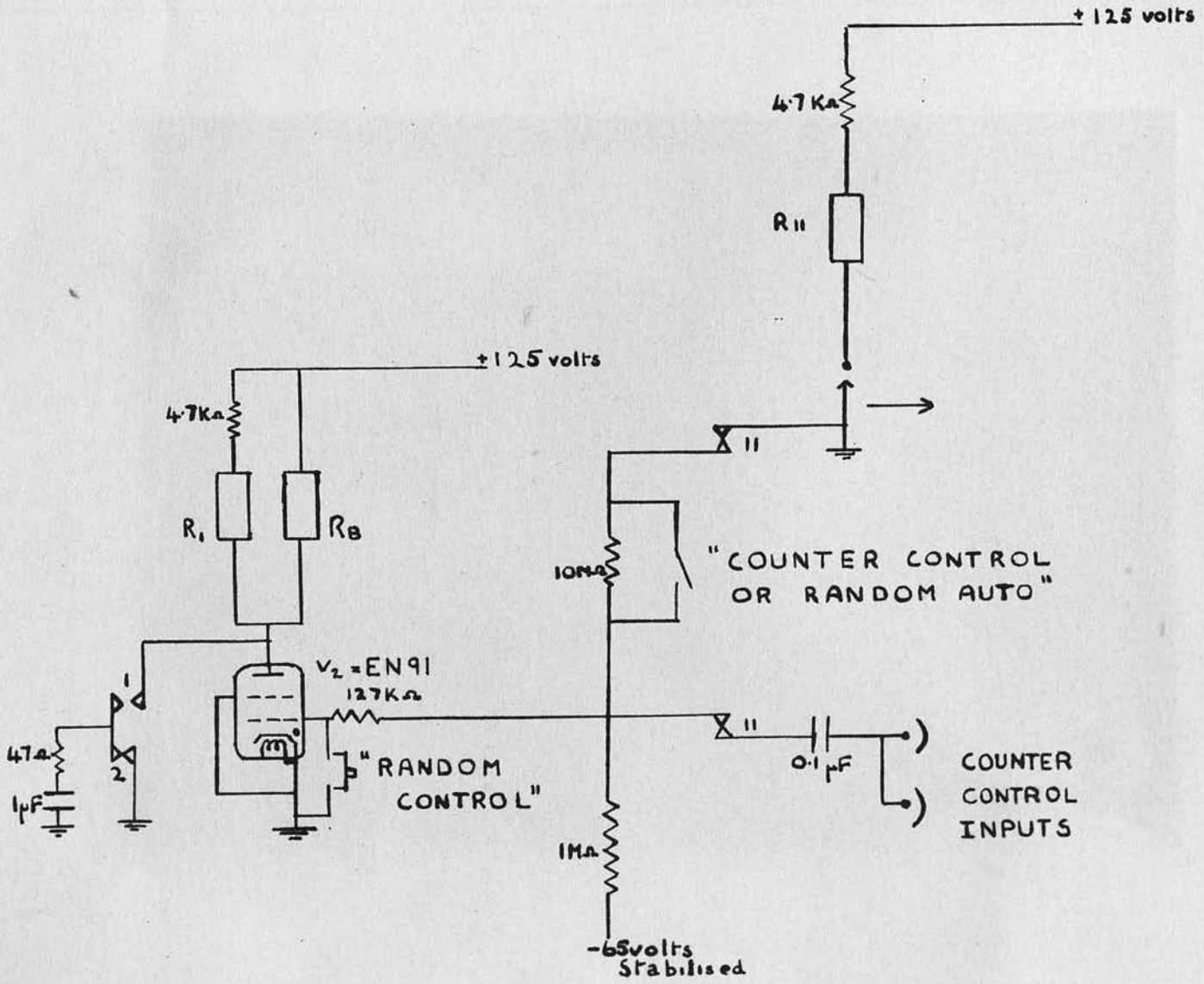

Figure 23. The triggering circuit. The numbers refer to the relay to which the contact belongs.

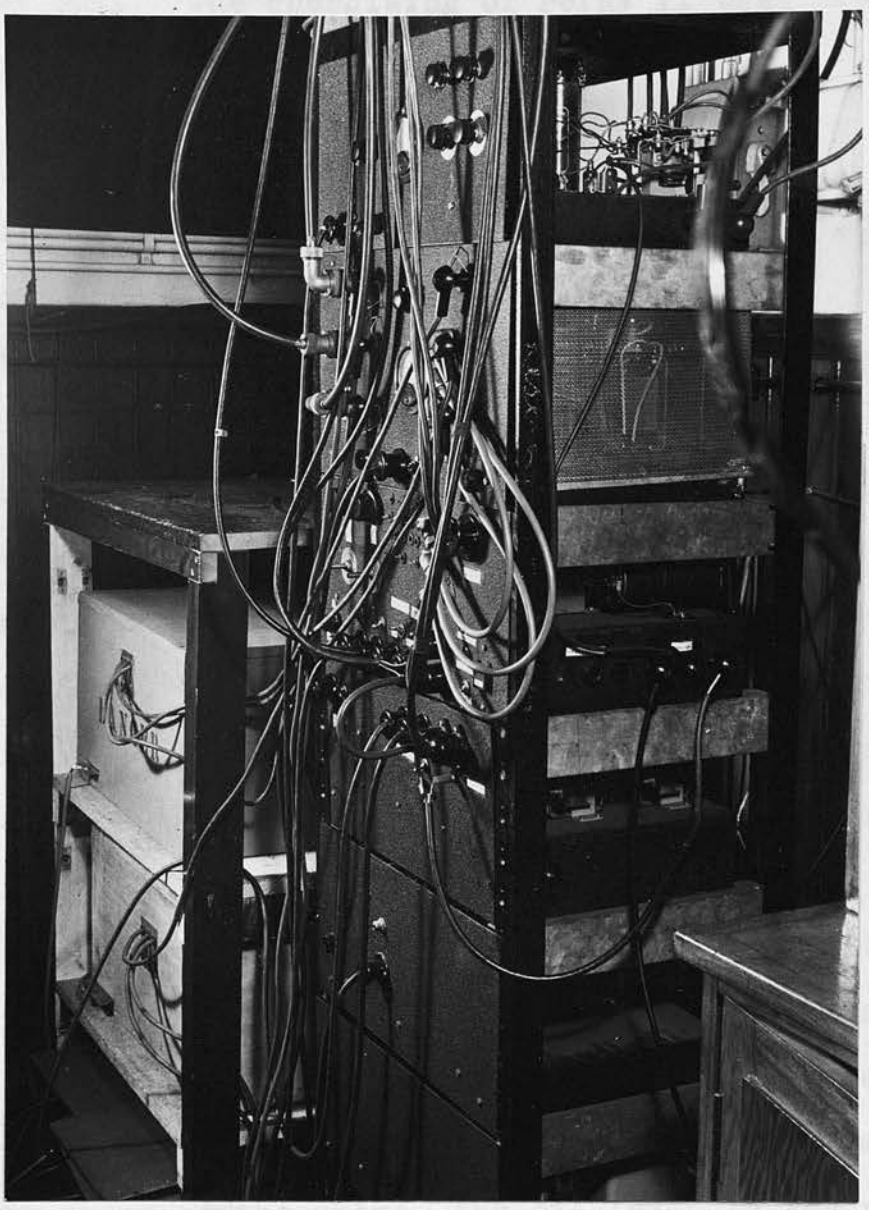

Figure 24. The control panel.

When the switch is closed, the 10 MΩ resistor is shorted out. The energising of relay 11 then fires the triggering thyratron and starts the cycle.

(6) Control of the High Pressure Pump.

In the original system, the operation of the pump was controlled by a pressure gauge, equipped with two adjustable contacts. When the relays controlling the motor and the solenoid valves of the pump were energised, the timing circuit was disconnected and the operation of pumping or letting out of oil was continued until the moving pointer touched one of the preset contacts of the gauge. This shorted the grid of the timing thyratron to earth and caused the uniselector to move on one step, de-energising the relay and stopping the operation.

It was found that the pressure regulation obtained with this system was not satisfactory, since the needle of the gauge tended to move in jerks, with a consequent uncertainty in the pressure at which contact was made.

In place of the above, the oil level in the pump was used as a pressure regulator. A float was introduced into the reservoir cylinder of the pump. This float carried a vertical rod to which two circular discs were attached. The positions of the discs on the rod could be adjusted.

Once the pump was started by the uniselector

circuit, the oil level dropped until the lower of the two discs pressed against the arm of a microswitch. The making of the microswitch moved on the uniselector in the same way as the pressure gauge had done in the previous system. The control of the oil level in the expansion cylinder of the chamber was effected by the upper disc in exactly the same way.

Since this is a control of oil levels rather than a direct pressure control, it is apparent that the rapid cycling of the gas in the portion of the chamber behind the diaphragm causes the temperature, and consequently the pressure, of the gas at the fixed oil levels to rise. This, in turn, causes the excess pressure between the back and front portions of the chamber after recompression to increase steadily during a continuous run of expansions. The effect is serious only at the faster rates of cycling, but, even at a total recycling period of two minutes, the back to front differential pressure does not reach a dangerous level in a run of fifty photographs.

(7) Photography.

Due to the long sensitive time of the high pressure chamber (approximately two seconds), it is possible to take a photograph, wind on the camera, and take a second photograph of the same event. This gives a method of deciding whether distortion is present or

not. Without some such system, this cannot be easily decided, unless the distortion is very bad, due to there being appreciable multiple scattering on many tracks. For this reason, facilities for the double flash were provided in the control system.

Illumination for the photograph was obtained by discharging condensers of total capacity 99 μF, charged to 2000 volts, through each of three flash tubes (Mullard LSD7; xenon filled). Since the charge on the condensers would be lethal if accidentally touched, they were contained in a totally enclosed wooden box, while the power pack which charged them was completely surrounded by wire mesh. In addition the charged condensers were not connected to the lamps until just before their discharge. Immediately after discharge the relay connecting them to the lamps was de-energised and a second bank, charged from a separate circuit, was connected in their place to provide the energy for the second flash. This bank was also disconnected during the recharge. This procedure reduced to a minimum the possibility of accident.

In the original runs of photographs, the sequence was altered to (1) expansion (2) first photograph (3) recompression (4) second photograph. It was hoped that information as to gas motion in the chamber and the re-evaporation of drops would be obtainable in this

way. The results will be discussed in a later section.

(8) Facilities Available.

The complete control system allows the cloud chamber to be used either as a counter-controlled chamber or as an automatic chamber, taking photographs at a preset rate. The recycling time of the chamber can be selected by a switch to be two, five or fifteen minutes. The delay between expansion and recompression can be varied continuously between 0.5 second and 2.35 seconds. One or two photographs of the same event, with the appropriate delay times also continuously variable, may be taken as desired.

For testing the chamber under the heavy ionisation conditions produced by accelerators, it is possible to allow a beam of γ-rays from a 5 millicurie Co^{60} source to enter the chamber for a period of approximately 0.2 second, at an appropriate part of the cycle. The source is contained in a large lead block. The lead immediately above the source may be pulled away for a short period by a magnet controlled by a relay in the uniselector circuit, and returned to its position above the source by a strong spring, when the magnet is de-energised.

Two safety devices are incorporated.

(1) If the expansion valve is held open after the recompression, the pumping operations do not start and

the cycle stops.

(2) To avoid damage to the flash condensers, the second bank cannot be switched on to the lamps unless the first bank is reconnected to its charging circuit.

The control system has been found to be reliable in operation and can safely be left running unattended, for a period of several hours.

Chapter X.

THE EXPERIMENTAL RESULTS.

The behaviour of the chamber under fast recompression conditions was examined for two filling materials, viz. nitrogen and argon. The chamber was filled to a pressure of 60 atmospheres, and pure ethyl alcohol was used as the condensant. The expansion ratio required for good tracks in argon was 1.05, while that for nitrogen was 1.09 (both at a temperature of 16°C). An electrostatic field of 1700 volts was applied between the clearing field electrodes. Before the start of the cycle, typical pressures were as follows

Recompression cylinder - 105 atmospheres
Expansion cylinder - 40 atmospheres
Back chamber - 62 atmospheres.

Repumping operations after the expansion and recompression required a time of 67 seconds, and this set a lower limit to the shortest recycling time obtainable with this particular system.

It was established in a preliminary run with nitrogen as the filling material that when operated in the conventional manner a recycling time of 12 minutes was necessary. If the chamber was used without fast recompression, and recycled at intervals of two minutes, it was found that the tracks had disappeared after two

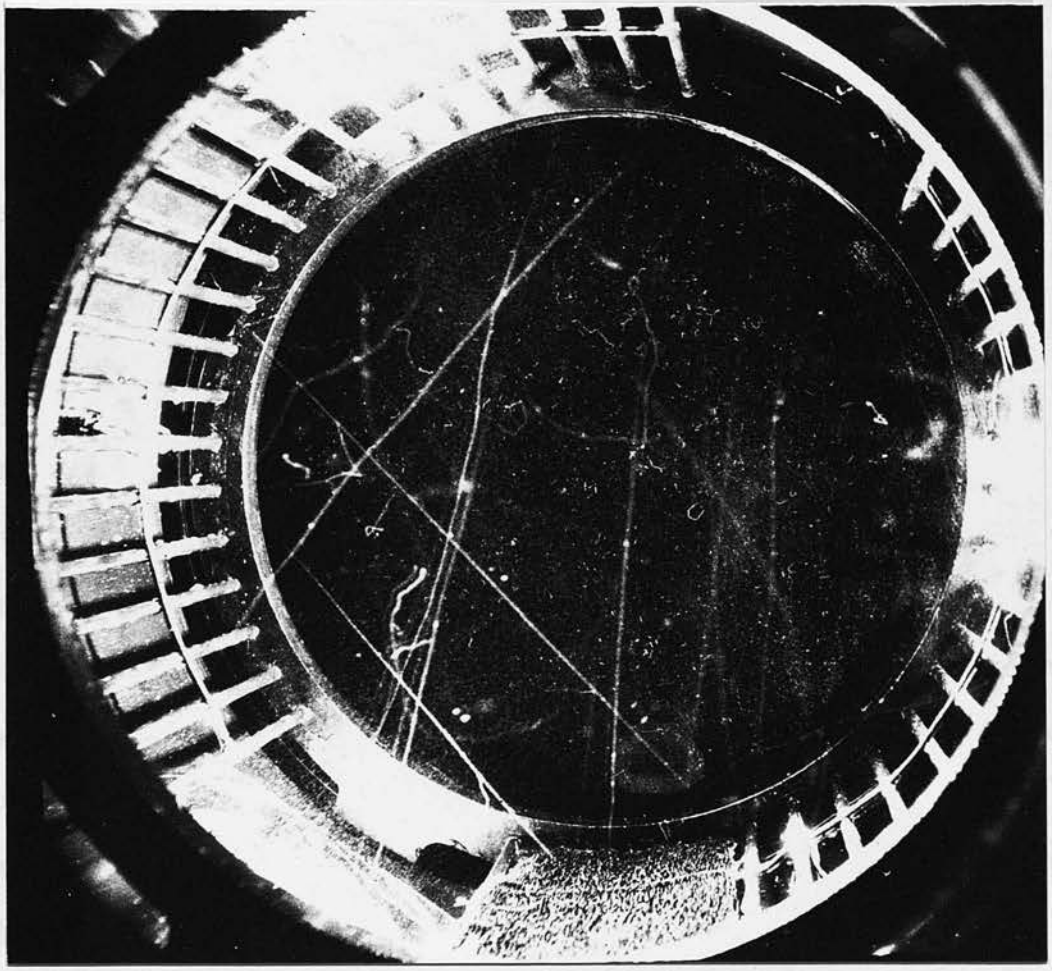

Figure 25. A typical photograph obtained with a two minute recycling period. This photograph was the 25th in such a series. The tracks are those of cosmic rays and the filling is 60 atmospheres of nitrogen.

expansions. Using the fast recompression cycle, it is possible to recycle the chamber usefully at two minute intervals. The effects of varying various parameters will be discussed below.

(1) The Delay before Recompression.

If the delay between the start of the expansion and the start of the recompression is less than 0.8 second (the maximum delay available with the present circuits was 1.3 seconds), the quality of the photographs remains satisfactory so long as the recycling time is not less than three minutes. In a run of thirty photographs, taken at two minute intervals, in which the recompression delay was 1 second, the condensation efficiency gradually decreased, and the average number of tracks per photograph also decreased, due to a gradual rise in the temperature of the gas as a whole. This rise in temperature was uniform over the body of the gas and must have been less than 0.5°C since tracks were visible over the whole volume of the chamber, in every photograph. After the first 15 photographs there was little evidence of rapid changes in the condensation efficiency, implying that the rise in temperature was very slow after this point.

It was found that for a recompression delay of 0.5 second and a two minute recycling period no appreciable loss in condensation efficiency can be detected

(see figure 25). It was found in the early stages of the work that, under the above conditions, there was often some distortion present on tracks which were made by particles crossing the chamber at or near the moment of expansion. Tracks of particles entering the chamber after the expansion showed much less, or no, distortion. This topic will be discussed in a later section.

It was not possible to take a run of photographs at intervals of much less than two minutes, owing to the time necessary to recharge the condenser banks used in the illumination circuits. A run of expansions at intervals of 1.5 minutes was taken using the minimum recompression delay. The track quality gradually deteriorated and distortion was present to an unacceptable degree. A short run of expansions, in which the tracks were examined visually, was taken using a recycling time of 67 seconds. In eight expansions the track quality had deteriorated markedly, the tracks were badly distorted and the background fog had increased to a great extent.

(2) The Speed of Expansion.

If the expansion valve was adjusted so that it did not open fully, with a consequent reduction in the speed of expansion, it was observed that a greater degree of

distortion was present compared with photographs taken with the valve fully open. This is presumably due to the greater expansion ratio necessary to produce the same degree of supersaturation, setting up more violent gas motions. In support of this, it was found that if, with the slower expansion, a lower condensation efficiency was used, the distortion was reduced.

The distortion mentioned in the previous section, which was found when a recycling period of two minutes was used, was caused by an unnecessary slowness of expansion. If the expansion valve was properly adjusted, it was possible to operate the chamber at intervals of two minutes, without serious distortion being present either in post-expansion tracks or tracks which were nearly counter-controlled. Pre-expansion tracks did show distortion, presumably due to slow gas motions.

Combining the considerations of this and the previous section, it is found that by recompressing within 0.5 second of the expansion and by ensuring that the expansion is as fast as possible, the chamber may be recycled at intervals of two minutes when filled to a pressure of 60 atmospheres of either argon or nitrogen. It is estimated that the expansion is completed within 0.25 second.

The Degree of Background Condensation.

One objection to the fast recompression system is that no provision is made for cleaning expansions. It might be expected that the background condensation would build up progressively. This was not found to be the case. At the end of a series of 65 photographs taken at intervals of two minutes, the background was no higher than at the beginning. It was found that if so large an expansion ratio was used that general cloud was formed, then subsequent fast expansions at the normal expansion ratio did not clean the chamber. If the expansion ratio was only slightly above that at which the background condensation started to obscure the tracks, then subsequent expansions were progressively dirtier and the background reached a point where tracks could no longer be seen. This confirms the finding stated in Chapter VII that it is not possible to re-evaporate the drops completely. It therefore follows that, for fast recompression to be applicable to a cloud chamber, that chamber must be capable of operating in the conventional manner without slow expansions. This condition is met by the chamber used in this work.

If immediately after an expansion and recompression one cleaning expansion is performed, the next fast expansion, after an interval of two minutes from the final repumping, shows a marked drop in the condensation

efficiency. This is to be expected from the arguments put forward in Chapter VII, and if a series of such expansions followed by a cleaning cycle is performed, it is indeed found that tracks disappear first from the top of the chamber. While the conditions of the above procedure are not identical to those of the overcompression cycle, it is to be expected that a similar loss of tracks at the top of the chamber should occur. This is confirmed in a private communication from the high pressure chamber group at University College, London, using a chamber adapted both to the overcompression system and to the fast recompression system. They report that fast recompression is superior to overcompression in nitrogen and hydrogen, but that the reverse is true in argon. This last is because of an inability to prevent the background increasing steadily during a series of expansions. The reason for this is not understood, since no difficulty has been experienced with the Edinburgh chamber when using argon as the filling material.

Operation of the Chamber under Heavy Ionisation Conditions.

In the work discussed above, the tracks were those formed by the cosmic radiation. A series of expansions was also carried out, for each gas, in which a beam of γ-rays, from a radioactive source, was allowed to

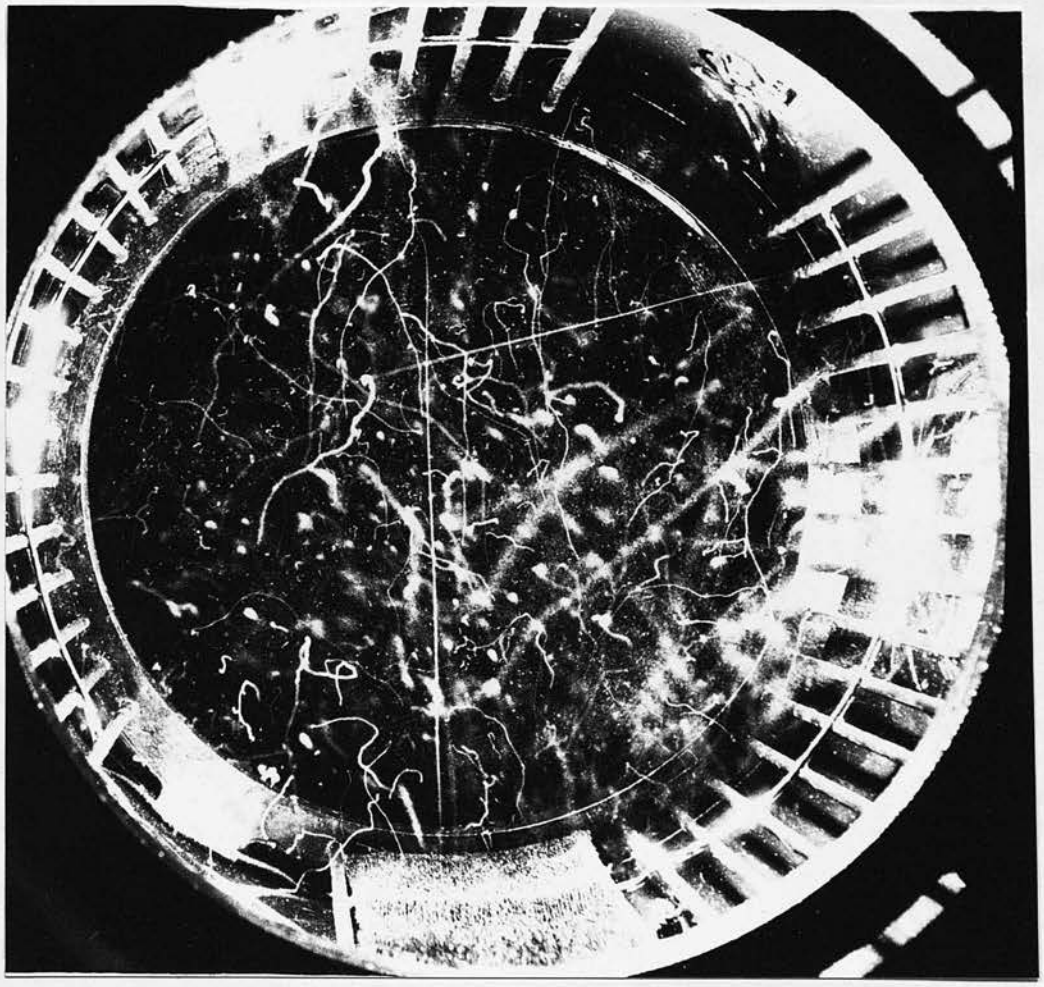

Figure 26. A typical photograph obtained under heavy ionisation conditions. The tracks are those produced by the 1.3 M.e.v. γ -rays from a 5 m.c. Co^{60} source.

enter the chamber some 200 milliseconds after the start of the expansion. It was thought desirable that the chamber should be tested under conditions of heavy ionisation, such as may be expected when working with a particle accelerator.

53 It had been found previously[53] that, when a similar high pressure chamber was operated in conjunction with the proton beam of the Harwell cyclotron, the chamber being operated in the conventional manner, there was a rapid loss of tracks in the upper part of the chamber. It was stated that this was considered to be due to a large proportion of the vapour being condensed and falling to the foot of the chamber. The rediffusion of vapour takes place slowly at this pressure. It would seem that this mechanism is unlikely to be the complete cause of the loss of tracks since the authors state that once the "vapour depleted" condition had been established, waiting periods of 1.5 hoursproduced no visible improvement. It is likely that temperature gradients play at least a large part in this phenomenon. In the present work no such vapour depletion was encountered over a period of 50 photographs. The γ-rays were those from a 2 millicurie radium bromide source, and in one series in argon they were allowed to pass into the chamber continuously. The ionisation produced by the γ-rays,

though much greater than that due to the cosmic radiation, was not so great as that used in the experiment of Griffith, where 600 protons were admitted to the chamber at each expansion, and it is possible that an effect due to a high proportion of the vapour being condensed may exist.

In conclusion, it appears that, with the present system, the limiting factor in the recycling time is the presence of distortion. It might be possible to reduce the recycling period to a small extent for the case of an experiment where the entry of the desired particles may be accurately controlled, for example by the pulsing of a particle accelerator at the appropriate part of the cycle. However, even in this case, a lower limit would be set at 1.5 minutes due to the onset of a net rise in temperature over the cycle as a whole. If a low condensation efficiency could be tolerated, it is considered that a long series of photographs could be obtained with recycling periods somewhat less than 1.5 minute. It is difficult to imagine an experiment in which this further reduction of the recycling period would outweigh the loss of information due to a low condensation efficiency.

Gas Motion during the Expansion and Compression.

In a large part of the present work, the camera

was rapidly wound-on after the photograph, and a second photograph of the same tracks was taken after the re-compression had been completed. It was hoped that measurements of position on corresponding points before, and after, the recompression would yield information about the gas motion. It was found that a region of extreme turbulence was set up near the walls of the chamber. Reference to figure 27 will show a case where the track has been snapped in two by the gas motion. This turbulence is to be expected, since the gas in this region will be heated by conduction from the walls, and will start to flow upwards - reference to figure 27 will show that this motion is well developed at a time 0.5 second after the start of the cycle. Similarly, after the recompression, this layer will cool down by conduction, and will tend to flow downwards along the wall and turbulent flow will be produced. This region does not extend far into the chamber.

In the useful, undisturbed, volume of the chamber, measurements of position were made on recognisable points on several tracks. These measurements were made directly off the film. The x and y coordinates in space of the point considered, with respect to the principal plane of one lens of the stereoscopic pair as origin, can be measured from the two projections of the point on to the film, through the poles of the

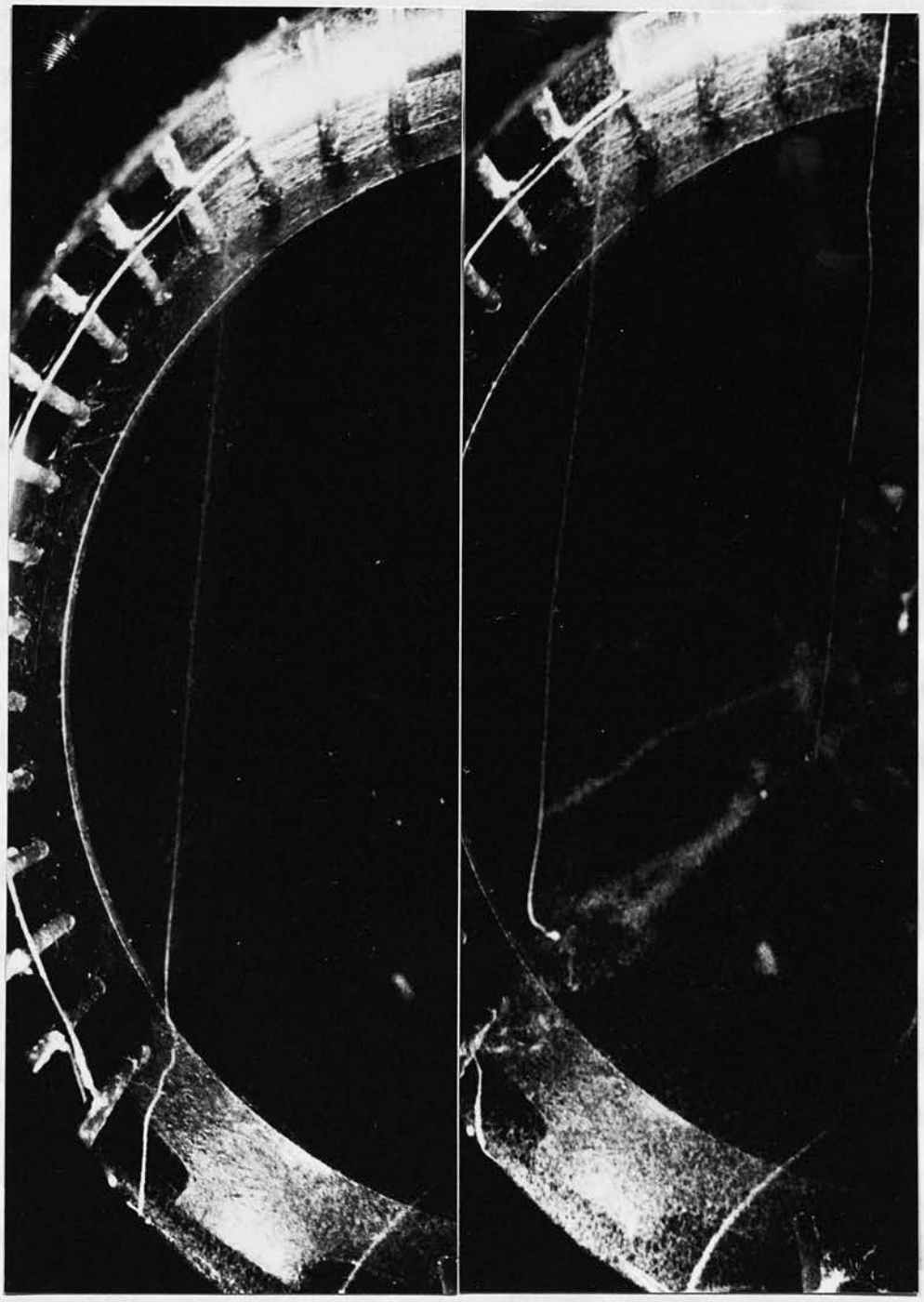

Figure 27. Photographs showing turbulent flow near the wall. The photograph to the left was obtained after the expansion. The photograph to the right is of the same track after the recompression.

lenses. The z coordinate in space may be obtained from the separation of the two images of the point considered and a knowledge of the magnification of the lenses.

In a chamber such as the one used in this work, the motion of the gas during the expansion would be expected to be along the axis of the chamber. Since the increase in volume required to produce a given expansion ratio depends on the volume considered, a purely axial expansion will produce a displacement proportional to the distance from the front of the chamber. For a track which dips in the chamber, the end nearer to the diaphragm will have been displaced in the direction of the expansion to a greater extent than the end nearer the front. The range and orientation of the line of droplets forming the track will therefore be different from that of the trajectory of the original ionising particle, all dimensions in the direction of the expansion having been multiplied by a factor equal to the expansion ratio. This effect will not occur for tracks entering the chamber after the expansion is completed, and will be reduced for tracks entering during the expansion. On the assumption that, for the undistorted portion of the gas, the recompression is the exact opposite of the expansion, the expansion ratio in each of three mutually perpendicular directions

may be measured.

Measurements made on tracks in argon showed that the calculated expansion ratio in the direction of the expansion was 1.015 ± .007 while in the other two directions they were 1.005 ± .007 and 0.987 ± 0.01. The known expansion ratio was 1.05. It was thought that this discrepancy was due to the tracks not moving with the gas, their motion being impeded by viscous forces. To verify this, a series of measurements were made on tracks in nitrogen. Since the expansion ratio in nitrogen is 1.09, the effect would be more easily measurable, and by measuring tracks with different degrees of condensation, and consequently different drop sizes, it was hoped to detect the variation of viscous drag with drop size.

For a track which had entered the chamber after the expansion, the expansion ratio in the axial direction was 1.05 ± .007, while for a pre-expansion track it was 1.03 ± 0.01. The expansion ratios in the radial directions were 0.99 ± 0.007 and 0.994 ± 0.005. From these figures, it seems clear that the expansion is very nearly purely axial. The observed variation of the axial expansion ratio with drop size is in the correct sense, if the viscous drag of the gas is the explanation of the low value of the measured expansion ratio.

In order to verify that the axial displacement is that expected from the volume change, it would be necessary to locate the original line of the ions, perhaps by a stringent counter telescope system.

Chapter XI.

CONCLUSIONS AND FUTURE PROGRAMME.

The fast recompression system has been found to be very successful. The recycling period of the high pressure chamber has been reduced to one sixth of that required for the conventional method of working and it is considered that it will now be a useful tool for use with the particle accelerators. It is proposed that the collaboration between the University of Edinburgh and University College, London, should continue. The Edinburgh chamber is to be taken to Geneva and operated with the 640 MeV synchrocyclotron at C.E.R.N., to investigate the reactions induced in the light gases hydrogen, deuterium and helium on bombardment by protons and π-mesons. A low beam current will be used so that, on average, one particle traverses the chamber per cycle. The chamber is to be counter-controlled by scintillation counters, using the simultaneous occurrence of a pulse from a scintillator placed in the beam path before it traverses the chamber, and the absence of a pulse from a second scintillator placed in the beam path after it traverses the chamber, to cause the expansion of the chamber. The high pressure chamber, now at London, is to be taken to Harwell to

carry out a similar experiment at a lower energy.

The reactions which can occur are very numerous, and it is considered that this field is one in which the high pressure chamber can make a valuable contribution.

REFERENCES.

1. Anderson, C.D. and Neddermeyer, S.H., Phys. Rev., 50, 263, 1936.

2. Williams, E.J. and Roberts, G.E., Nature, 145, 102, 1940.

3. Rossi, B. and Nereson, N., Phys. Rev., 62, 417, 1942.

4. Conversi, M., Pancini, E. and Picciono, C., Phys. Rev., 71, 209, 1947.

5. Powell, C.F. and Occhialini, G.P.S., Nature, 159, 186, 1947.

6. Wataghin, G., Santos, M.D. de S. and Pompeia, P.A., Phys. Rev., 57, 339, 1940.

7. Rochester, G.D. and Butler, C.C., Nature, 160, 855, 1947.

8. Leighton, R.B., Wanless, S.D. and Anderson, C.D., Phys. Rev., 89, 148, 1953.

9. Rochester, G.D. and Butler, C.C., Reports on Progress in Physics, 1953, 365.

10. Brown, R.H., Camerini, U., Fowler, P.H., Murhead, H., Powell, C.F. and Riston, D.M., Nature, 163, 82, 1949.

11. Gell-Mann, M. and Pais, A., Proc. Glasgow Conference on Mesons, 1954.

12. Donald, R.A., Evans, G.R. et al., Nuovo Cimento, Supplemento No. 2, 272, 1955.

13. Evans, G.R., Report of London Cloud Chamber Conference, p. 67, 1955.

14. Baxter, P. and Stannard, F.R., Proc. Phys. Soc. A, 70, 17, 1957.

15. Fowler, P.H., Phil. Mag., 41, 169, 1950.

16. Williams, E.J., Proc. Roy. Soc. A, 169, 531, 1939.

17. Biswas, S., George, E.C. and Peters, B., Proc. Ind. Acad. Sci. A, 38, 418, 1953.

18. Williams, E.J., Ph.D. Thesis, University of Wales, 1955.

19. Bullock, F., Proc. Phys. Soc. A, 70, 134, 1957.

20. Rangarao, B.V., Private communication (to be published).

21. George, E.P., Redding, J.L. and Trent, P.T., Proc. Phys. Soc. A, 66, 553, 1953.

22. Kannanagra, M.L.T. and Shrikantia, G.S., Phil. Mag., 44, 1091, 1953.

23. Leontic, B. and Wolfendale, A.W., Phil. Mag., 44, 1101, 1953.

24. McDiarmid, I.B., Phil. Mag., 45, 933, 1954.
Phil. Mag., 46, 177, 1955.

25. Rochester, G.D. and Wolfendale, A.W., Phil. Mag., 45, 980, 1954.

26. Molière, G., Zeits. Naturforsch., 3A, 78, 1948.

27. Olbert, S., Phys. Rev. 87, 319, 1952.

28. Rose, M.E., Phys. Rev., 73, 279, 1948.

29. Hofstadter, R., Fechter, H.R. and McIntyre, J.A., Phys. Rev., 92, 978, 1951.
Phys. Rev., 95, 512, 1954.

30. Blackett, P.M.S., Proc. Roy. Soc. A, 159, 1937.

31. Wilson, J.G., Nature, 158, 415, 1949.

32. Jones, H., Rev. Mod. Phys., 11, 235, 1939.

33. Heitler, W., Quantum Theory of Radiation.

34. Greisen, K., Phys. Rev., 61, 212, 1942.

35. Amaldi, E. and Gatto, R., Nuovo Cimento, 7, 553, 1950.

36. Anderson, CD., Fermi, E., Nagle, D.E. and Yodh, G.B., Phys. Rev., 86, 793, 1952.

37. Clarke, J.O. and Major, J.V., Phil. Mag., 2, 37, 1957.

38. Sard, R.D. and Crouch, M.F., Prog. in Cosmic Ray Physics, Vol. 2, p. 1.

39. Leighton, R.B., Anderson, C.D. and Seriff, A.J., Phys. Rev., 75, 1432, 1949.

40. Wheeler, J.A., Rev. Mod. Phys., 21, 133, 1949.

41. Evans, G.R., Evans, W.H., Griffith, T.C. and Muller, H., Proceedings of the Bristol Conference, 1951, p. 33.

42. Lederman, L.M., Circulated Reports from Nevis Laboratory, 1957.

43. Eisenberg, Y., Report on the Pisa Conference, 1955, p. 484.

44. Alvarez, L.W., Bradner, H., Falk-Vairant, P., Gow, J.D., Rosenfeld, A.H., Solmitz, F.T. and Tripp, R.D., Nuovo Cimento, Vol. V, No. 5, p. 1027, 1957.

45. Gatto, R., Nuovo Cimento, Vol. V, No. 5, p. 1021, 1957.

46. Gaerttner, E.R. and Yeater, M.L., Rev. Sci. Inst., 20, 588, 1949.

47. Goldwasser, E.L. and Nicolai, V.O., Report of the London Conference on Cloud Chambers, p. 152, 1955.

48. Emigh, C.R., Rev. Sci. Inst., 25, 221, 1954.

49. Walker, J., Tagliaferri, D., Bower, J.C. and Hedley, D.W., J. Sci. Inst., 33, 113, 1956.

50. Williams, E.J., Proc. Camb. Phil. Soc., 35, 512, 1939.

51. Duff, M. and Morris, N., Report on the London Conference on Cloud Chambers, p. 78, 1955.

52. Kluyver, J.C. and Endt, P.M., Physica, 16, 257, 1950.

53. Banford, A.P., Duncanson, W.E., Griffith, T.C. and Williams, W.S.C., Report of the London Conference on Cloud Chambers, p. 104, 1955.

ACKNOWLEDGMENTS.

I wish to thank Professor N. Feather, F.R.S. for the use of his laboratory facilities, and Professor H.S.W. Massey, F.R.S. for the opportunity to participate in the work at La Marmolada.

I am deeply indebted to Dr. G.R. Evans for having suggested the subjects of this thesis, for his advice and for the benefit of his experience.

I am grateful to Professor A. Rostagni of the University of Padua for permission to use the laboratory at La Marmolada and to the directors of the Societa Adriatica di Elletricitta for the invaluable help that they afforded. I also wish to thank Dr. A. Loria of the University of Padua for his help in matters of organisation.

Mr. A. Headridge and his staff have given valuable help in the construction of apparatus.

I am indebted to the Postgraduate Studentships Committee of the University of Edinburgh for financial assistance.